CONTRACT REPORT S-75-5

SOIL STABILIZATION

by

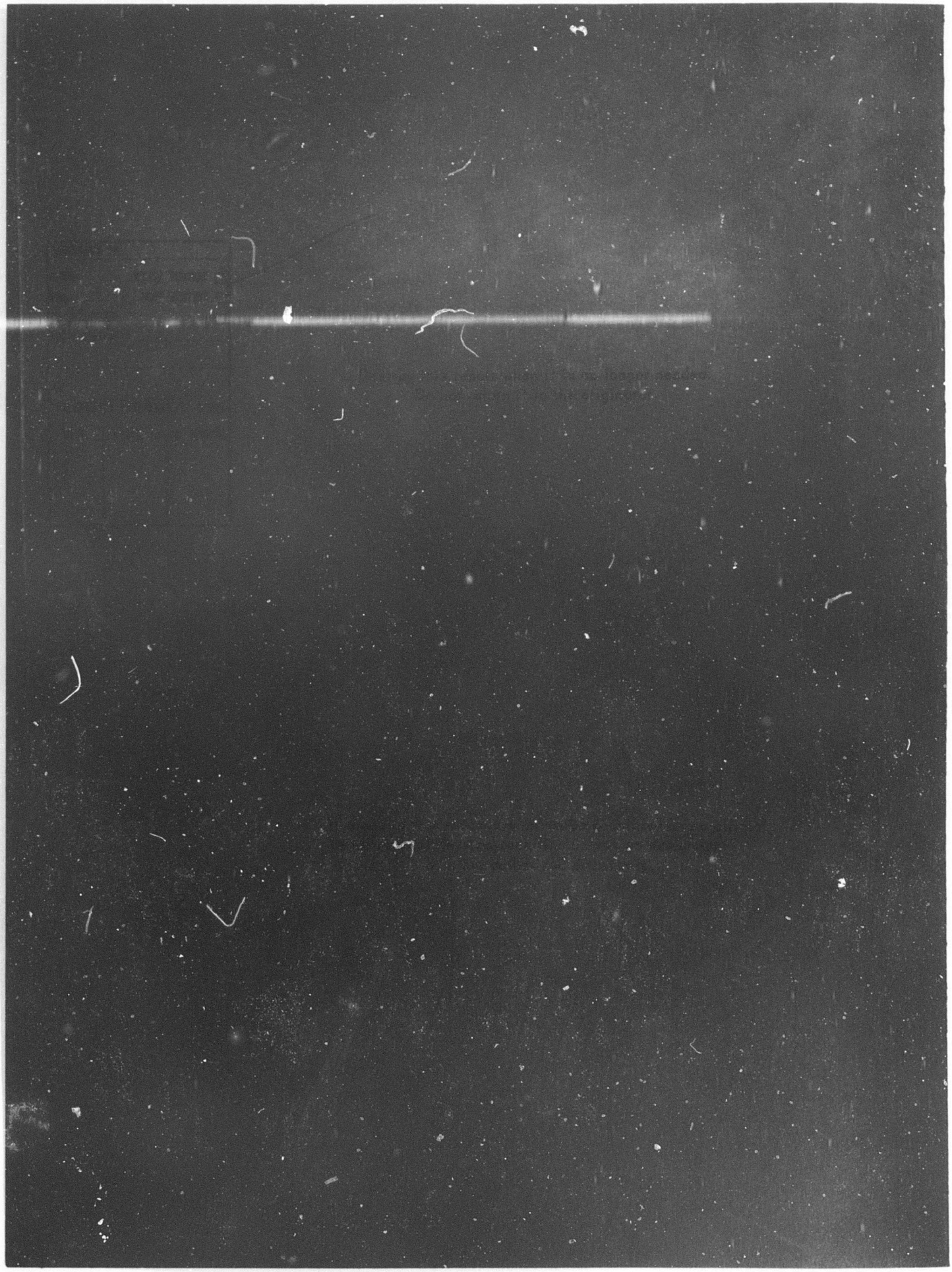

Contract Report No. 3-63

Soil Stabilization Phase Report No. 7

A DURABILITY TEST FOR STABILIZED SOILS

by

Anwar E.Z. Wissa
Jose Guillermo Paniagua

Sponsored by

U.S. Army Materiel Command
Project No. DA IT061102B52A-01

Conducted for

U.S. Army Engineer Waterways Experiment Station
Vicksburg, Mississippi

under

Contract No. DA-22-079-eng-465

Research Report No. R69-32
Soil Mechanics Division
Department of Civil Engineering
Massachusetts Institute of Technology

June , 1969

Soils Publication No. 239

FOREWORD

This report is the seventh in a series of reports on soil stabilization issued by the Massachusetts Institute of Technology for the U. S. Army Materiel Command under Project Number DA IT061102B52A-01. The work was conducted during fiscal year 1968-1969 under Contract No. DA-22-079-eng-465 between the U. S. Army Engineer Waterways Experiment Station (WES), Vicksburg, Mississippi, and the Soils Research Laboratory of the Department of Civil Engineering at the Massachusetts Institute of Technology.

The work covered by this report was conducted by Mr. Jose Guillermo Paniagua, Research Assistant in Soils, under the direct supervision of Dr. Anwar E. Z. Wissa, Assistant Professor of Civil Engineering. Dr. Wissa and Mr. Paniagua prepared the report.

The contract was monitored by Mr. G. R. Kozan, former Chief, Stabilization Section, Expedient Surfaces Branch, under the general supervision of Mr. A. A. Maxwell, Acting Chief, Soils Division, WES. Contracting Officer was COL L. A. Brown, CE.

TABLE OF CONTENTS

LIST OF TABLES

LIST OF FIGURES

APPENDIX D DETAIL DRAWINGS, ASSEMBLING INSTRUCTIONS, AND SPECIFICATIONS FOR THE REVISED DURABILITY TENSILE TESTING APPARATUS

D.1 COMPACTION MOLD AND ACCESSORIES

SUMMARY

This report describes and evaluates a new testing procedure for determining the surface durability of stabilized soils by measuring the change in tensile strength at the surface of test specimens (slabs) subjected to laboratory cycles of weathering. This test, called the Durability Tensile Test, is shown to be potentially a more direct and reproducible method than the standard ASTM Durability Test for evaluating stabilized soils.

A prototype apparatus has been constructed to measure the surface tensile strength over approximately 4.0 cm^2 circular areas of a 5-inch-square slab, one inch thick. Preliminary tests on three slabs show that the measured strength is related to the effective cohesion of the soil system. For example, increases in curing or dry density which result in an increase in effective cohesion also produce an increase in measured tensile strength. Weathering cycles, which have been shown elsewhere to cause a loss in effective cohesion, also result in a loss in tensile strength. Therefore the Durability Tensile Test appears to be a rational method of evaluating durability characteristics.

Based on the experience obtained with the prototype apparatus, a modified version is recommended to improve reproducibility and to simplify the testing procedure.

BLANK PAGE

Chapter 1
INTRODUCTION

1.1 GENERALITIES

Soil Stabilization, in the broadest sense, is the alteration of any property of a soil to improve its engineering performance (Lambe, 1961). One of the most commonly used methods for improving the strength and moisture stability properties of soils is by the addition of a small amount of a cementing agent such as portland cement or hydrated lime. The feasibility of using such a method is primarily determined by economic considerations, i.e., the amount of cementing agent needed to achieve the desired alteration. Soil stabilization techniques can often offer low cost solutions to some earthwork and foundation problems. For this reason a considerable amount of research has been undertaken over the last thirty years in this field. The development of chemical additives to be used as cementing agents, an understanding of the mechanism involved in soil stabilization and the determination of the parameters that control the behavior of stabilized soil masses are therefore necessary for the production of economical designs with good performance characteristics.

1.2 PURPOSE OF THE INVESTIGATION

The purpose of this investigation was to develop an apparatus and testing technique to evaluate the ability of stabilized soils to resist the disruptive effect of shrinkage and expensive forces produced by periodic moisture changes or freezing usually referred to as "cyclic weathering".

The effects of cyclic weathering on a stabilized soil mass are most severe at the surface where the loss of cohesive strength can manifest itself by loss of material from the surface in the form of dust or scales.

The testing technique selected in this investigation involved the measurement of the tensile strength of the surface of a stabilized specimen, i.e., the cohesive strength. This can be done at different levels of weathering (number of cycles of weathering). This proposed test will be referred to as the "DURABILITY TENSILE TEST."

This technique serves to evaluate the susceptibility to dusting and scaling of a given mix by measuring the losses in tensile strength of the surface when subjected to cyclic weathering in the laboratory. The results obtained using this technique are believed to be a more rational measure of the durability characteristics of stabilized soils than the presently used empirical methods (ASTM Designations D559-57 and D560-57). However, since these empirical methods have already been extensively correlated with field performance, it would be desirable to attempt to indirectly correlate the tensile durability test with field performance via the ASTM standard tests.

1.3 SCOPE OF THE TEST PROGRAM

A testing apparatus was developed and used to conduct tensile durability tests on stabilized soil specimens (slabs). Tests were run on static compacted specimens of a clayey silt stabilized with 5% portland cement. Two specimens were used to study the reproducibility of the equipment and a third specimen to study the effects of weathering. Eighteen tension tests were run on each slab.

Based on the results of this investigation, a tentative test procedure was developed and the testing equipment redesigned to simplify its use and improve its performance.

Chapter 2
BACKGROUND

2.1 DEFINITIONS

2.1.1 Soil-cement

Soil-cement is a mixture of soil with measured amounts of portland cement and water, compacted to high density.

2.1.2 Durability of Soil-cement

Durability of soil-cement is the ability of the soil-cement mass to retain its structural stability when subjected to detrimental cycles of wetting and drying or freezing and thawing (e.g., ASTM Designations D559-57 and D560-57).

2.2 HISTORICAL REVIEW

Portland cement has proved to be a good stabilizing agent for most soils. Exceptions are soils with high contents of sulphates and chlorides due to the formation of an expansive and disruptive calcium sulphoaluminate (sherwood, 1962). Also, cement does not react well with organic soils.

Soil-cement has been widely used for over 30 years both in the United States and in most other countries mainly as base course for roads and airfields, and also as slope protection for embankments and canals.

During the development of soil-cement as a construction material, observation of performance showed that some mixes did not retain their structural integrity.

The disruptive effect of the shrinkage and expansive forces introduced by moisture changes in the soil-cement mass was identified as the primary cause of the observed behavior. Freezing has also been shown to cause disintegration of soil-cement.

In engineering works using soil-cement, it is sometimes necessary to only rely on the cohesive strength of the mass, for example when soil-cement is used to provide an erosion-resistant surface for embankments or canals.

In other instances it is desirable to be able to count on a cohesive resistance which adds to the strength of the mass, thus increasing its load-bearing capacity especially by providing tensile strength, which for unstabilized soils is negligible. The design of base courses for pavements is an example where this marginal strength characteristic of tensile resistance is sought in an effort to reduce pavement thicknesses. This is particularly true for sands where the addition of cement does not alter the frictional behavior and solely increases its cohesive resistance (Wissa and Ladd, 1964). It is not clear, however, whether it is realistic to count on the tensile strength characteristic of a soil-cement base which undergoes repetitive loading due to traffic.

An extensive research program by the Portland Cement Association (PCA) in 1935 resulted in design criteria for soil-cement based on the results of some laboratory tests (Norling, 1963). These criteria provided the necessary guidelines for the production of soil-cement with "good and durable engineering properties."

The laboratory tests used to evaluate performance are the wet-dry test (ASTM D559-57), the freeze-thaw (ASTM D560-57), and the unconfined compressive strength

test. Using these testing procedures, the acceptance criteria recommended by the PCA and adopted as standards by ASTM are:

1. "Soil-cement losses during 12 cycles of either the wet-dry or freeze-thaw test shall conform to the following limits: Soil groups A-1, A-2-4, A-2-5, and A-3, not over 14 percent. Soil groups A-2-6, A-2-7, A-4 and A-5, not over 10 per cent. Soil groups A-6 and A-7 not over 7 per cent."
2. "Maximum volume at any time during either test shall not exceed the volume at time of molding by more than 2 per cent."
3. "Maximum moisture content at any time during either test shall not exceed that quantity which will completely fill the voids of the specimen at time of molding."
4. "Compressive strength of soil-cement specimens soaked in water 1 to 4 hours prior to test shall increase both with age and with cement content at and above the cement content which produced results meeting requirements 1, 2, and 3."

The criteria 1, 2, and 3 above presumably indicate whether or not the soil-cement is effectively resisting the disruptive forces resulting from cyclic weathering.

Criterion 4 indicates whether or not the soil is interfering with the normal hydration process of the cement.

The wet-dry and the freeze-thaw tests were developed to reproduce in the laboratory the disruptive effect of weathering. The wet-dry test simulates shrinkage forces, and the freeze-thaw test expansive forces.

The number of cycles of wet-dry or freeze-thaw and the other procedural details were selected to produce reasonable data in a practical length of time (Norling, 1963). A brushing procedure after each cycle was introduced in an effort to improve the consistence and reproducibility of the "weight loss" measurements. These procedures were adopted by ASTM.* The tensile durability test described in Chapter 3 is a substitute to the brushing procedure and has the advantage of being more rational and does not depend on the operator's ability to perform the test.

*ASTM Designations D559-57 and D560-57.

Chapter 3
TEST APPARATUS, MATERIALS, AND PROCEDURES

3.1 TESTING EQUIPMENT

3.1.1 Compaction Mold and Accessories

All the parts of the compaction mold and its accessories were made of aluminum to minimize cost. Detail drawings of the parts are presented in Appendix A. The base plate "A" and the top plate "B" in Figs. 3.1 and 3.2 were used as plungers for two-end static compaction. Spacer bars "D" were made to separate the plunger pieces from the mold at different stages during the compaction operation.

Brass screed plates "L", 1/3" in thickness, were used to distribute the soil-cement mix uniformly inside the mold before compaction (Fig. 3.3).

3.1.2 Compaction Equipment

A 5-ton compression test machine was used to provide the necessary compaction effort (Fig. 3.2). A suitable hydraulic press could have been substituted for the compression test machine. The mold was centered in the load frame by means of a vertical pin connection between the center of the bottom plate and the pedestal of the compression machine (Fig. 3.4).

A proving ring with 10,000-pounds capacity served to measure the applied compressive force. The center line of the proving ring was aligned with the center of the top plate "B" by means of two steel pieces "E" and "F" shown in Figs. 3.2 and 3.4. They also served the purpose of distributing the applied force over a larger area at the top plunger.

An air-bubble level was used to ensure horizontal alignment of all parts of the compaction assembly before compaction.

3.1.3 Tensile Test Equipment

The tension tests were performed by means of several pieces of equipment designed and assembled to achieve the desired purpose. These pieces of equipment can be grouped into the following categories according to their function.

1. Specimen supports.
2. Guiding block and accessories.
3. Tensile force application system.
4. Measuring devices and recording instruments.

3.1.3.1 Specimen Supports

A spacer block, "B" in Figs. 3.5 and 3.6,* is used over the bottom plunger "A" to raise the level of the top surface of the test specimen above the surface of the compaction mold. The bottom plunger then acts as the base plate for the tensile testing equipment. The mold "C" (Fig. 3.7) provides lateral support to the sample.

The base plate is located on the testing table between the two guide angles "C" (Fig. 3.5) and is prevented from vertical movements by the base clamps "D", which are fastened to the vertical legs of the guide angles. This locks the base plate laterally, but it can still slide

---

*In Figs. 3.6 through 3.8 a sample already tested is shown because a specimen not tested was not available at the time the photograph was taken.

longitudinally. In Fig. 3.8 two air-bubble levels "D" are shown in the position used to level the specimens and the mold.

3.1.3.2 Guiding Block and Accessories

The guiding block of the tensile test assembly contains the shafts and cylinders via which the tensile force is applied to the slab (Fig. 3.9). An arm connected to the shaft is used to measure the vertical displacement during the tension test (Figs. 3.9 and 3.10). Detail drawings are given in Appendix A. The shafts are 60 Rockwell case-hardened stainless steel and each one is guided through the guiding block by two Thompson high-precision ball bushings for linear motion. The bushings ensure the stability of the center line and minimized friction of the shafts during testing.

Two long bars, "F" in Fig. 3.10, run through the guiding block and the mold "B" and are screwed to the base plate "A". With the wing nuts "S" (Fig. 3.11) the guiding block is fastened to the base.

The tension loading caps "C", made of stainless steel, screw on to the lower end of the testing shafts (Fig. 3.9).

3.1.3.3 Tensile Force Application System

The system used for applying the tensile load to the shafts and loading caps is shown in Figs. 3.12 and 3.13.

A "Boston Gear" electric motor with a rated output torque of 133 in.-lbs. and output speed of 35 RPM is used to apply the tensile load. The output shaft rotation of the motor is transferred to the gear box "M" by means of the steel sprockets "J" and "L" and the chain "K", which increases the speed from 35 RPM at the output of the motor to 70 RPM at the input of the gear box "M".

The gear box "M" with a ratio of 1-to-900 is coupled to the gear box "N", which has a ratio of 1-to-100, resulting in the drive shaft "O" having a speed of 7.77×10^{-4} RPM.

The pulley "P" rotates together with the drive shaft while being able to slide along its length. This is provided by means of a key that locks the pulley to the shaft for rotary movement only, as shown in Fig. 3.14a. The drive shaft is supported by a ball bushing at the opposite end of the connection with the gear box "N". (Fig. 3.12).

The cable "C" in Fig. 3.12 and 3.13 is firmly attached to the driving pulley "P" by feeding it through a hole drilled along a chord of the pulley and clamping it with two screws as shown in Fig. 3.14b.

The radius of the driving pulley being 0.75 in. results in a linear velocity of the cable of 3.66×10^{-3} in./min or 0.22 in./hr.

In Fig. 3.15, the cable "C" runs around the pulley "B", which is mounted on a ball bushing to reduce friction at this point. The pulley-ball bushing assembly is mounted on the shaft "O", which is supported at both ends by the frame "A". The pulley-ball bushing assembly can easily slide along the length of the shaft.

The end of the cable is fastened to the force transducer-support cylinder "H" by means of the clamping nut "I" as shown in Figs. 3.15 and 3.16b.

As shown in Fig. 3.16c, the force transducer "G" screws into the bottom part of the cylinder "H". This cylinder has a 1 inch diameter hole, bored at right angles to the axis of the cylinder.

The upper beam "K" of the yoke in Fig. 3.17 runs inside the transverse hole in the cylinder and rests on the transducer head. The lower beam "L" of the yoke has a hole in its center through which the threaded end of the testing shaft "A" passes and is fastened with the nut "M".

With this assembly a tensile force in the cable, which has its reaction in the testing shaft, is measured as a compression force on the head of the transducer.

3.1.3.4 Measuring Devices and Recording Instruments

A Dynesco force transducer with 200-pounds capacity (compression) was used to measure the applied forces. Its location and mounting details were explained in the preceding section. The calibration curve for the force transducer is given in Appendix B.

Excitation to the transducer is provided by a constant voltage direct current power supply. The excitation voltage used was 6.2 volts. The electrical cable of the transducer is a four-conductor shielded cable; two for input excitation voltage, two for output signal, and the grounded shield. The output voltage signal from the transducer is read at the central data acquisition system of the Soils Laboratory via a terminal box "G", Fig. 3.13, (a diagram of internal wiring of the terminal box is presented in Appendix B.). The data acquisition system consists of a cross-bar scanner, a digital voltmeter, a line printer, and a digital clock. The resolution of the voltmeter is 10 microvolts. A direct current displacement transducer (DCDT) was used to measure displacements during the tension tests. The transducer was excited from the same constant voltage supply as the force transducer, and the output signal was recorded by the data acquisition system as explained above. This transducer could easily respond to 0.0001 inch displacements.

A calibration table of this transducer is presented in Appendix B.

3.1.4 Miscellaneous Equipment

The following list covers all additional miscellaneous equipment used:

a) Oven at a temperature of $105^{\circ} \pm 5^{\circ}C$
b) Oven at a temperature of $70^{\circ} \pm 5^{\circ}C$
c) Balance. Capacity 800 gms. Accuracy = 0.1 gm.
d) Balance. Capacity 100 gms. Accuracy = 0.001 gm.
e) Balance. Capacity 200 gms. Accuracy = 0.2 gms.
f) Beaker
g) Aluminum pan
h) Squeeze bottle
i) Graduated glass jar. Accuracy 1 cc.
j) Optical micrometer. Accuracy = 0.001 in.
k) Micrometer. Accuracy = 0.001 in.
l) Glass plates 6" x 6" x 1/4"
m) Thin polyvinyldene chloride film.
n) Aluminum foil
o) Hysol epoxy-patch
p) Water-content determination cans
q) Spoon and small scoop
r) Air-bubble level
s) Constant temperature bath ($T = 70^{\circ}C$)

3.2 MATERIALS

3.2.1 Soil

The soil used for this investigation was the fraction passing #40 sieve of a glacial till called Massachusetts clayey silt (M-21). This clayey silt is classified as ML-CL according to the Unified Soils Classification System. The method used to obtain the fraction passing #40 sieve was as follows:

a) The natural till was first ovendried and then passed through a #4 sieve to remove the gravel-size particles.
b) The fraction passing #4 sieve was then ground in a mill to break down lumps.
c) The material was then passed through a #40 sieve.
d) To ensure homogeneity of the soil, the fraction passing #40 sieve was then spread over an area of approximately 4 x 4 feet, (100 pounds of material) divided quarterly, and mixed using a scoop, first each quarter of soil within itself and then all the quarters among themselves.
e) The material was then stored for use in a closed 20-gal. galvanized steel can.

This particular soil was selected for two reasons: first, because it is available locally and second, because numerous research projects in soil stabilization at M.I.T. have used this soil in the past.

The properties of this soil are given in Table 1, Appendix C. The grain-size distribution of the fraction passing #40 sieve is shown in Figure C.1, Appendix C.

3.2.2 The Stabilizer

Commercial grade, Type I portland cement was used as the stabilizing agent. All the cement used was taken from a batch stored in a tightly closed can. All the specimens tested were prepared using this cement in a proportion equal to 5% by weight of the oven-dried soil. Some physical properties of the soil-cement mixture were given by Wissa and Ladd (1964) and are shown in Table 1 of Appendix C.

3.3 LABORATORY PROCEDURES

3.3.1 Preparation of Specimens

3.3.1.1 Proportioning and Mixing

To achieve a 5% cement content by weight, 900 gms. of air-dry M-21 were mixed by hand for ten minutes with 45 grams of portland cement Type I.

Water was then added to achieve the desired molding water content and hand mixed for 10 minutes. A damp cloth was then placed over the mix to reduce moisture losses by evaporation during compaction.

3.3.1.2 Compacting

The method of compaction used was two end static. When the top and bottom plunger pieces reach the end of their travel distance, a fixed volume of 27.5 in^3 or 0.01592 ft^3 remains inside the mold; therefore all specimens have this volume, and the dry density is controlled by varying either the water content or the amount of mix placed inside the mold. Obviously, different compaction efforts will be necessary for different final densities. Alternatively, the samples could have been compacted at constant effort by increasing the amount of soil used, to prevent the plungers from reaching the ends of their travel.

The compaction data for the three specimens used in this investigation are given in Tables 1, 2, 3, and 4, Appendix C.

While placing the mix in the mold, the screed plates were used to evenly distribute the mix in an effort to ensure uniform compaction at all points of the specimen (see Fig. 3.3).

Three sizes of spacer bars were used between the mold and the top and bottom plungers to ensure even compaction at both ends of the specimen. This was important since both surfaces of the specimen were used for tension tests and therefore had to have the same molding density.

3.3.1.3 Curing of Specimens

When compaction was completed, the sample was extruded from the mold and placed between two glass plates, then wrapped with three layers of thin polyvinyldene chloride film and sealed with adhesive tape. The sample was wrapped once more using aluminum foil and sealed with a silicone rubber.

Two methods of curing were used:

a) Cold Cure

In this method the sample was stored in a humid room where the temperature averaged 24°C.

b) Hot Cure

In this method, the sample was placed inside a glass jar which in turn was placed inside a constant temperature bath at 70°C.

3.3.2 Tension Test

3.3.2.1 Locating the Specimen for testing

Stage I (Fig. 3.5) Locate the base plate "A" between the centering guides "C". Place the base clamps "D" and fix them with the bolts "F". Place the pedestal block "B" over the base plate.

Stage II (Fig. 3.6) Place the sample over the pedestal block "B".

Stage III (Fig. 3.7) Slide down the mold "C" over the specimen.

Stage IV (Fig. 3.8)* Level the mold using the leveling screws "C" and air-bubble levels "D". Bring the surface of the mold flush level with the surface of the sample.

---

*See footnote in page 9

3.3.2.2 Gluing of Testing Cylinders

The original design of the loading caps (Fig. 3.9) did not include the cup form at the gluing end; instead, it was a horizontal flat surface. Great difficulties were experienced in controlling the spreading of the epoxy used as gluing agent and the design was changed to the cup shape mentioned.

Two types of Hysol epoxies were tried as gluing agents; one of high viscosity and the other one of low viscosity. Neither of the two consistencies were satisfactory. A satisfactory consistency was finally achieved by mixing the two epoxies in a ratio of 1 part by volume of the low viscosity one to four parts by volume of the highly viscous one.

The mixture of epoxies was then poured in the cup-shaped end of the loading caps in excess of the cup capacity. By running a straight knife or razor blade on the shoulders of the cup end, the surface of the epoxy was made flushed with that of the shoulder. Finally an extra amount of epoxy (about 0.2 cc) was poured into the center of the cup.

An amount of epoxy in excess of the cup capacity was found necessary to provide some overflow when the caps came in contact with the specimen's surface. Otherwise, some empty or unglued pockets were left within the testing area.

In several tests where unglued areas occured, the failure load measured was substantially lower than in identical tests where all the area under the loading cup was glued well. An attempt to correct the test results for the percentage of unglued area did not yield satisfactory results; in part due to the difficulty in

measuring the percent of the area that did not bond. Further, a brittle mode of failure characterized the tension tests performed in this investigation. Under these conditions, concentration of stresses around an unglued pocket can induce fast propagation of the failure surface along cracks or planes of weakness in the vicinity of this region and the failure load is substantially reduced. It is believed that this is the cause for the non proportionality between the reduction in load capacity and the amount of unglued area.

3.3.2.3 Assembling the Tension Test System

The following steps were taken to assemble the tension test system:

(a) Prepare three loading caps with epoxy as explained in Section 3.3.2.2.

(b) Screw the loading caps to the testing shafts.

(c) Insert the testing shafts through the guiding block, from the bottom, as shown in Fig. 3.9.

(d) Place the testing shaft locks "G" (Fig. 3.11) and lock the shaft in its upper most position.

(e) Place the guiding block over the specimen and mold but resting on two spacers, which keeps the guiding block above the sample and mold to permit visual inspection during the subsequent gluing operation. Locate the testing sites by passing the two long rods "F" (Fig. 3.11) through the bored holes in the guiding block and through the desired bored holes in the mold "D". (There are six bored holes in the mold "D" which are aligned in pairs on opposite sides of the mold shoulder to permit the location of the guiding block into three different positions). The rods are then screwed into the base plate.

(f) Release the testing shafts by removing the locks "G" (Fig. 3.11) and allow the loading cups to glue to the surface of the specimen under their own weight. Allow minimum of twelve hours for the epoxy to harden.

(g) Remove the spacers and allow the guiding block to slide down onto the mold and/or sample surface.*

3.3.2.4 Conducting the Tension Test

The following steps were taken to run the tension tests:

(a) Fasten the guiding block using the wing nuts "S" (Fig. 3.11).

(b) Place the extension arm "H" as shown in Fig. 3.10.

(c) Attach the displacement transducer "I" (Fig. 3.17) in its position and in contact with the extension arm "B" as shown.

(d) Align the center of the lower beam of the yoke over the center of the shaft to be pulled. For this operation, two horizontal adjustments are necessary: (i) sliding the sample supports and guiding block already assembled in the longitudinal direction; (ii) sliding of the pulley "B" (Fig. 3.15) along its shaft (in the transverse direction).

(e) Bring the yoke "C" (Fig. 3.17) down and pass

---

*As shown later it is recommended to have the block rest on the sample rather than on the mold.

the upper threaded end of the testing shaft through the hold in the lower beam of the yoke. Place the nut "M" and fasten.

(f) Center the yoke and the transducer-supporting cylinder "F" (Fig. 3.17) such that the head of the transducer is located at the center of the upper beam "K" of the yoke.

(g) Switch on the data acquisition system and select one-minute interval readings. (Keep transducers continuously excited even during periods of no testing.)

(h) Switch on the motor to begin the application of load.

(i) When the maximum load capacity is reached in any one test and a sudden failure occurs, turn the motor off immediately.

(j) Remove the yoke and extension arm from the testing shaft.

(k) Move the complete assembly to bring the next testing shaft under the center of the yoke as explained in (d) above.

(l) Repeat stages (b) through (h) until the three shaft sites are tested.

3.3.2.5 Data Collection from the Tension Test

A record of the output voltages from both the force transducer, the displacement transducer, and the excitation voltage, as well as time of day, is printed on a paper tape by the data acquisition system at the time interval selected (one minute). The voltage can be converted to load in kilograms or pounds and displacements in inches or centimeters, using the corresponding calibration charts for these devices. At the end of testing the three sites, the tension test system was dismantled and

the loading cups removed from the shafts.

Each loading cup was placed between the centering bars "B" of the optical micrometer shown in Fig. 3.18 to measure the diameter of the soil pulled out from the specimen surface (which remains glued to the loading cup, see Fig. 3.19). The centering bars "B" are held in a position such that a cylinder touching the sides of both bars has a diameter coinciding with the center of the cross hair lines of the telescope "C". A diameter is measured by turning the knob "F", which displaces the telescope horizontally until the center of the cross-hair lines is at the border of the soil area and a reading of the scale "H" is taken.

Then the knob is turned until the center of the cross-hair line is at the diametrically opposite extreme of the soil area, and another reading of the scale is taken. The length of the diameter is the difference of the two readings taken.

Then the cylinder is rotated approximately 90° and another diameter measured. The average of these two diameters is used to compute the average area of soil pulled from the specimen surface.

Finally, to remove the soil and epoxy from the cup of the loading caps, they are rapidly heated with a Bunsen burner. Upon heating, the epoxy separates completely from the cup and the loading caps can be re-used.

3.3.3 Wet-dry Cyclic Weathering

The selected wet-dry cycles of weathering following curing were:

(a) Submerge the specimen in tap water for a period of eight hours.

(b) Place the specimens in an oven at 70°C for a period of sixteen hours. A record of weight and measurements of the length and width of the specimen was made before and after both the wet and dry periods of every cycle.

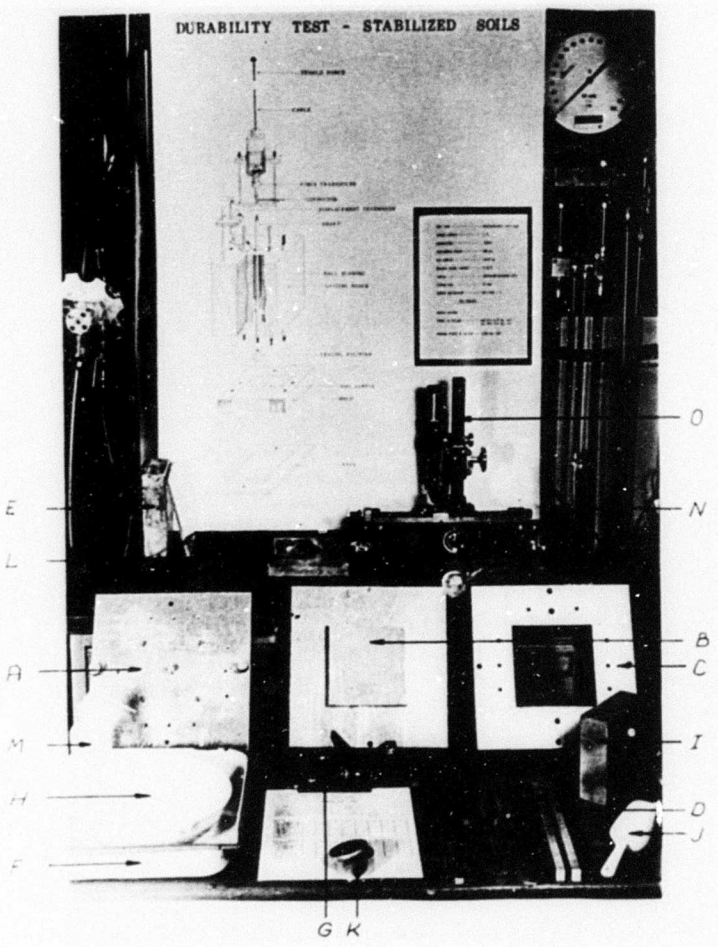

A Base plate
B Top plate
C Mold
D Spacer bars
E Sample
F Aluminum Pan
G Air bubble level
H Beaker
I Extruder block
J Scoop
K Water content can
L Screed plates
M Squeeze bottle
N Calibrated glass container (accuracy,1.0cc)
O Optical micrometer

Fig. 3.1 Components of Compaction Equipment

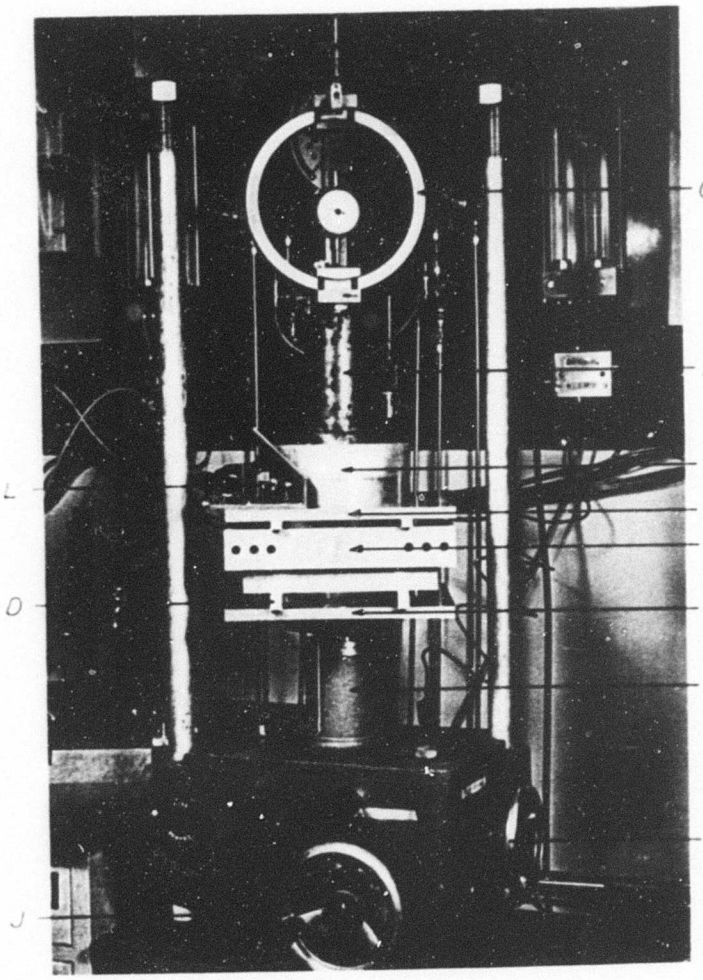

A Base plate
B Top plate
C Mold
D Spacer bar
E Block for alignment
F Piston for alignment
G Proving ring
H Pedestal of the compression machine
I Optical micrometer
J Wheel for slow manual control
K Wheel for fast manual control
L Air-bubble level

3.2 Compaction Equipment Assembled for Operation

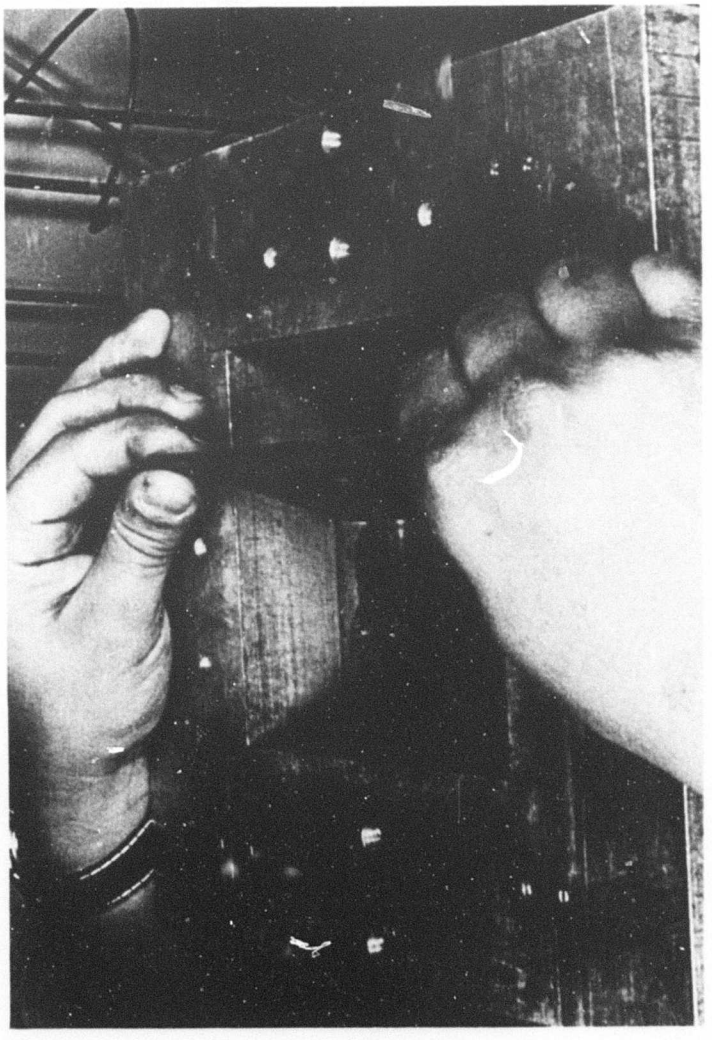

Fig. 3.3 Placement of Soil in the Mold

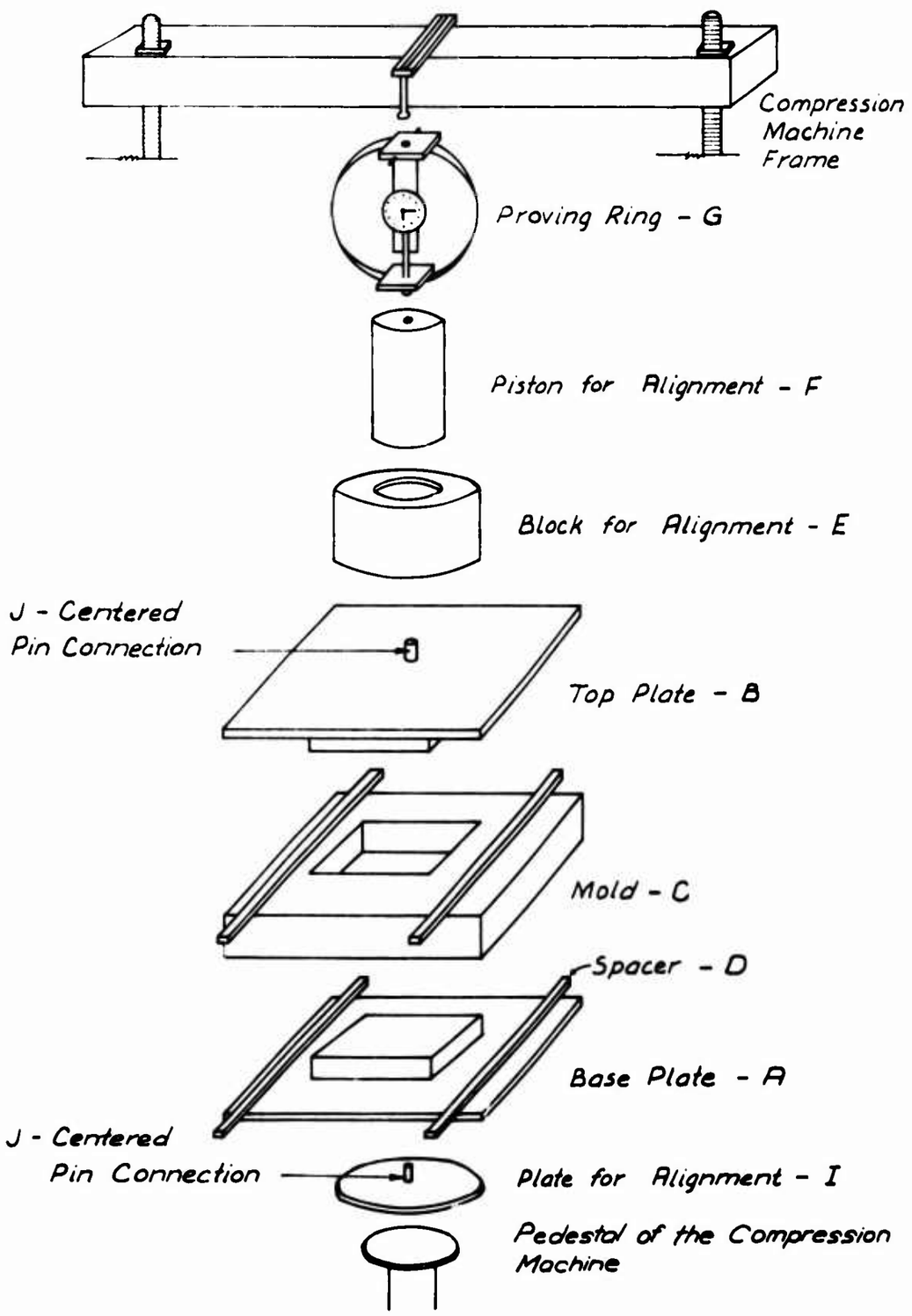

FIG. 3.4 ASSEMBLY FOR COMPACTION

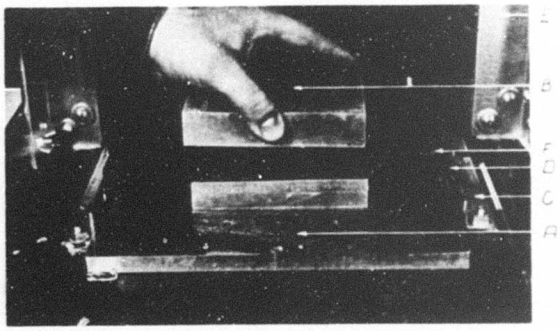

A Base Plate
B Spacer block
C Guiding Angle
D Base clamps
E Frame

FIG. 3.5 STAGE I

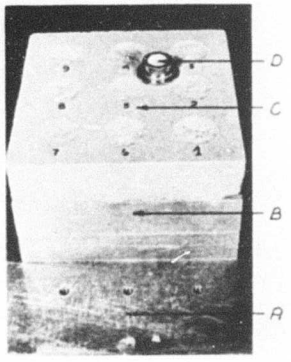

A Base Plate
B Spacer block
C Sample
D Air bubble level

FIG 3.6 STAGE II

Assembling for Tension Test*

*An already tested sample is shown in the sequence of assembling for testing because it was the only one available at the time the photographs were taken.

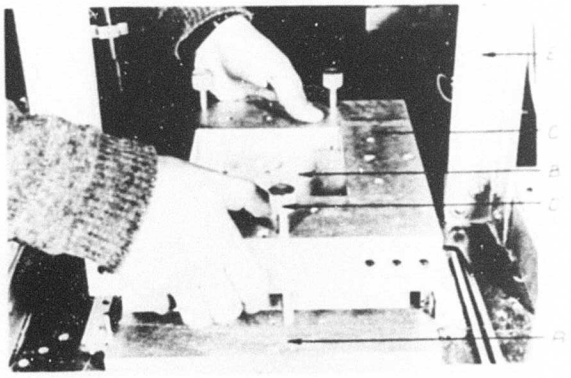

FIG 3.7 STAGE III

A Base plate
B Sample
C Mold
D Leveling Screws
E Frame

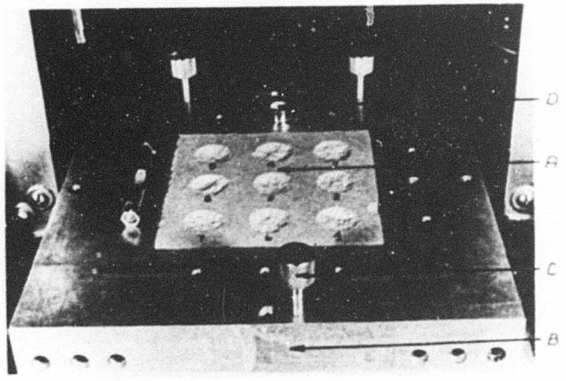

FIG. 3.8 STAGE IV

A Sample
B Mold
C Leveling Screws
D Air bubble level

Assembling for Tension Test*

*See Footnote in page 27

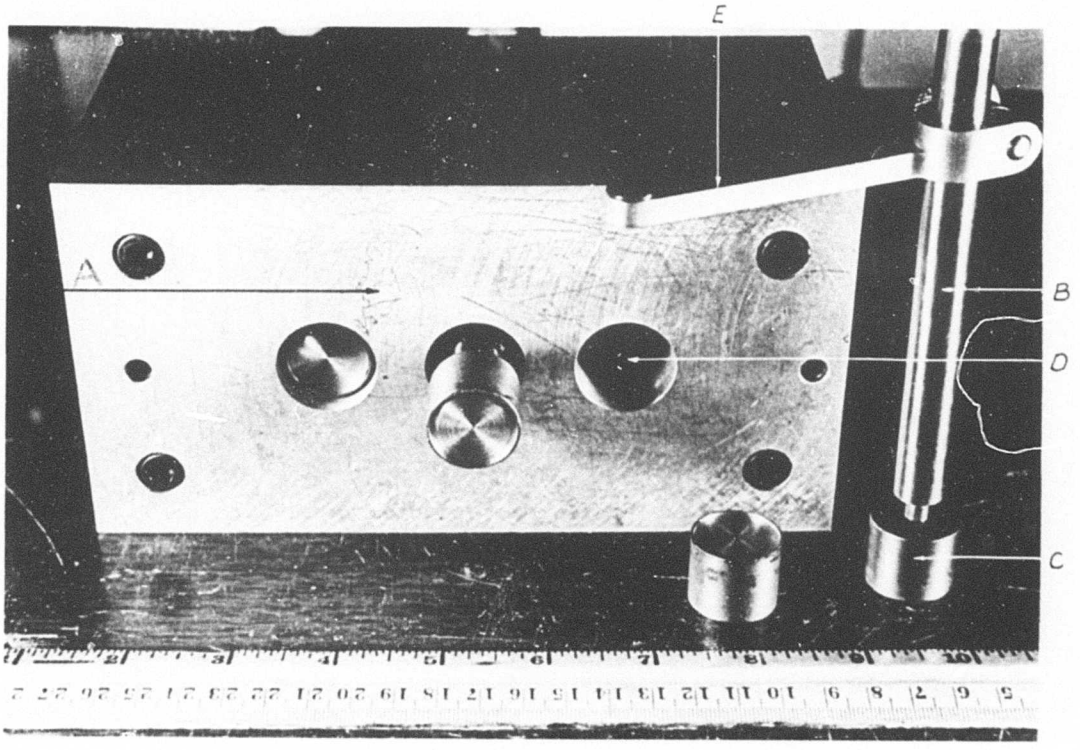

A - Guiding block

B - Testing shaft

C - Loading cap

D - O-ring

E - Extension arm

Fig. 3.9 Guiding Block and Additaments

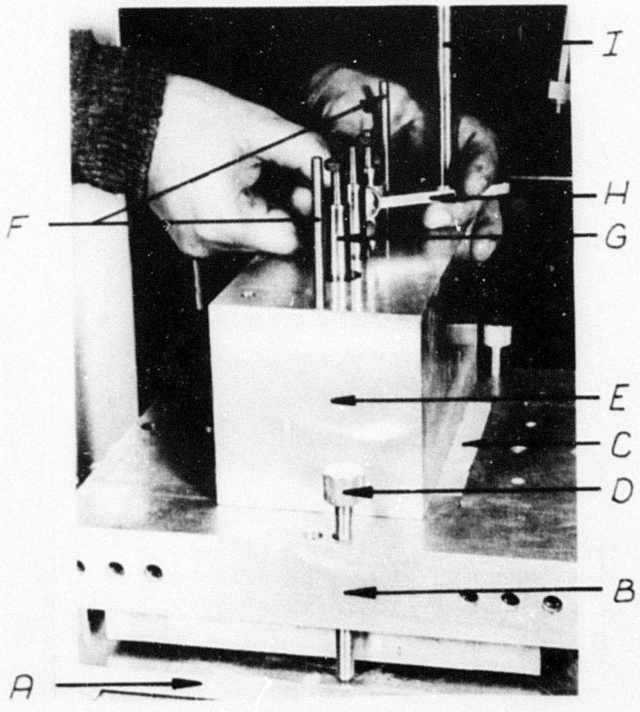

A - Base Plate

B - Mold

C - Sample

D - Leveling screw

E - Guiding block

F - Threaded rod

G - Testing shaft

H - Extension arm

I - Rod for mounting the Displacement Transducer (DCDT)

Fig. 3.10 Assembling for Tension Test - Stage V

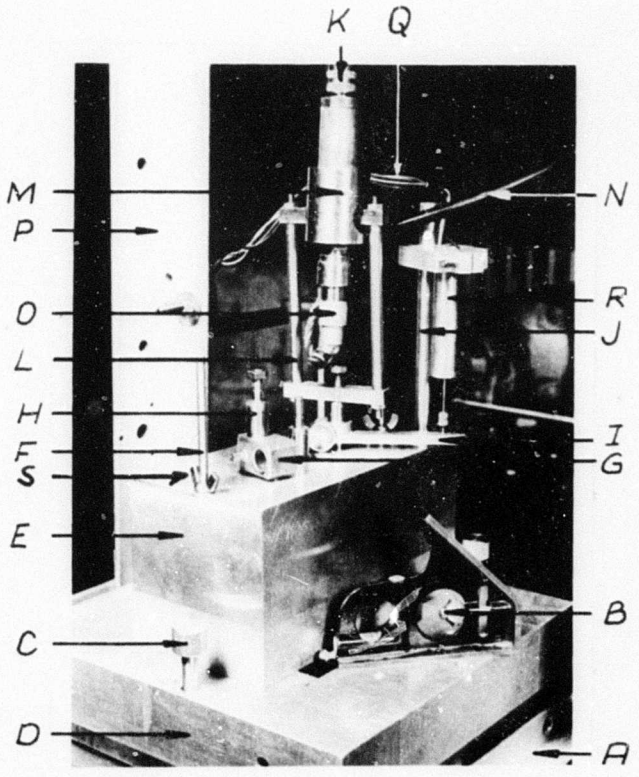

A - Guiding Angle
B - Air bubble level
C - Leveling screw
D - Mold
E - Guiding block
F - Threaded rod
G - Shaft locks
H - Testing shaft
I - Extension arm
J - Rod for mounting the DCDT
K - Clamping nut
L - Yoke
M - Force Transducer support cylinder
N - Force Transducer conductor cable
O - Force Transducer
P - Frame
Q - DCDT conductor cable
R - Displacement Transducer (DCDT)
S - Wing nut

Fig. 3.11 Assembling for Tension Test - Stage VI

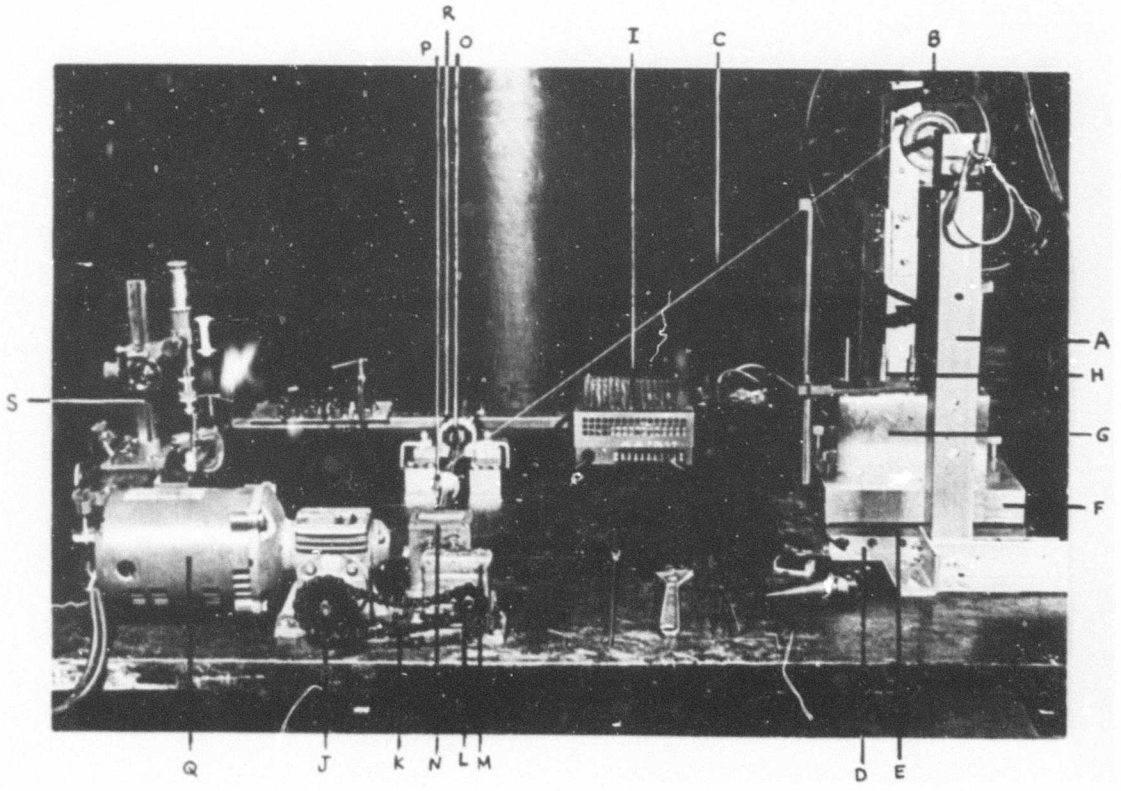

A - Frame
B - Pulley
C - Cable
D - Guiding angle
E - Base clamp
F - Mold
G - Guiding block
H - Testing shaft
I - Electrical power supply
J - Steel sprocket
K - Chain
L - Steel Sprocket
M - Gear box (ratio 1 to 900)
N - Gear box (ratio 1 to 100)
O - Drive shaft
P - Pulley
Q - Electric motor
R - Ball bearing
S - Optical micrometer

Fig. 3.12 Tensile Force Application System

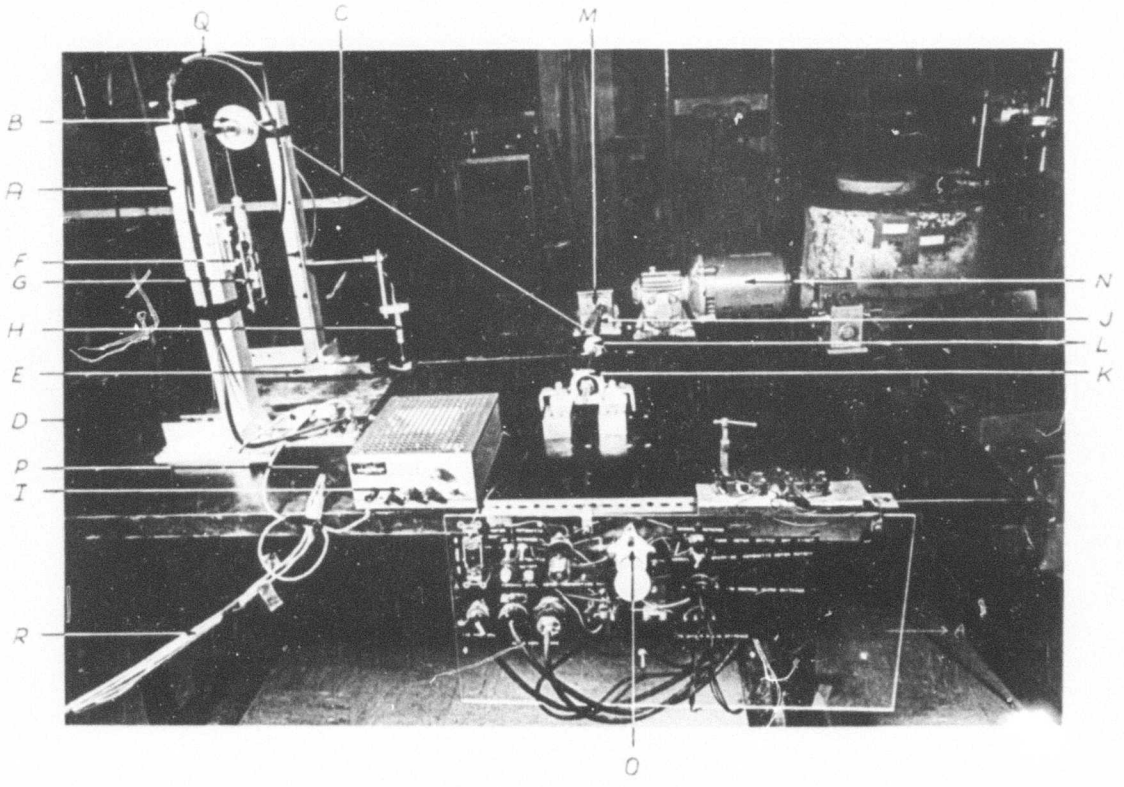

A - Frame
B - Pulley
C - Cable
D - Guiding Angle
E - Base clamp
F - Yoke
G - Force transducer
H - Displacement transducer (DCDT)
I - Electrical power supply
J - Drive shaft
K - Ball bearing
L - Pulley
M - Gear box (ratio 1 to 100)
N - Electric motor
O - Electric motor controll panel
P - Terminal box for transducer conductor cables
Q - Force transducer and DCDT conductor cables
R - Conductor cables to data aquisition system

Fig. 3.13 Tensile Force Application System

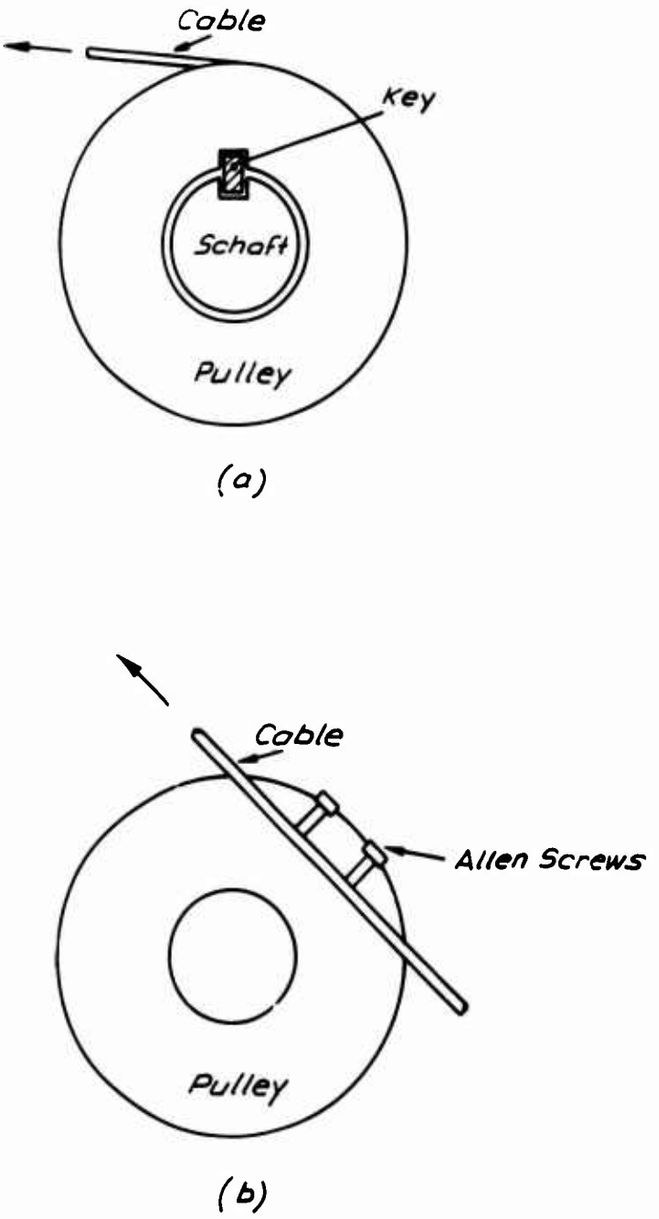

FIG. 3.14 DRIVE SHAFT AND PULLEY

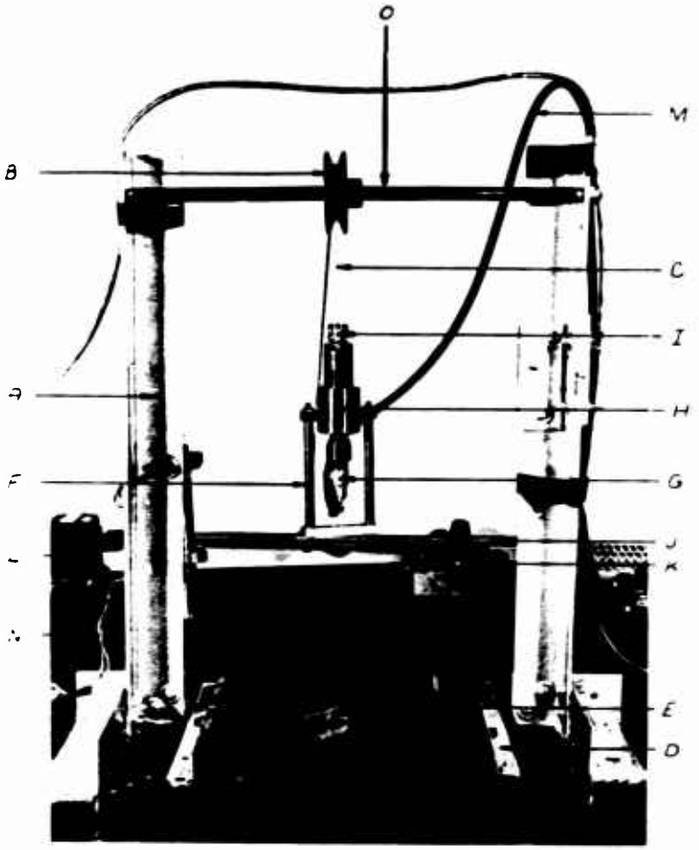

A - Frame

B - Pulley

C - Cable

D - Guiding angle

E - Base clamp

F - Yoke

G - Force transducer

H - Force transducer support cylinder

I - Clamping nut

J - Drive shaft

K - Ball bearing

L - Gear box (ratio 1 to 100)

M - Force transducer conductor cable

N - Displacement transducer conductor cable

Fig. 3.15 Tension Force Application System

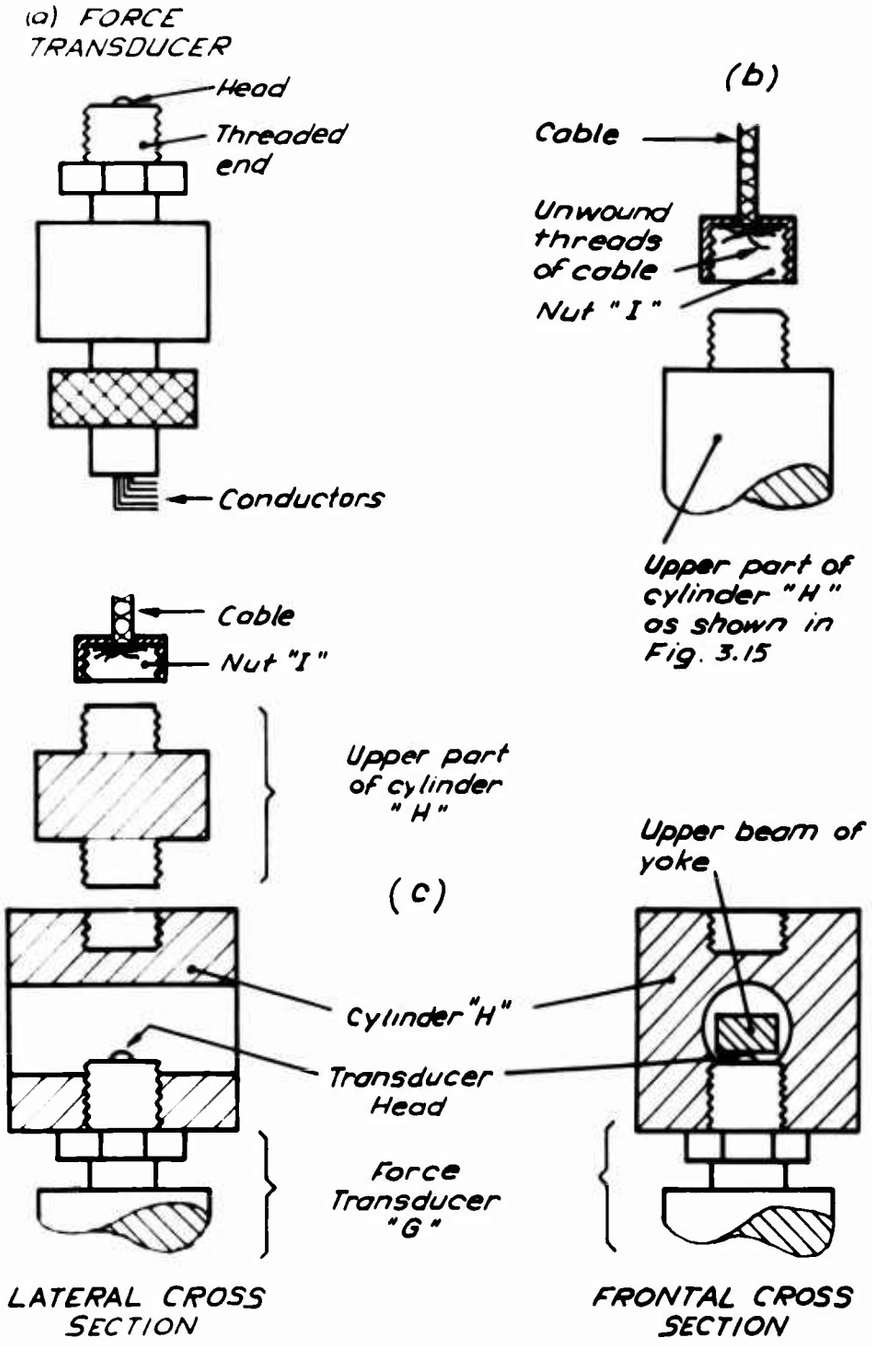

FIG. 3.16 FORCE APPLICATION SYSTEM
(accessory parts)

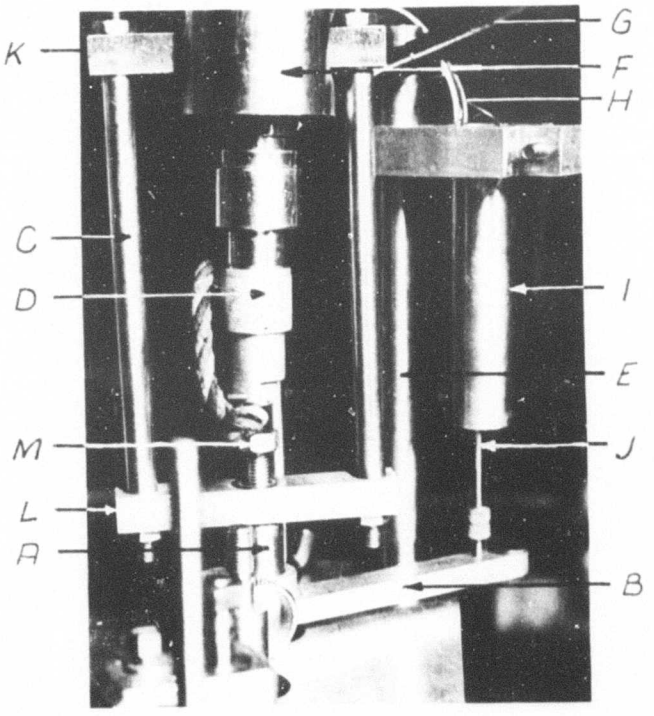

A - Testing shaft
B - Extension arm
C - Yoke
D - Force transducer
E - Rod for mounting DCDT
F - Force transducer support cylinder
G - Force transducer conductor cable
H - Displacement transducer (DCDT)conductor cable
I - Displacement transducer (DCDT)
J - DCDT core
K - Upper beam of Yoke
L - Lower beam of Yoke
M - Testing shaft clamping nut

Fig. 3.17 Assembling for Tension Test

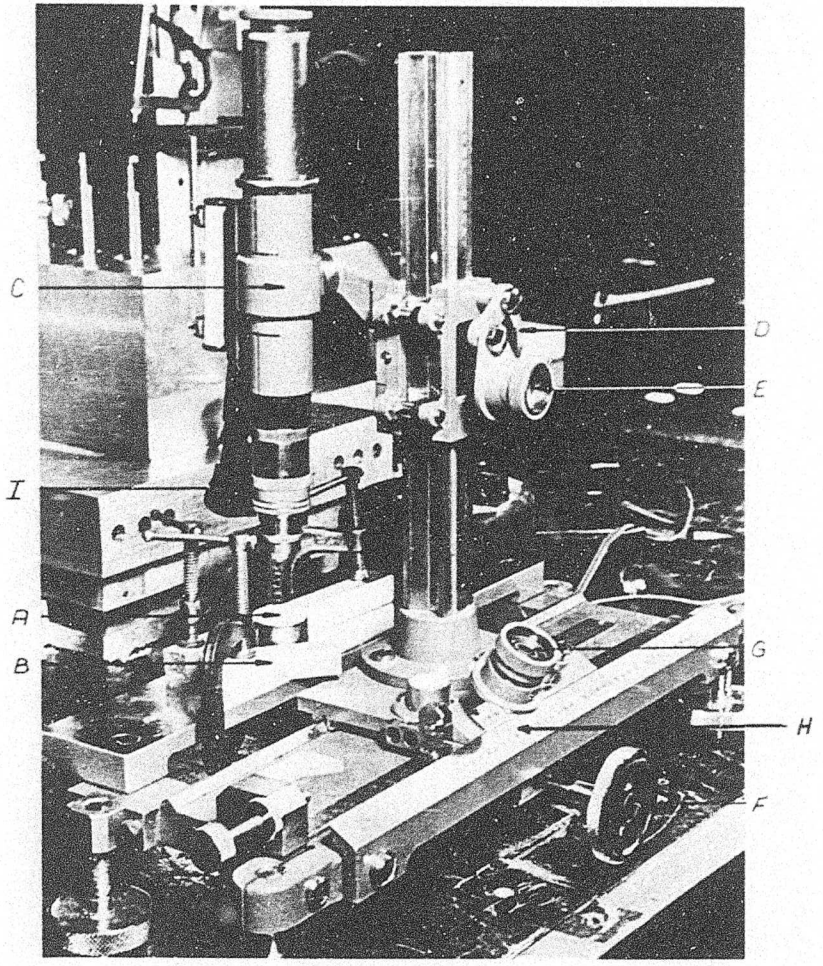

A - Loading cap after test

B - Centering bars

C - Telescope

D - Vertical displacement knob

E - Magnifying glass

F - Horizontal displacement knob

G - Magnifying glass

H - Scale

I - Light source

Fig. 3.18 Optical Micrometer

Fig. 3.19 Loading Caps Before and After Testing

Chapter 4
EVALUATION OF TESTING EQUIPMENT AND PROCEDURES - DISCUSSION OF RESULTS

4.1. MIXING, COMPACTING, AND CURING

4.1.1 Mixing

The standard hand-mixing procedure as described in Section 3.5.1.1 is considered satisfactory in all respects to ensure a uniform distribution of the cement in the mix.

4.1.2 Compacting

Difficulty was experienced during the compaction operation due to tilting of the plunging pieces, especially in the specimen compacted to a high density. This leads to nonuniform densities at different points on the surfaces, which could result in significant variations of the tensile strength measurement.

4.1.3 Curing

The samples did not loose moisture or change in dimensions during curing which indicates that the method used of sealed curing is satisfactory.

4.2 GLUING OPERATION

The simple method of preparing and placing the epoxy in the cup of the loading cap as described in Section 3.3.2.2 is considered to be satisfactory. However, based on the experience obtained with the 54 tests run in this investigation, the following procedure is recommended for lowering the loading caps and allowing the epoxy to bond to the surface of the specimen.

(a) Place two spacers between the mold surface and the bottom of the guiding block to permit visual inspection during gluing.

(d) Release the testing shafts. The epoxy in the cup comes in contact with the specimen's surface and begins to spread under the weight of the shaft and loading cap.

(c) When a small outflow of epoxy is observed around the loading cap, the shafts are again locked. This prevents further application of load to the epoxy layer and therefore the outflow stops.

(d) Remove the spacers; bring the guiding block to rest on the surface of the sample. Lower the testing shaft locks to the new level of the surface of the guiding block, and tighten them to prevent any further squeezing of epoxy from the cups.

The epoxy then hardens with the surface of the specimen in contact with the bottom of the guiding block, which ensures that the center line of the testing shaft is normal to the specimen surface.

4.3 TENSION LOAD APPLICATION

4.3.1 Rate of Loading

As explained in Section 3.1.3.3, the cable used to transmit the tensile force winds around the pulley "L" (Fig. 3.13) at a speed of 0.2928 inches/hour, or 0.00488 inches/minute. The average rate of loading was about 0.3 kg/min.

The data acquisition system was set to take readings at one-minute intervals; therefore, because the failure is sudden, any one of the test runs could have a failure load underestimated by a maximum of 0.3 kg.

This represents a maximum error of about 2% for the tests with the lowest tensile capacity (considering only the good tests) or about 0.5% for the tests with high tensile capacity. This error, while not significant in this investigation (compared to other errors discussed later), can be substantially reduced by recording the transducer outputs on X-Y analog plotter, thus permitting the tests to be conducted at a faster rate.

4.3.2 Force Application

During several tests, it was observed that a small vertical misalignment between the transducer and the yoke (see Fig. 4.1a) had occurred. To investigate the influence of this misalignment, a tilt was intentionally introduced when the transducer read 32.9 kg. This resulted in a change of 2 kg, or about 6%, in the measured force. If this error was solely due to tilting of the transducer as shown in Fig. 4.1a, it would represent a tilt of 10° from the vertical. However, the tilting also introduces a displacement of the loading cup, which also will result in a change in force on the specimen since this is a strain-controlled test.

The effect of misalignment can be computed from the force diagrams shown in Fig. 4.1c. The angles of inclination shown in the sketches of Fig. 4.1 are exaggerated for the purpose of illustrating the discussion.

First assume that the shaft cannot tilt. If the tensile force T in the cable is at an angle α and the transducer remains vertical at its contact point with the upper beam of the yoke, the transducer measures the vertical force $S_n = T \cos \alpha$ (Fig. 4.1c). At the upper part of the shaft, there is a vertical force $P_n = T \cos \alpha$ and at the loading cap $R_n = P_n - P_t f$, where the force

$P_t f^*$ is the frictional force developed between shaft and bushings. This case is an over simplification since some friction exists between the transducer head and the yoke beam causing some tilting of the transducer.

Still assuming that the shaft cannot tilt, if the transducer rotates by an angle B< α, the force measured by the transducer is now $Q_n = T \cos(\alpha - B)$. The vertical force at the top of the shaft is still P_n and the force transmitted to the testing cylinder is still $P_n - P_t f.^*$ The friction force $P_t f^*$ is the same as in Case A, but now the force P_n, which is still equal to T cos α, is smaller than the force measured by the transducer, Q_n. Therefore one would measure a higher force than the force really applied to the glued area. For B = 3° and $\alpha = 5^\circ$ (the maximum angles that probably could occur without being visually noticed), the measured load would be 1.003 times the load applied to the cap. Excluding piston friction, this is insignificant.

Now, suppose the testing shaft has some lateral play so that it can also tilt slightly with respect to the vertical; this will reduce the difference between the measured and applied force. However, tilting of the testing shaft produces a situation of nonuniform distribution of the tensile stresses on the glued area (see Fig. 4.1d). This situation can lead to a substantial decrease in the measured tensile strength at the surface since the soil is brittle in tension and therefore local failure in the zone of the highest tensile

---

*The friction force $P_t f$ is very small for the lateral loading conditions of this testing system.

stress will cause premature crack propagation over the entire test site.

In the prototype guiding block used for this investigation, there was some play between the ball bushings that guide the shafts and their housings. Therefore the last situation presented above is close to the actual one that occurred during this testing program. This situation can be avoided by specifying closer machining for the housings. The sources of tilt or deviation from the vertical alignment between the testing shafts and the transducer supporting cylinder were:

(a) Deformation of the shaft containing the pulley "B" under load as shown in Fig. 4.1e.

(b) Distortion of the frame "A" (Fig. 3.13) while applying the load.

(c) Initial misalignment of the transducer with respect to the testing shaft because it was done visually.

Other problems encountered with the force application system were:

(a) The shaft "J" (Fig. 3.13) bent substantially during the tests.

(b) The cable stored considerable strain energy, which upon failure of the sample was released. The amount of deformation stored in the cable was larger than the remaining travel distance of the loading caps inside the guiding block (see Fig. 3.9); therefore, the cylinders came to a sudden stop against the inside shoulder of the guiding block, resulting in an impact

force being applied to the transducer which on several occasions produced a shift in the zero reading of the force transducer. Rubber o-rings were therefore placed on the shoulders where the loading caps come to a stop, to dampen the impact. This reduced the frequency of zero shifts occurring to the force transducer. However, even infrequent zero shift of the transducer is undesirable.

From this discussion it is concluded that vertical alignment of the transducer is not important. However, two corrective measures are needed to improve the performance of the loading mechanism. First, machining of a new guiding block, with press-fit installation of the ball bearing bushings in their housings. Secondly, change the load application system to that presented in Chapter 5, in which loading via a cable has been replaced by a relatively rigid system that will not store significant strain energy for the loading conditions expected. The revised system also reduces aligning problems.

4.3.3 Displacement Measurements

Vertical deformations during loading were obtained with a direct current displacement transducer (DCDT) mounted as shown in Fig. 4.2. The total deflection to failure was in the order of 0.001 inches, and for this order of magnitude, the DCDT was not sufficiently sensitive. Further, minor movements of the guiding block to which the DCDT was attached, and play in the testing shafts resulted in erratic load-deformation data, which was primarily due to the erratic displacement measurements.

For this reason no useful information was obtained from the deformation data.

4.4 DISCUSSION OF TENSION TEST RESULTS

Three specimens were prepared for running tension tests. Fig. 4.3 shows a slab (specimen) before and after testing. The slabs were labelled I, II, and III. Slab I was compacted to a density of 115.1 pcf at molding water content of 15.0%. It was cured at room temperature (cold cure) for a period of 58 days. Slab II was compacted to a dry density of 114.03 pcf with molding water content of 13.1% and was cured at 70°C (hot cure) for a period of 60 days. Specimen III was compacted to a dry density of 120.3 pcf at a molding water content of 14.1% and was cured at 70° (hot cure) for a period of 74 days. These data are presented in Table 4.1. Accidently, for Specimen III, the temperature in the curing bath went up to 90°C for a period of one day. All the specimens were sealed during curing time.

Specimens I and II were tested continuously without subjecting them to cyclic weathering (Tables 4.2 and 4.3). The objective was to study the reproducibility of the strength measured using different testing techniques, i.e. gluing of the loading caps to the specimen surface and application of the tensile force.

Specimen III was tested after 0, 1, 2, 4, 8, and 12 cycles of wet-dry (Table 4.4).

4.4.1 Confined Versus Unconfined Tests

Tests 10, 11, 12, 13, 14, and 15 were performed with the guiding block completely separated from the specimen's surface. This was achieved by placing two spacers between the top surface of the specimen and the bottom surface of the guiding block. The areas pulled out in these tests had a very irregular shape and no reasonable estimate of the failure area could be made (Figs. 4.5 and 4.6f through 4.6j). This situation will be referred to as unconfined testing and is shown schematically in Fig. 4.6f.

In the second situation, the guiding block rested on the surface of the slab during testing, resulting in confining the area surrounding the loading cap. In this case the failure area was circular and well defined. (see Figs. 4.6a through 4.6e). This procedure was used with tests 37 through 54. It is referred to as confined testing and is shown in Fig. 4.6a.

In the confined case, the application of the tensile force "T" through the loading cap produces a tensile stress "f_t" acting on the glued area and compressive stress "f_c" is developed as a reaction on the contact area between the guiding block and the specimen's surface around the testing area as shown schematically in Figs. 4.6b and c.

In the unconfined case, the spacer bars were placed far away from the testing area; therefore, no compressive stresses occurred around the testing area, which was in tension (see Fig. 4.6g).

In the confined tests, a very regular failure surface was produced versus a very irregular one for

the unconfined test, as sketched in Figs. 4.6e and 4.6j. In the unconfined tests, while cracks probably start propagating from beneath the loading cap where the tensile stresses are greatest, they could extend into the unconfined zone beyond the loaded area resulting in a poorly defined failure area.

In the confined tests, the main effect of the compressive stresses around the test area is to restrict crack propagation beyond the loading cap zone, since in brittle materials compressive stresses tend to prevent crack propagation. On the other hand, the compressive stress field in the ring area surrounding the loading cap extends under the area that is subjected to the tensile state of stress during testing. The actual distribution of the compressive stresses acting around the loading cap is unknown for two reasons:

(a) Due to the configuration of the guiding block surface (the effect of the two unstressed areas where the other two loading caps are located, Fig. 3.9), one does not really know how the compressive stresses are distributed around and away from the tensile area, although one may reasonably assume that they will have higher values at the border around the testing area.

(b) There is an initial compressive stress acting on the sample produced by the weight of the block plus the tightness with which the guiding block is fastened.

For these reasons, it has not been possible to make a precise quantitative analysis of the effects of confinement; nevertheless, it is possible to obtain an approximate solution based on some simplifying assumptions to facilitate the evaluation of the effects of confinement.

The weight of the guiding block plus the force produced by the tightening of the guiding block fastening screws is assumed to be about 10 kg. This force divided by the contact area between the soil specimen and the guiding block gives a compressive stress of 0.011 kg/cm^2. Of the tests run, the smallest average tensile stress measured at failure was in the order of 4 kg/cm^2. Therefore, the effect that the initial compressive stress field has on the tensile stress field under the loading cap during testing is small and can be neglected. The most important compressive stresses are developed around the testing area as a reaction to the applied tensile stresses. To investigate the effects of these stresses, two assumptions will be made to simplify the problem. First, it will be assumed that the reaction to the tensile stresses acting under the loading cap is concentrated in a ring area of width equal to the radius of the area in tension (0.5 in.) and second, that these stresses are uniformly distributed over the annular area.

If only compressive stresses were acting on a ring area, as shown in Fig. 4.7a, the distribution of stresses under the surface at a depth of 0.25 in. (corresponding to a depth just below the average failure surface) can be obtained by applying superposition of the stresses under the loading in the situations shown in Fig. 4.7b and c. It was assumed that the material is homogeneous,

isotropic, and lineraly elastic. Use was made of the solution from theory of elasticity for the vertical stresses induced by a uniform load on a circular area. In this way, the distribution presented in Fig. 4.7d was obtained, for the vertical stresses induced by a uniform load on a ring area (see Table 4.5).

In a similar manner, the stress distribution under a uniform tensile force per unit area, as shown in Fig. 4.8, was obtained. Having assumed that the reaction to the tensile force applied to the loading cap during testing is uniformly distributed on a ring area of thickness 0.5 in., the force per unit area on the ring area (compressive) is one third of the force per unit area under the loading cap (see Fig. 4.9). Therefore, during testing, the loading condition under the test site and its surrounding zone is as shown in Fig. 4.10a where the compressive force per unit area on the ring area is one third of the tensile force per unit area under the loading cap. The stress distribution shown in Fig. 4.10b was obtained by superposing the ordinates of the diagrams shown in Fig. 4.8b and one third of the ordinates of Fig. 4.7d.

The distribution of vertical stresses shown in Figs. 4.8b and 4.10b therefore correspond to unconfined and confined testing, respectively. It can be seen that under the testing area, the effect of confinement is small even for the depth for which these plots were obtained ($\Delta\sigma_v/\Delta_{qt}$ under the center line of 0.87 for the confined cases versus 0.90 for the unconfined case).

At shallower depths, the effect of confinement on the stress field under the tensile zone will be even smaller.

From the above analysis, the following qualitative conclusions are drawn:

(a) In the confined case failure occurs also by tension.

(b) For depths within the range at which the failure surface develops, as measured in the experiments, the maximum tensile stress under the testing area is only slightly reduced due to the surrounding compressive stresses in the confined tests.

(c) The effect of confinement produces a less jagged and a more repeatable failure area, making it possible to get a good estimate of the average failure tensile stress.

The material tested in this investigation exhibits brittle behavior under tensile stresses. Inperfections and minor cracks existing prior to testing will play an important role in the shape of the failure surface that develops and will reduce the magnitude of the strength measured. Essentially, failure will develop by propagation of cracks. These cracks can be either preexisting or induced. Preexisting cracks are produced during compaction and curing. Induced cracks are produced during weathering cycles, which cause differential shrinkage and/or expansion of the soil mass. Therefore, for a given mix and curing conditions (i.e. a given pattern of preexisting cracks) and for given weathering conditions (induced cracks), the crack pattern prior to testing will be the same in both confined and unconfined testing since the confinement prior to testing has been

shown to be small. In the confined tests during the propagation of a crack, it may come under the zone where the compressive stress field acts. This imposes a restriction to the continuous propagation of the crack, and it will stop propagating or change direction. In either case, more energy will have to be supplied to the system before this crack can continue to propagate, which means raising the tensile stress required to achieve failure. For this reason, one would expect to measure higher failure loads in confined tests than in unconfined tests.

The experimental results from Specimen I (Table 4.2) showed the following:

(a) Tests 10 through 15 of this slab were run unconfined because excessive spreading of the epoxy interfered with movement of the loading cap into the guiding block. In these tests the average diameter of the glued area was about 1.05 inches, which is larger than the average diameter of the remaining tests on this slab (0.93 inches). Further, the actual failure area of the unconfined tests was larger than the glued area due to spreading of the cracks and was estimated to be 1.1 inches. The average tensile force at failure of the unconfined tests was 24.96 kg, which with an estimated average failure area of 6.13 cm^2 (1.1 inches diameter) gives a failure stress of 4.1 kg/cm^2. Similarly, the confined

tests failed at an average load of 20.56 kg,* which with an average failure area of 4.35 cm^2 gives a failure stress of 4.73 kg/cm^2. It is seen from the above test results that the average tensile stress at failure for the confined tests was about 12% higher than for the unconfined tests. This is due to the effect of confinement in restricting crack propagation.

(b) The standard deviation of the failure load in the unconfined tests was 6.07 versus 2.52 for the confined tests. Therefore confinement reduces considerably the scatter in the measured failure load (see Table 4.6).

(c) Confinement always resulted in a very regular circular failure area which could be easily measured versus the jagged area produced in the unconfined tests.

4.4.2 Effect of Poor Bonding (See Fig. 4.4)

In some of the tests (see Tables 4.2, 4.3, and 4.4), a part of the area under the loading cap did not bond to the specimen surface, due to lack of sufficient epoxy in the cup of the loading cap. This resulted in a lowering of the measured tensile force at failure. In these cases an estimate of the percentage of the total area that was not bonded was made in order to obtain the effective area subjected to the tensile loading. The average tensile stress at failure, based on the estimated effective area (P/A), was significantly lower than the average stress at failure for the tests where

---

*This average excludes test results in which the loading caps were poorly bonded to the specimen surface.

good bonding occurred. The reason for the nonproportionality between the reduction in failure load and the reduction in effective area was discussed in Section 3.3.2.2.

The percent decrease in the computed failure stress for the tests having incomplete surface bonding compared to those with complete bonding was between 15% and 33% for Slab I, 30% to 55% for Slab II, and 10% to 20% for Slab III.

Differences of these magnitudes cannot be tolerated and therefore results of tests where incomplete bonding occurs must be discarded.

The frequency with which incomplete bonding occurred during the testing of the three specimens used in this investigation was 31% (17 tests out of a total of 54 tests run), which is relatively high. This was the result of using various gluing techniques, many of which proved unsatisfactory. With the procedure ultimately recommended in Section 4.2, the occurrence of an unglued area under the loading caps is eliminated.

4.4.3 Eccentricity of Loading

During the testing of Slab II, some significant eccentricity in applying the tensile force to the loaded area resulted from the procedure used in this series of tests.

As shown in Fig. 4.11, the guiding block rested on the shoulders of the mold that provides lateral support to the sample and not on the surface of the specimen. When the tensile force "T" was applied, the specimen was lifted up until it came in contact with the bottom of the guiding block and from then on, the test resembled the situation described as a confined test in Section 4.4.1.

Under this condition, the specimen has a tendency to tilt, and friction can be developed between the sides of the sample and the mold in the locations shown circled

"A" and "B" in Fig. 4.11. This causes the force "T" to be eccentrically applied with respect to the bonded area. This eccentricity resulted in a standard deviation of the tensile stress at failure for Slab II of $\pm$ 1.01 kg/cm^2 compared to $\pm$ 0.38 kg/cm^2 and $\pm$ 0.34 kg/cm^2 for Slabs I and III, respectively, which were run with the guiding block resting on the specimen from the beginning of the tests.

These results indicate that the maximum tensile strength is very sensitive to eccentric loading conditions. Therefore it is recommended that the slabs remain confined immediately after gluding, i.e., with the guiding block resting directly on the specimen surface.

4.4.4 Effect of Molding Conditions

Slabs II and III had different molding conditions (a dry density of 114.0 pcf and a molding water content of 13.1% for Slab II, versus a dry density of 120.3 pcf and molding water content of 14.1% for Slab III), but were subjected to the same curing method and curing time prior to initial testing (see Table 4.1).

Comparing the average maximum tensile strength computed for tests 37 and 39 (Table 4.4) on Slab III (P/A avg = 14.3 kg/cm^2), which were run after curing but prior to cyclic weathering, with the average maximum tensile strength for Slab II (P/A avg = 6.34 kg/cm^2), it can be seen that an increase in molding dry density of 5.5% produced a large increase in the tensile strength. This trend agrees with triaxial test results, obtained with similar soil-cement systems, which showed a large increase in effective cohesions intercept of the Mohr-Coulomb envelope, with increasing as-molded dry density (Wissa and Feferbaum, 1969).

From the triaxial test results given in the above report, it was also shown that the effective cohesion intercept of M-21 soil plus 5% portland cement is very sensitive to molding dry density; therefore, small variations in the as-molded dry density of the surface of a slab will result in relatively large variations in the measured tensile strength.

Some tilting of the plunging pieces while applying the static compaction effort and nonuniform distribution of the amount of soil-cement mix in the mold prior to compaction could not be eliminated in this investigation and therefore resulted in some variation in the as-molded dry density of the slabs. This variation is probably responsible for part of the scatter obtained in the maximum tensile strengths measured. The recommendation in Chapter 6 to change the shape of the compaction mold from square to circular, to use impact rather than static compaction, and to use only the bottom surface of the compacted specimens for tensile testing should minimize surface density variations.

4.4.5 Effect of Curing Method

The average tensile strength of Slabs I and II show the effect of curing method. Slab I was cold cured and Slab II was hot cured, while they were similar in all other respects (mixing, molding conditions, and curing time).

The results presented in Table 4.6 show that the hot-cured specimen had a higher maximum tensile strength (P/A avg. = 6.34 kg/cm^2) than the cold-cured specimen (P/A avg. = 4.73 kg/cm^2). This trend agrees with the observation made by Clare and Pollard (1954), who showed that increasing the curing temperature increases the

unconfined compressive strength of cement stabilized soils.

4.4.6 Effect of Weathering

Tensile Tests were run on Slab III after 0, 1, 2, 4, 8, and 12 cycles of wet-dry as shown in Table 4.4.

During the first two cycles of weathering, there was approximately 15% loss in tensile strength; however, with further cycling, essentially no further loss of tensile strength occurred (see Fig. 4.12). These results indicate that this soil-cement system, and for the hot-curing condition, losses some strength during the first cycles of wetting and drying, but subsequent cycling does not cause any further deterioration. Therefore, this system should be expected to withstand field wetting and drying as well. On the other hand, if the system had shown continuous loss in tensile strength with increasing number of cycles of weathering, the mix would probably deteriorate under field weathering conditions.

A record of changes in length of the specimen (Tables 4.7 and 4.8) as well as changes in water absorption during each cycle (see Fig. 4.13), indicates that the change in volume of the specimen was less than 2% during cyclic weathering and that the amount of water absorbed was less than the amount of water necessary to fill all the voids of the sample in the as-molded conditions. These results, together with the tensile strength data, support the conclusion that a soil-cement mix with the characteristics of Specimen III can resist the effect of cyclic wetting and drying in the field.

TABLE 4.1 COMPACTING AND CURING DATA

Specimen	Wet density (pcf)	Water content (%)	Dry density (pcf)	Curing Method	Time of curing (days)
I	132.4	15.0	115.1	cold	58
II	129.0	13.1	114.0	hot	60
III	137.3	14.1	120.3	hot	74

TABLE 4.2 TEST DATA FOR SPECIMEN I

WEATHERING No. OR CYCLES	Test No	V_o (mv.)	V_i (VOLTS)	P (kg)	DIAMETER COMPARATOR READING (IN)	DIAMETER (IN)	DIAMETER COMPARATOR READ. V_o (IN)	DIAMETER (IN)	AVERAGE DIAMETER (IN)	AVERAGE AREA (cm^2)	P/A (kg/cm^2)	COMMENTS
0	1	4.43	6.2001	21.25	3.345 2.398	.947	3.342 2.399	.943	.945	4.525	4.70	
	2	3.55	6.2006	17.58	3.311 2.400	.911	3.314 2.404	.910	.910	4.196	4.19	
	3	3.43	6.2011	17.09	3.307 2.409	.898	3.308 2.405	.903	.900	4.102	4.17	
0	4	5.15	6.2000	24.18	3.344 2.394	.950	3.346 2.392	.954	.952	4.573	5.29	
	5	4.26	6.2001	20.51	3.340 2.415	.925	3.346 2.411	.935	.930	4.383	4.68	
	6	2.37	6.2001	12.72	3.315 2.426	.889	3.305 2.413	.892	.890	4.014	3.17	Imperfect bonding
0	7	3.41	6.2000	17.00	3.341 2.411	.930	3.341 2.410	.931	.930	4.383	3.88	Imperfect bonding
	8	2.77	6.1999	14.36								Imperfect bonding
	9	0.46	6.2001	4.85								Imperfect bonding
0	10	6.20	6.2001	28.50								Run unconfined
	11	7.01	6.1995	31.84								Run unconfined
	12	3.56	6.1992	17.62								Run unconfined
0	13	6.76	6.2003	30.81								Run unconfined
	14	5.25	6.2002	24.59								Run unconfined
	15	3.26	6.1999	16.39								Run unconfined
0	16	4.83	6.2002	22.86	3.351 2.411	.940	3.351 2.410	.941	.940	4.477	5.11	
	17	4.24	6.2005	20.43	3.307 2.411	.896	3.310 2.403	.907	.901	4.110	4.97	
	18	3.30	6.2009	16.55	3.307 2.408	.899	3.307 2.405	.902	.900	4.106	4.03	Imperfect bonding

TABLE 4.3 TEST DATA [illegible]

WEATHERING NO. OF CYCLES	TEST NO.	V_o	V_s	P	DIAMETRAL COMPRESSIVE LOADING READING (LB)		DIAMETRAL COMPRESSIVE LOADING READING (LB)		AVERAGE DIAMETER			
0	19	3.62	6.2079	17.85	3.315 2.428	.887	3.317 2.428	.889	.888	4.992	4.47	
	20	3.76	6.2077	18.43	3.312 2.402	.910	3.335 2.418	.917	.913	4.228	4.36	Imperfect bonding
	21	3.35	6.2078	16.74	3.329 2.435	.894	3.312 2.415	.897	.895	4.065	4.12	Imperfect bonding
0	22	9.24	6.2061	40.99	3.366 2.403	.963	3.370 2.377	.993	.978	4.847	8.46	
	23	8.00	6.2061	35.89	3.362 2.378	.984	3.368 2.378	.990	.987	4.936	7.21	
	24	5.61	6.2081	26.04	3.349 2.407	.942	3.354 2.420	.934	.938	4.458	5.84	
0	25	5.99	6.2053	27.62	3.369 2.380	.989	3.370 2.386	.984	.986	4.931	5.60	
	26	6.38	6.2057	29.22	3.371 2.380	.991	3.368 2.380	.988	.989	4.956	5.89	
	27	2.23	6.2053	12.13	3.332 2.410	.922	3.348 2.425	.923	.922	4.307	2.82	Imperfect bonding
0	28	4.98	6.2084	23.45	3.313 2.425	.888	3.316 2.425	.889	.888	3.996	5.87	
	29	4.21	6.2080	20.28	3.321 2.461	.860	3.342 2.442	.899	.879	3.919	5.17	
	30	2.68	6.2086	13.98	3.335 2.425	.910	3.325 2.420	.905	.907	4.173	3.35	Imperfect bonding
0	31	5.23	6.2089	24.48	3.339 2.420	.919	3.346 2.408	.938	.929	4.368	5.60	
	32	6.69	6.2085	30.48	3.343 2.381	.962	3.345 2.381	.964	.963	4.699	6.49	
	33	8.68	6.2089	38.67	3.369 2.376	.993	3.368 2.399	.969	.981	4.876	7.93	
0	34	3.90	6.2088	19.00	3.293 2.480	.813	3.287 2.470	.817	.815	3.366	5.64	
	35	2.80	6.2084	14.47								Imperfect bonding
	36											Not performed because of broken edge of this site

TABLE 4.4 TEST DATA FOR SPECIMEN III

WEATHERING No. OF CYCLES	TEST No	V_o (mv)	V_i (VOLTS)	P (kg)	DIAMETER COMPARATOR READING (IN)	DIAMETER (IN)	DIAMETER COMPARATOR READING (IN)	DIAMETER (IN)	AVERAGE DIAMETER (IN)	AVERAGE AREA (cm^2)	P/A (kn/cm^2)	COMMENTS
0	37	15 52	6 2108	66 81	3.365 2 393	.972	3 360 2.398	962	967	4 738	14 10	
	38	11.89	6 2108	51 06	3 360 2 423	.937	3.340 2.423	917	927	4 354	11 73	Imperfect banding
	39	16 29	6 2106	69 17	3 365 2 393	.970	3 363 2.393	970	970	4 767	14 51	
1	40	8 93	6 2113	37 28	3 325 2 407	.918	3 350 2 418	912	.915	4 84	8.78	Imperfect banding
	41	2 39	6 2114	11 52	3.284 2.448	.836	3 294 2 448	846	841	3 58	3 22	Imperfect banding
	42	7 67	6 2114	33 24	3 310 2 473	.837	— —	—	.837	3 55	9.36	Imperfect banding
2	43	13 22	6.2117	56 07	3 351 2 407	.944	3 353 2 407	946	945	4525	12 39	
	44	10 90	6 2115	46.49	3.309 2 438	.871	3.313 2.438	874	872	3 853	12 07	
	45	10 53	6 2117	44 02	3 333 2 436	.897	3 330 2 429	.901	.899	4 095	10 75	Imperfect banding
4	46	10 83	6 2117	46 07	3 391 2.455	896	3.392 2 451	.901	.898	4 091	11 26	
	47	11 90	6 2120	50 48	3 396 2 455	891	3 345 2 409	.936	914	4 23	11 93	
	48	9 10	6 2117	38.96	3 363 2.466	898	3 358 2 459	899	898	4 086	9 53	Imperfect banding
8	49	12 32	6 2127	52 28	3 341 2 421	920	3 329 2 408	921	921	4 298	12 21	
	50	11 72	6 2126	49 81	3 351 2 410	921	3 335 2 416	919	920	4 289	11 61	
	51	12 37	6 2130	52 48	3 359 2 407	932	3 359 2 395	944	938	4 458	11 77	
12	52	6 88	6.2137	29 72	— —		— —					Imperfect banding
	53	12 57	6 2132	53 31	3 515 2.419	.896	— —					Imperfect banding
	54	6 37	6 2139	27 67	— —		— —					Imperfect banding

For z = 0.25 inches

Element	Due to Δq_i as shown in Fig. 4.7 b					Due to Δq_i as shown in Fig 4.8 and 4.7c					
	R(in)	x(in)	z/R	x/R	$\Delta\sigma_v/\Delta q_i$	R(in)	x(in)	z/R	x/R	$\Delta\sigma_v/\Delta q_i$	NET $\Delta\sigma_v/\Delta q_i$
1	1.00	0	.25	0	1.00	.50	0	.5	0	0.9	0.1
2	1.00	.25	.25	.25	≈1.00	.50	.25	.5	.5	.84	0.16
3	"	.50	"	.50	≈1.00	"	.50	"	1.0	.42	0.58
4	"	.75	"	.75	0.9	"	.75	"	1.5	.075	0.825
5	"	.80	"	.80	0.84	"	.80	"	1.6	.05	0.79
6	"	1.00	"	1.00	0.45	"	1.00	"	2.0	.025	0.425

TABLE 4.5

STRESS DISTRIBUTION UNDER UNIFORM LOAD AND UNDER RING LOAD

TABLE 4.6 COMPARATIVE RESULTS

Specimen	δ_d (lb/ft^3)	ω (%)	Curing	Time curing (days)	P/A* avg. (kg/cm^2)	STANDARD DEVIATION		
						Ultimate Load "P"		Ultimate P/A*
						Unconfined	Confined	
I	115.08	14.99	cold	58	4.73	6.07	2.52	0.38
II	114.03	13.13	hot	60	6.34	—	6.47	1.01
III	120.33	14.13	hot	74	11.89	—	3.25	0.34

*Confined tests only

TABLE 4.7 DATA FROM CYCLIC WEATHERING OF SPECIMEN III

WEATHERING CYCLES	WEIGHT BEFORE SOAKING (gms)	LENGTH BEFORE SOAKING		WEIGHT AFTER SOAKING (gms)	Δ_w (gms)	LENGTH AFTER SOAKING		WEIGHT AFTER OVEN DRYING (gms)	Δ_w (gms)	LENGTH AFTER OVEN DRYING	
		A-A (in)	B-B (in)			A-A (in)	B-B (in)			A-A (in)	B-B (in)
1	876.20	—	—	959.50	83.30	—	—	876.95	82.55	—	—
2	874.23	—	—	967.64	93.41	—	—	880.72	86.92	4.980	5.003
3	875.02	4.980	5.003	968.21	93.19	4.985	5.006	870.72	97.49	4.981	5.003
4	870.72	4.981	5.003	970.40	99.68	4.983	5.005	875.47	94.93	4.980	5.002
5	872.65	4.980	5.002	969.41	96.76	4.983	5.005	860.60	108.81	4.980	5.000
6	860.60	4.980	5.000	970.53	109.93	4.983	5.005	867.30	103.23	4.980	5.001
7	867.30	4.980	5.001	970.37	103.07	4.983	5.004	864.54	105.83	4.980	5.003
8	864.54	4.980	5.003	970.55	106.01	4.983	5.005	870.87	99.68	4.980	5.002
9	866.90	4.980	5.002	969.48	102.58	4.983	5.005	856.93	112.55	4.979	5.000
10	856.93	4.979	5.000	969.32	112.39	4.984	5.005	858.80	110.52	4.980	5.001
11	858.80	4.980	5.001	969.67	110.87	4.983	5.005	856.70	112.97	4.979	5.000
12	856.70	4.979	5.000	969.63	112.93	4.982	5.004	856.84	112.79	4.980	5.003

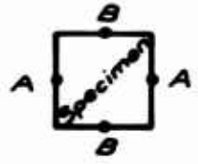

TABLE 4.8 CHANGES IN LENGTH OF SPECIMEN III DURING WEATHERING CYCLING

No. of Cycles	$\bar{A}$-$\bar{A}$ Dry-Wet	$\bar{B}$-$\bar{B}$ Dry-Wet	$\bar{A}$-$\bar{A}$ Wet-Dry	$\bar{B}$-$\bar{B}$ Wet-Dry
1	-	-	-	-
2	-	-	-	-
3	.005	.003	.004	.003
4	.002	.002	.003	.003
5	.003	.003	.003	.005
6	.003	.005	.003	.004
7	.003	.003	.003	.001
8	.003	.002	.003	.003
9	.003	.003	.004	.005
10	.005	.005	.004	.004
11	.003	.004	.004	.005
12	.003	.004	.002	.001

*Refer to Fig. 4.13

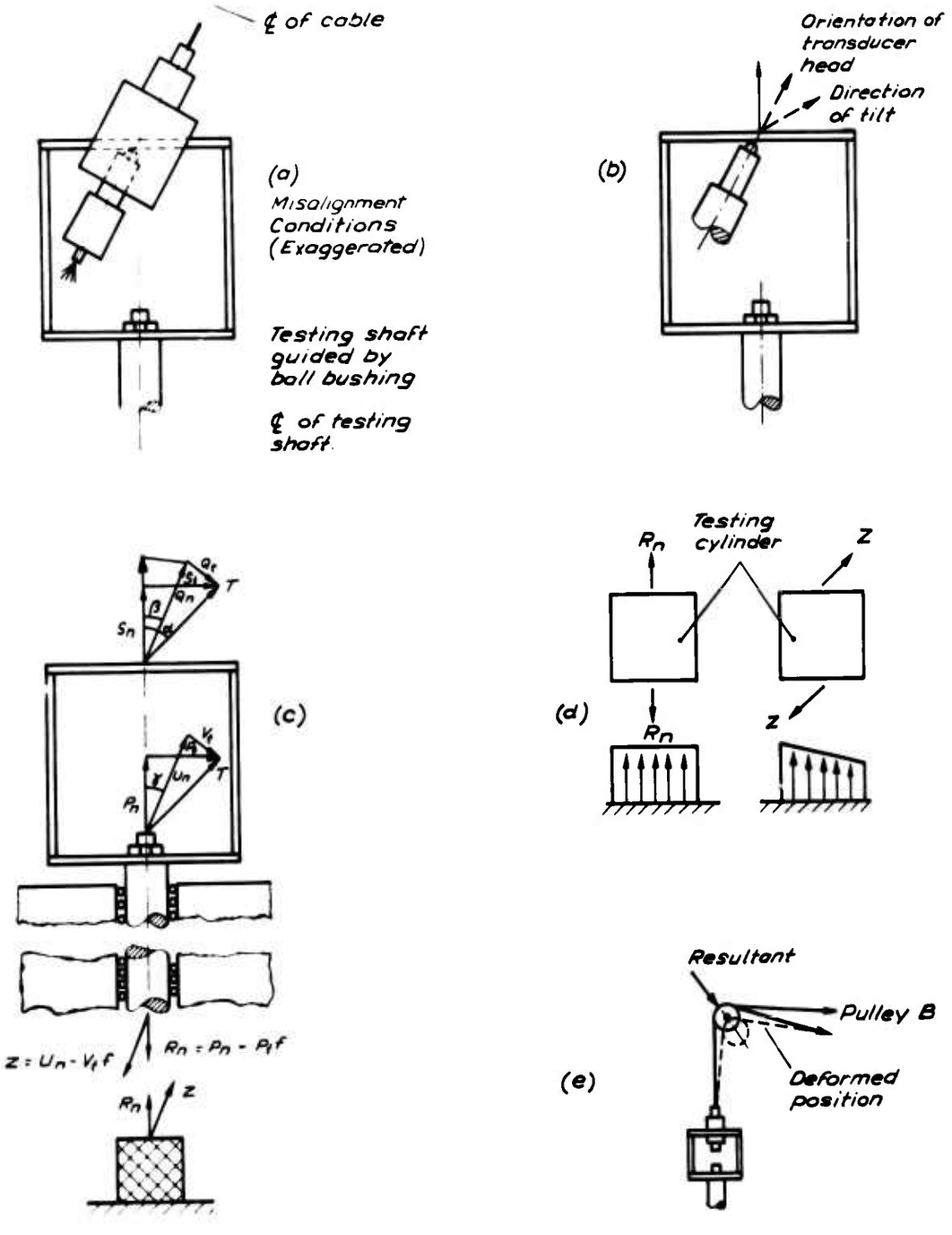

FIG. 4.1 TILTING DURING TESTING

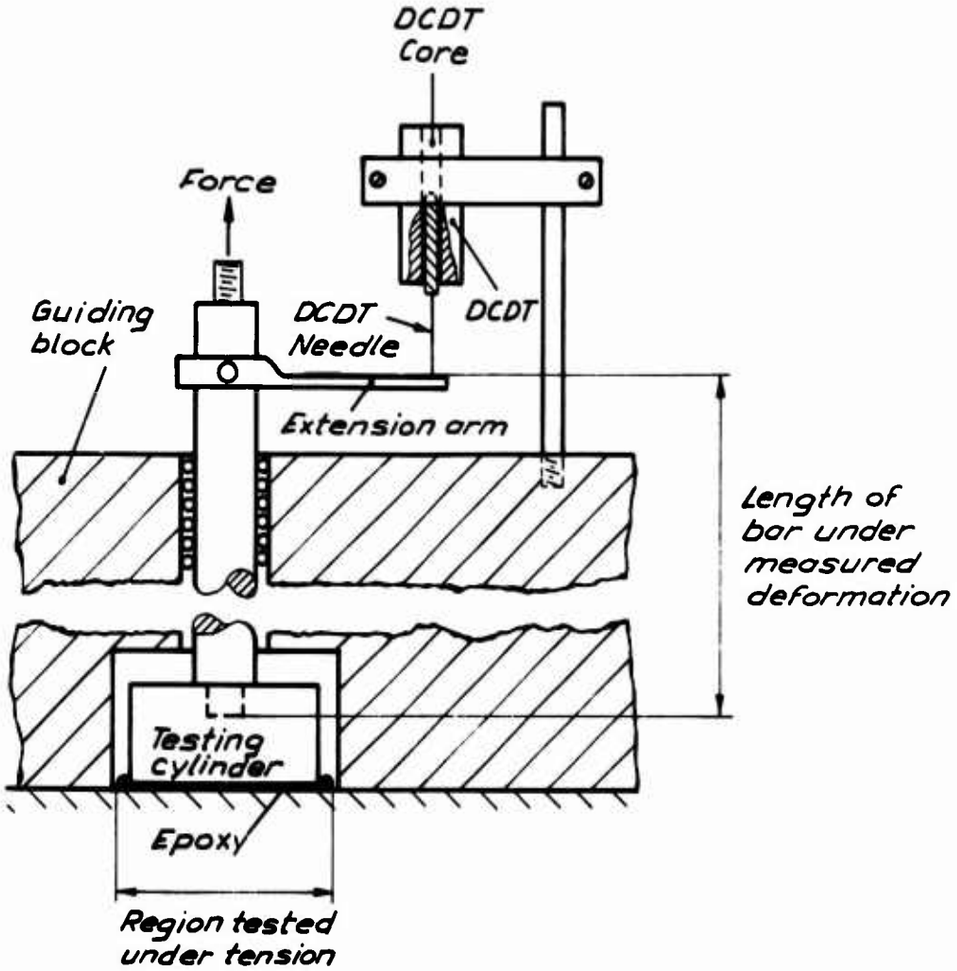

FIG. 4.2 INSTALLATION OF DCDT

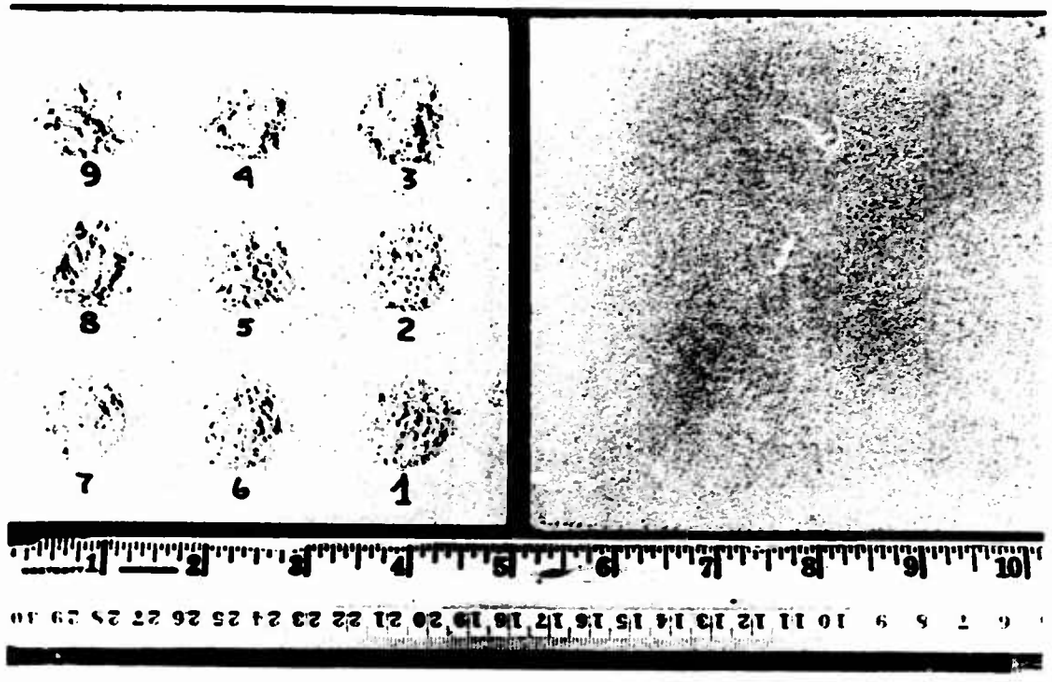

Fig. 4.3 Specimens Before and After Testing

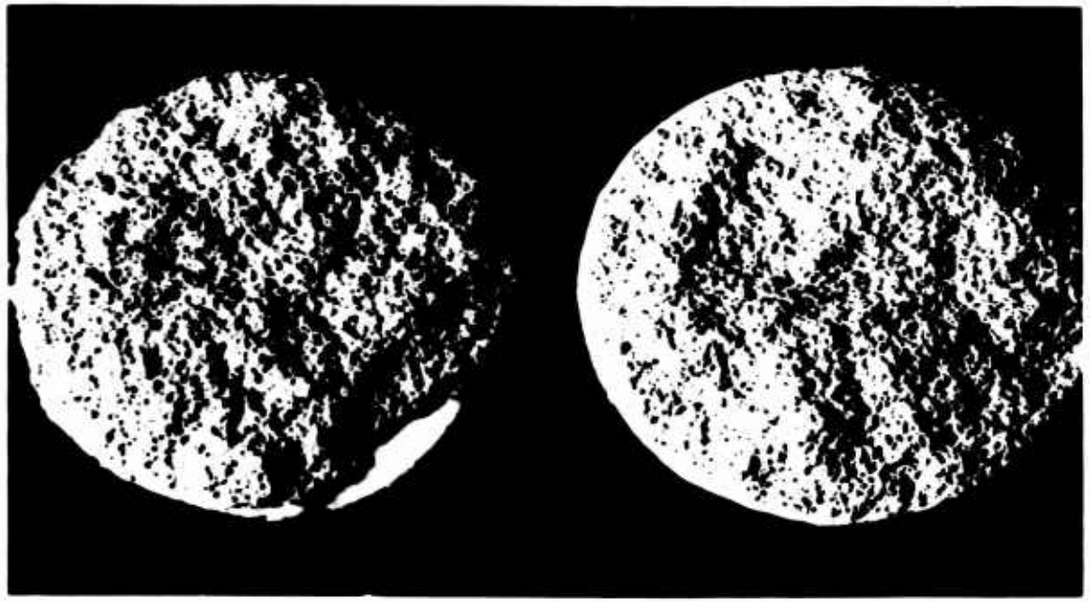

Fig. 4.4 Faulty Bonded Area Versus Well-Bonded Area

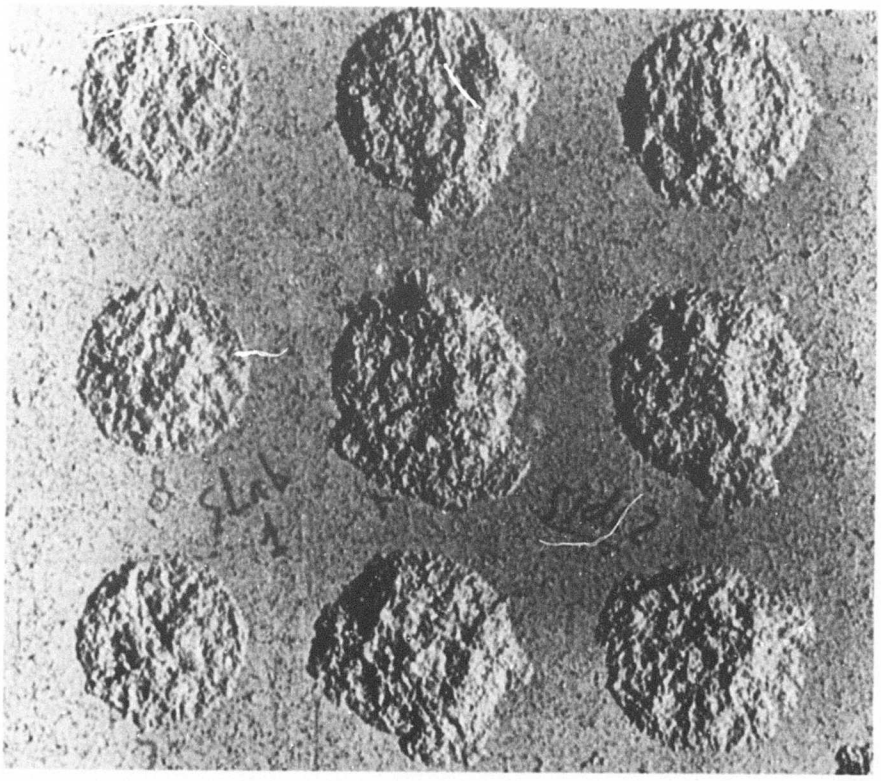

Fig. 4.5 Tested Area Under Confined Tests
Versus Unconfined Tests

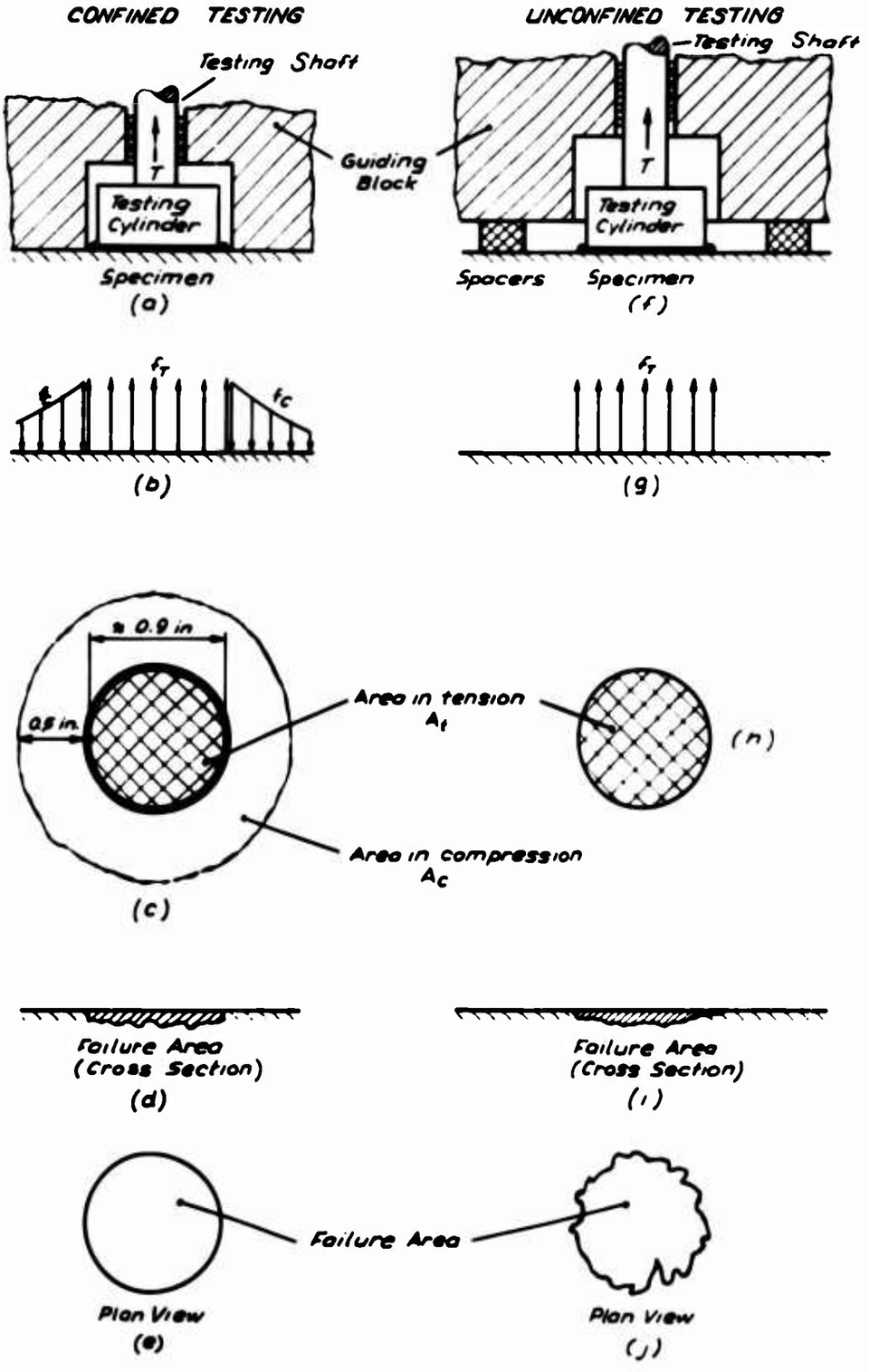

FIG. 4.6 CONFINED VERSUS UNCONFINED TENSION TEST

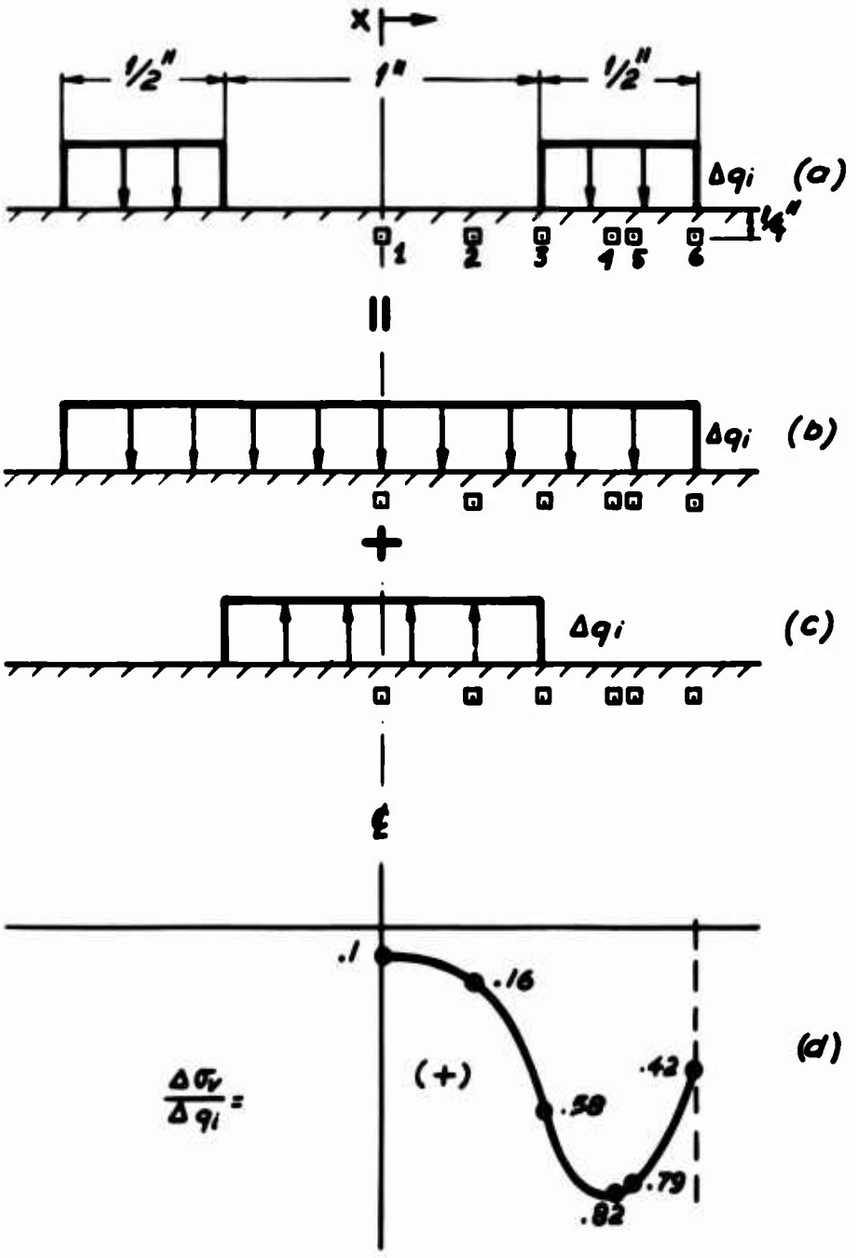

FIG. 4.7 STRESS DISTRIBUTION UNDER A UNIFORM RING LOAD

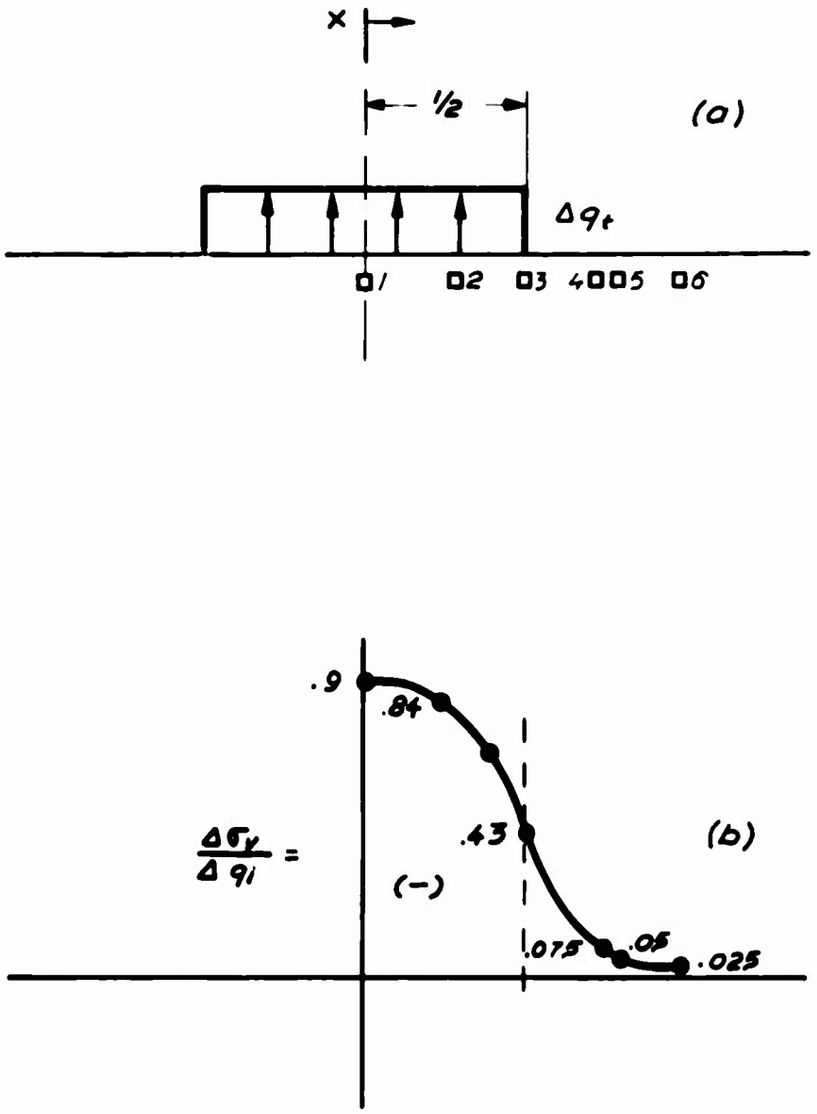

FIG. 4.8 STRESS DISTRIBUTION UNDER A UNIFORM CIRCULAR LOAD

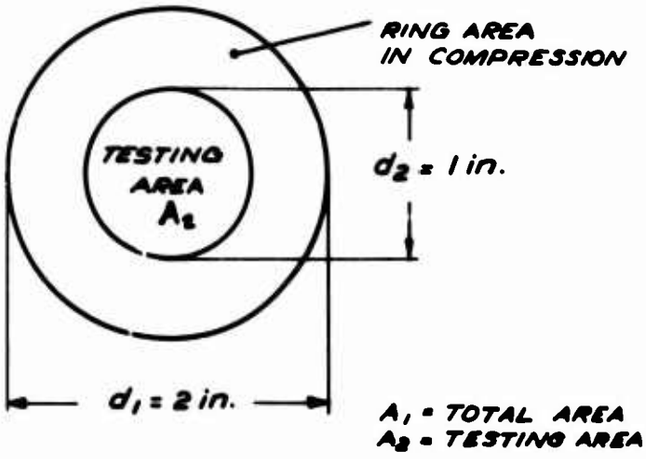

$$A_1 = \frac{\pi d_1^2}{4} \qquad A_2 = \frac{\pi d_2^2}{4}$$

$$A_{Ring} = A_1 - A_2 = \frac{\pi}{4}(d_1^2 - d_2^2) = \frac{\pi}{4}(4-1) = \frac{3\pi}{4}$$

$$\text{Area Ratio} = \frac{A_{Ring}}{A_2} = \frac{\frac{3\pi}{4}}{\frac{\pi}{4}} = 3$$

Δq = Load per unit area = $\frac{F}{A}$

Δq_t = Load per unit area on testing area

Δq_c = Load per unit area on Ring Area

$\therefore$ For the same force F

$$\frac{\Delta q_c}{\Delta q_t} = \frac{F/A_{Ring}}{F/A_2} = \frac{A_2}{A_{Ring}} = \frac{1}{3} \quad \therefore \quad \Delta q_c = \frac{\Delta q_t}{3}$$

FIG. 4.9 RELATION BETWEEN TESTING AREA AND RING AREA

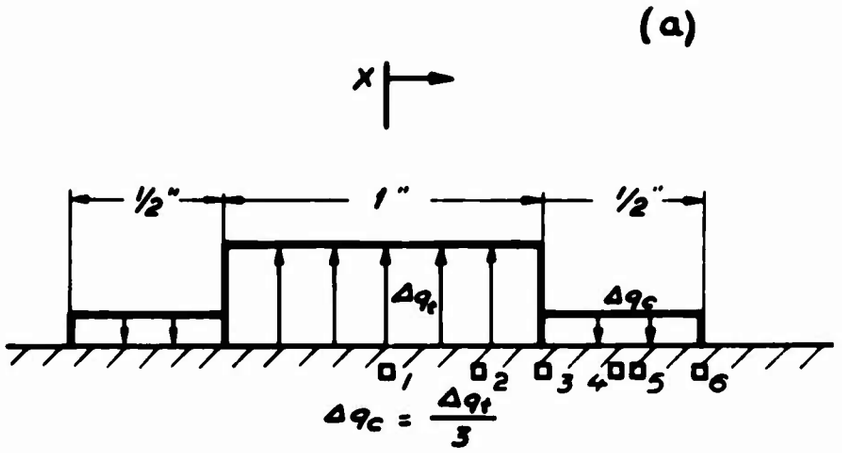

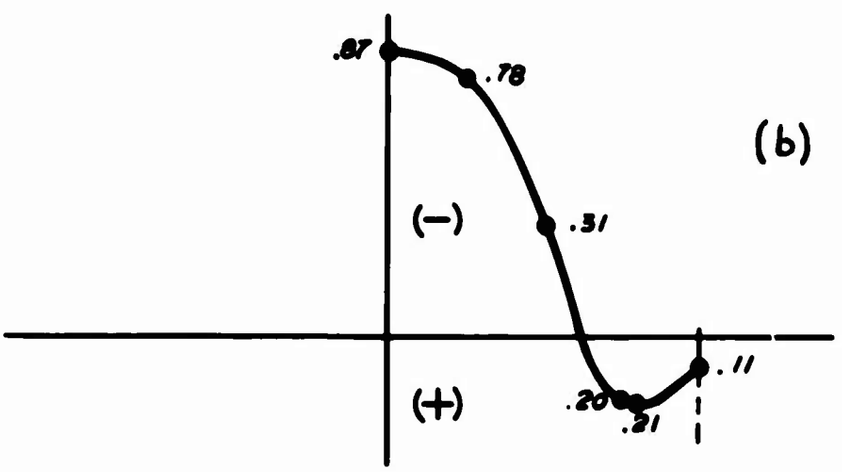

FIG. 4.10 STRESS DISTRIBUTION DURING TENSILE TEST

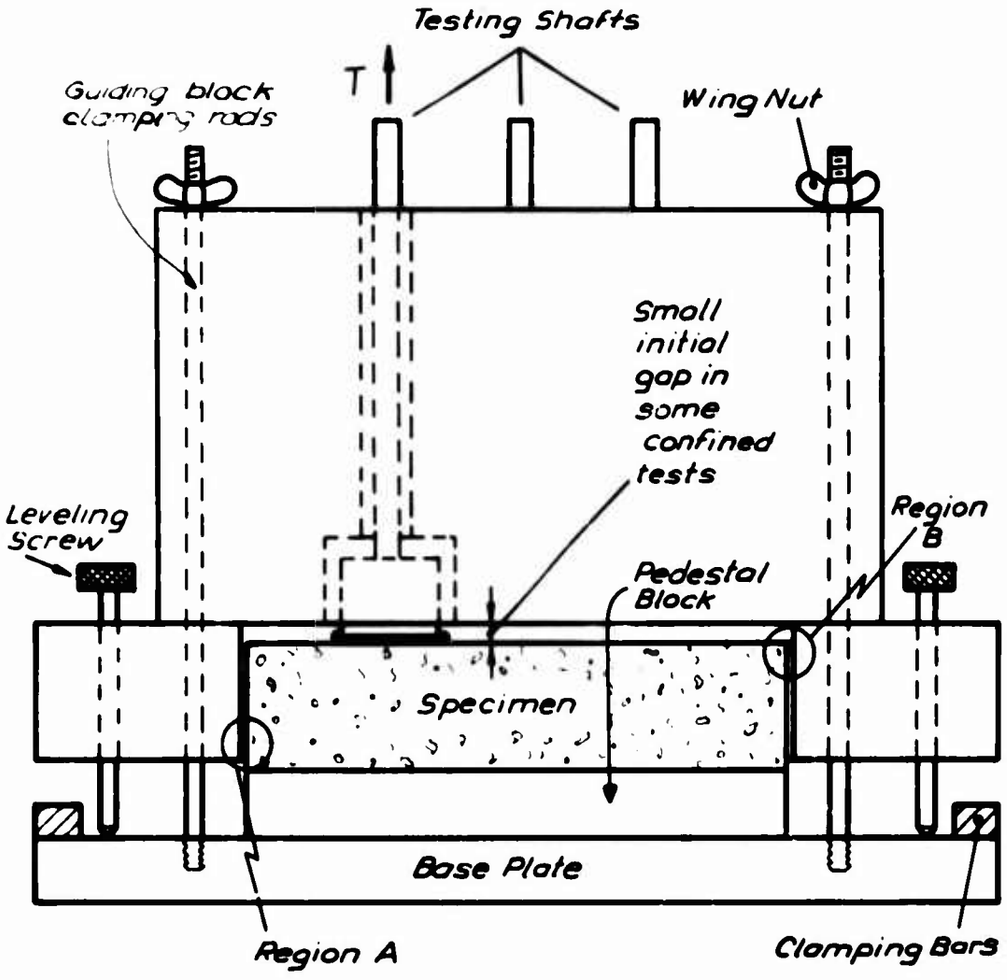

FIG. 4.11 ECCENTRIC LOADING

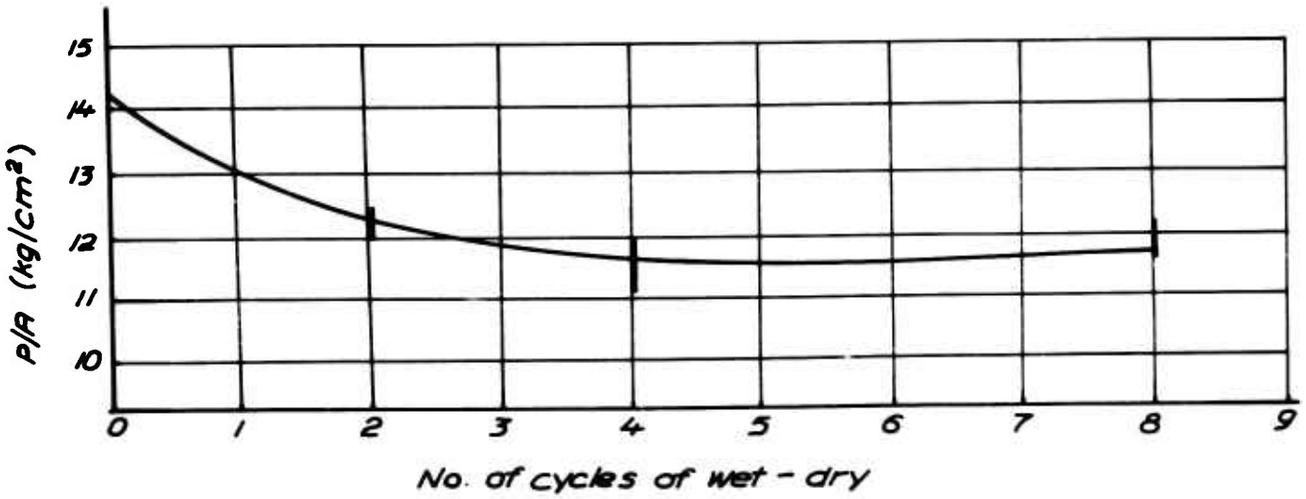

FIG. 4.12
TENSILE STRENGTH Vs CYCLIC WEATHERING

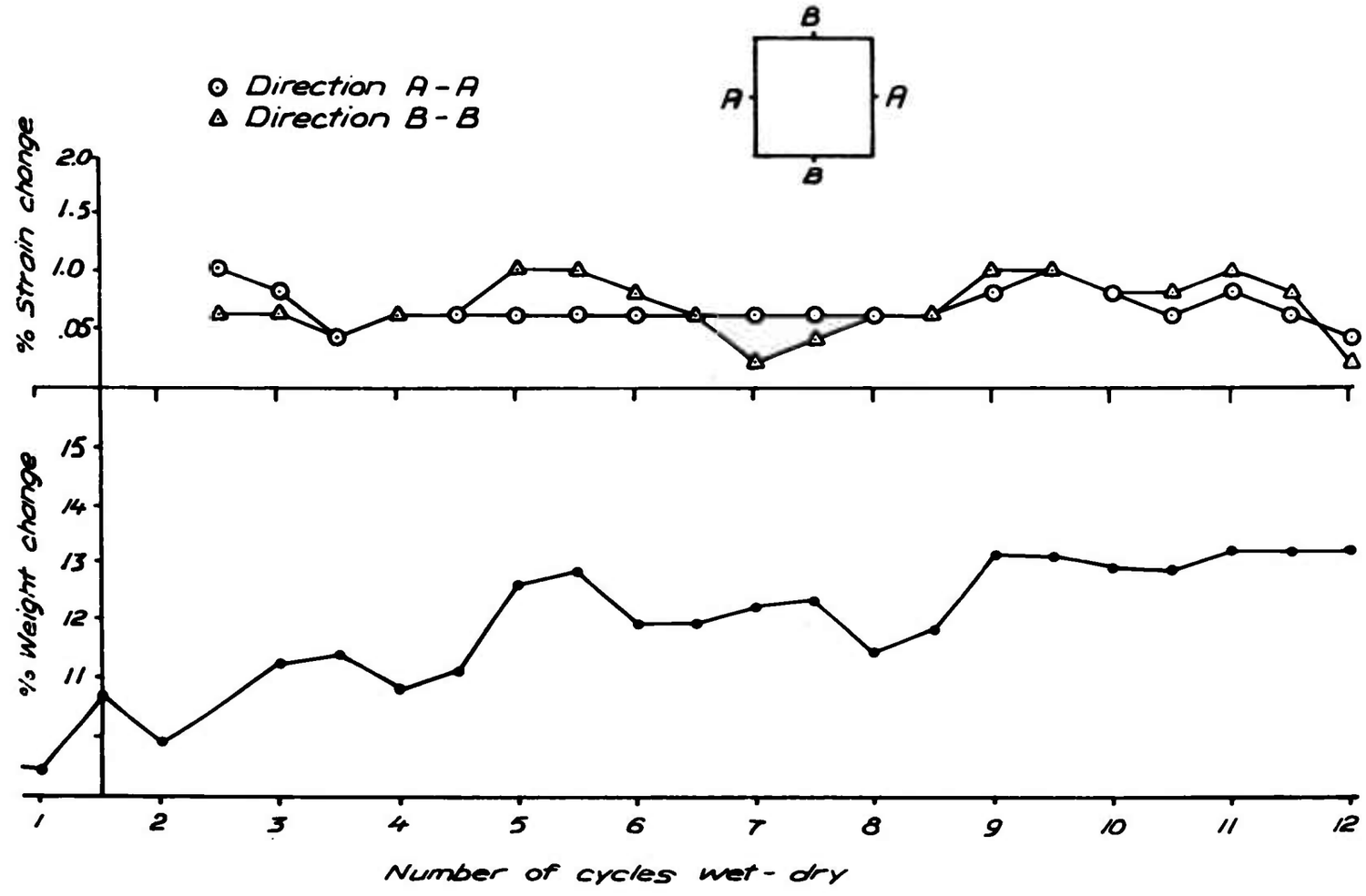

FIG. 4.13 PERCENT STRAIN AND WEIGHT CHANGES DURING WET-DRY CYCLES

Chapter 5
MODIFIED APPARATUS AND PROCEDURES FOR THE DURABILITY TENSILE TEST

5.1 COMPACTION

In Chapter 4 it was stated that even with careful placing and screeding of the loose mix of soil-cement in the square mold, it was difficult to obtain uniform static compaction over such a large area (5 in. x 5 in.). To simplify the compaction procedure and to improve uniformity of the compacted specimen, it is recommended that the shape of the mold be changed from a 5-inch square to a six-inch circle. This will make it possible to use impact compaction (Standard of Modified AASHO compaction). Detail drawings of the proposed mold and compaction accessory pieces are given in Appendix DI. The following procedure is recommended:

a) Once compaction is completed, remove the top collar of the assembly and trim the top surface of the specimen flushed with the mold's surface using a sharp straight bar.

b) Extrude approximately one-half inch of the specimen from the mold and introduce two short pins through the sides of the sample, coinciding with the two groove marks on the side of the mold. These marks determine a diameter on the specimen which will serve as a reference line to orient the specimen in the tension test apparatus.

c) Complete extrusion of the sample from the mold.

d) Measure the diameter of the specimen across the pin marks and weigh the specimen.

e) Seal the specimen in the manner described in Section 3.3.1.3 and store for curing.

5.2 TENSION TEST

In Chapter 4 it was stated that the high flexibility of the tension test apparatus made it impossible to obtain good deformation data during the surface tension tests. The prototype equipment used in this investigation (Chapter 3) occupied a relatively large area and a more compact unit is desirable.

Further, since a circular shape is being recommended for the specimens (Section 5.1), the parts of the assembly that support the specimen must be changed accordingly. In order to meet the above requirements, the design presented in Sections 5.2.1 to 5.2.3 is recommended for performing tension tests on the surface of stabilized specimens.

The imporved characteristics of this new design are:

a) A very rigid frame made with standard steel members to house the tension test.

b) A compact and relatively rigid tension force application system firmly fixed to the frame mentioned above.

c) An assembly of parts to support circular specimens, having three degrees of motion to permit the location of the tension test sites directly under the force application system.

d) A guiding block coupled with the specimen support assembly in order to perform eighteen

tension tests on one surface of the specimen with no less than 1/4 in. separation between test sites.

5.2.1 The Assembly Frame

The assembly frame houses the complete tension test apparatus. It has been designed as a very rigid frame in order that its deformations are negligible under the working loads for which the tension test apparatus is designed. A perspective view of the assembly frame is shown in Fig. 5.1 and detail drawings are given in Appendix D.II.

5.2.2 Specimen Supports, Guiding Block, and Accessories

The pieces of equipment associated with this assembly were redesigned to accommodate round compacted specimens and are shown in Figs. 5.2 and 5.3.

A special feature of this assembly is the provision of aligning and locating the guiding block in six different positions relative to the test specimen. In this way, the three testing shafts of the guiding block mark a total of 18 test sites with no less than 1/4 inch between adjacent sites. Furthermore, this assembly is provided with three degrees of movement, two in a horizontal plane at right angles to each other and a third of rotation around the central axes of the whole assembly. This is necessary in order to locate the different testing sites directly under the force application system, which in this new design is bolted in a fixed position to the assembly frame.

Another improvement is the provision of an open watertight chamber for soaking the test specimen during testing.

Detail drawings are presented in Appendix D.III with a description of each individual piece and assembling instructions.

5.2.3 Force Application System (or Drive Mechanism)

As mentioned in Section 5.2, the drive mechanism now recommended for the application of the tensile force has been redesigned as a relatively rigid and compact unit capable of applying a tensile (or compressive) force of 450 kg (see Figs. 5.4, 5.5, and 5.6). It is estimated that the maximum load that will normally be encountered in tension tests on stabilized soils is 100 kg.

The drive mechanism is firmly bolted to the assembly frame and is then an integral part of the frame. Detail drawings and part specifications are given in Appendix D.IV.

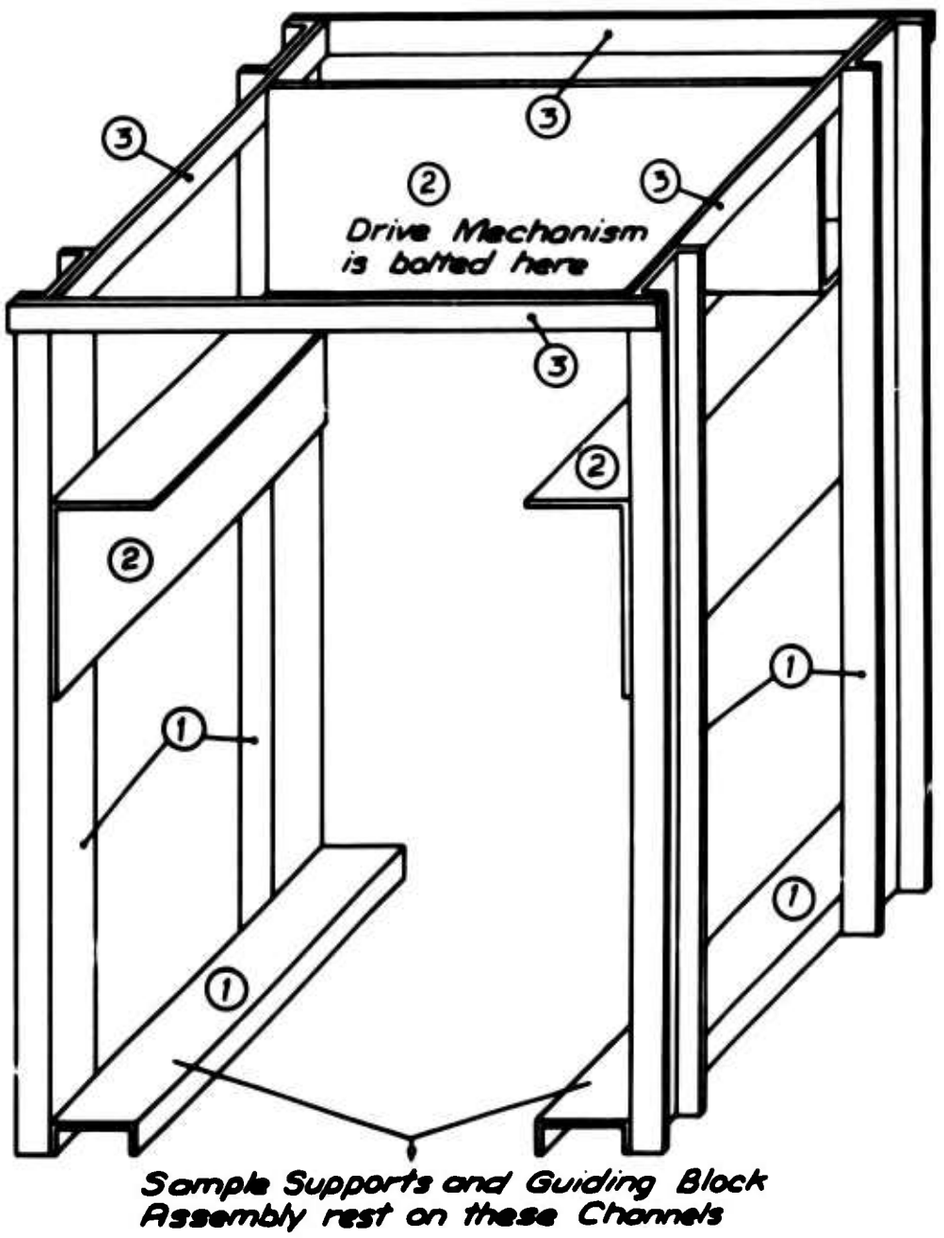

FIG. 5.1 ASSEMBLY FRAME

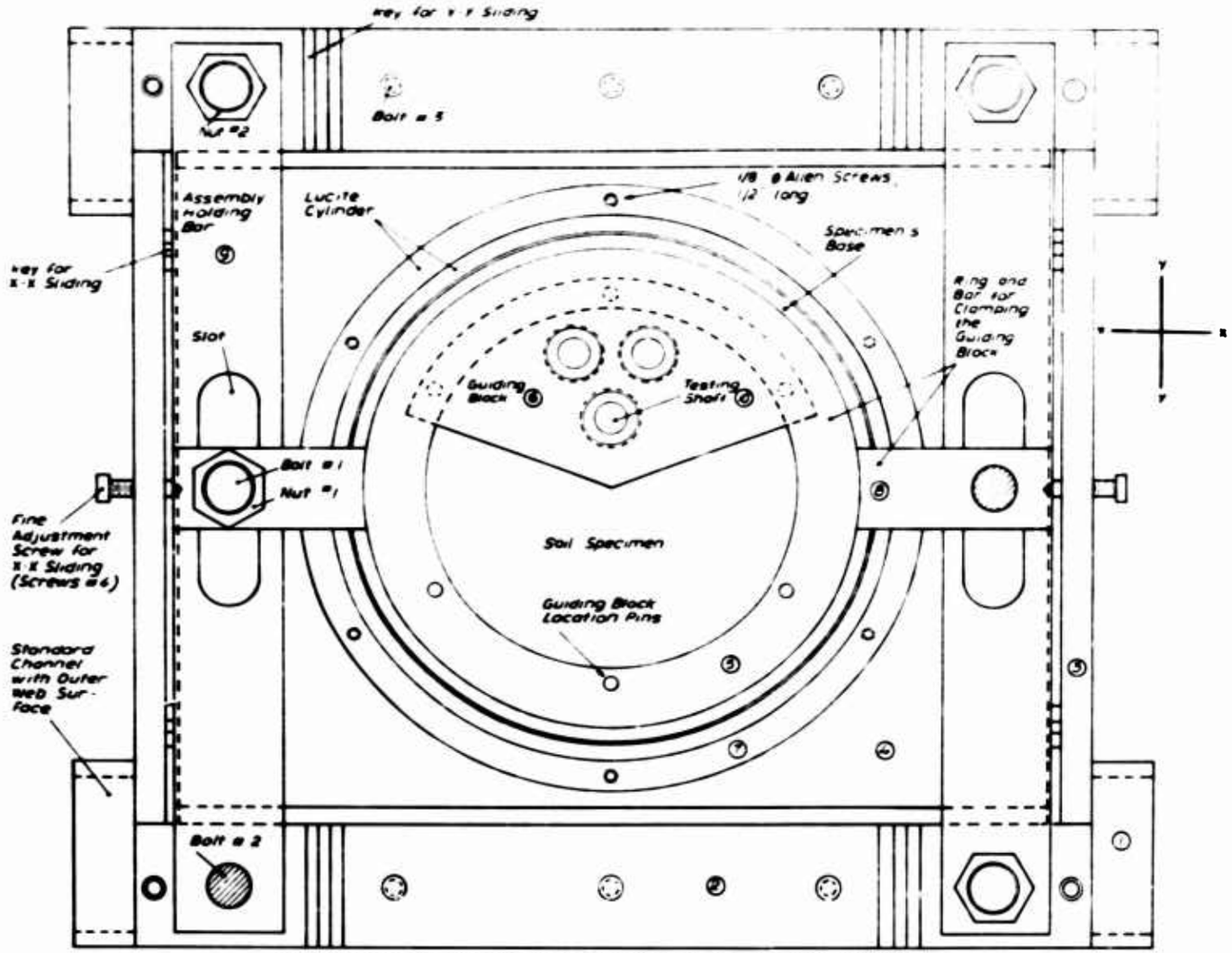

FIG 32 SPECIMEN SUPPORT, GUIDING BLOCK AND ACCESSORIES (PLAN VIEW)

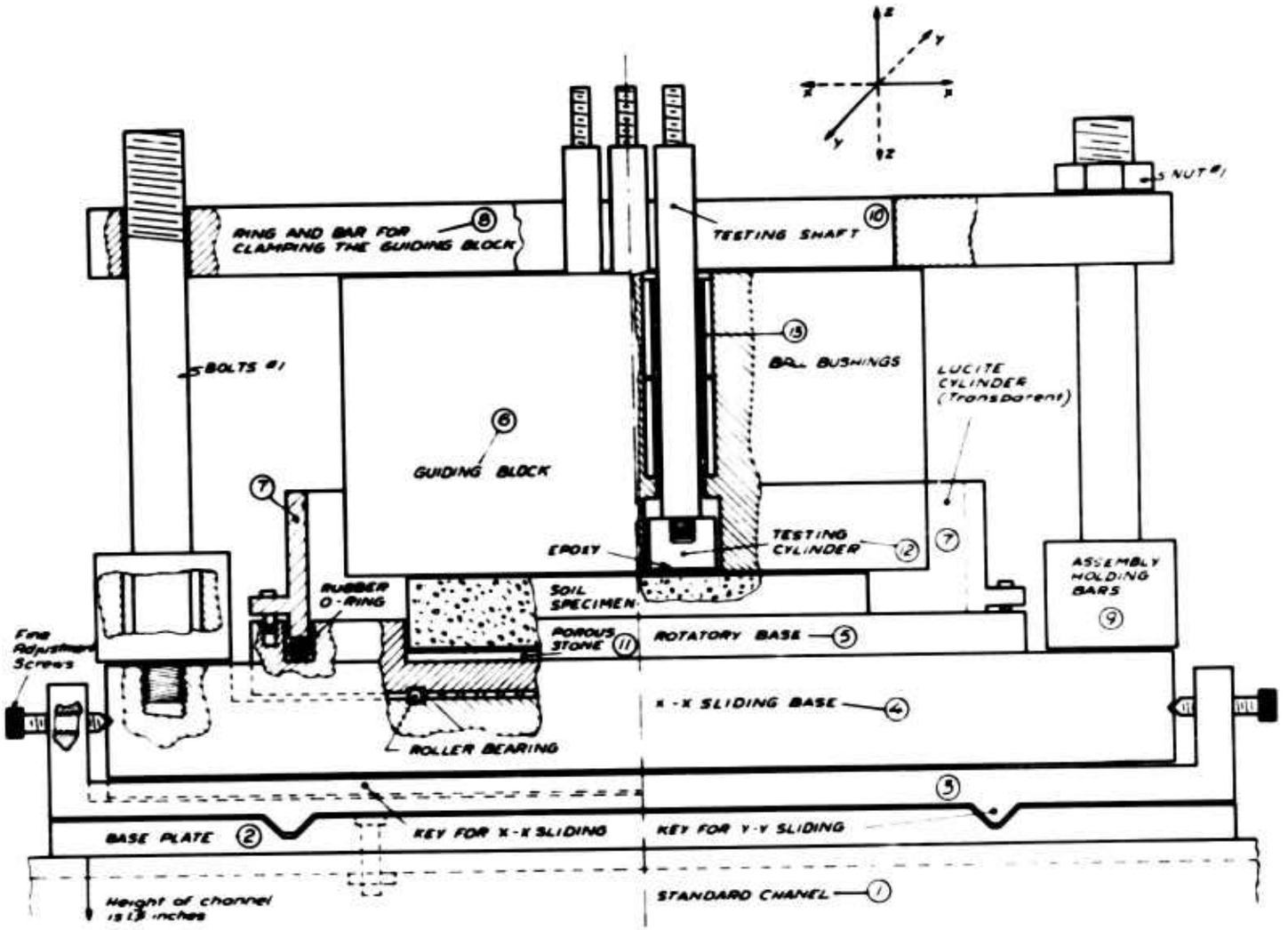

FIGURE 5.3 SPECIMEN SUPPORTS, GUIDING BLOCK, AND ACCESORIES (CROSS SECTION)

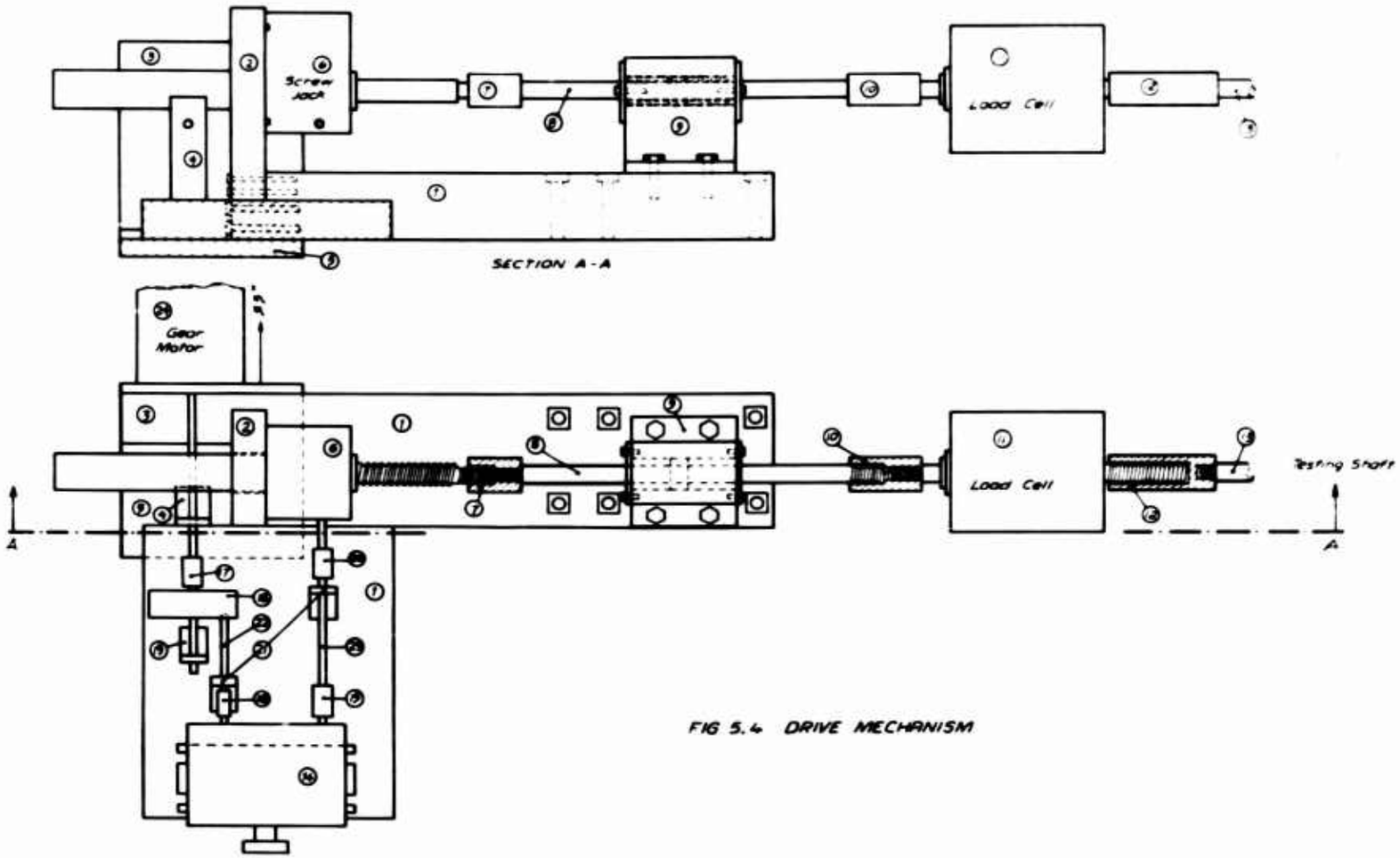

FIG 5.4 DRIVE MECHANISM

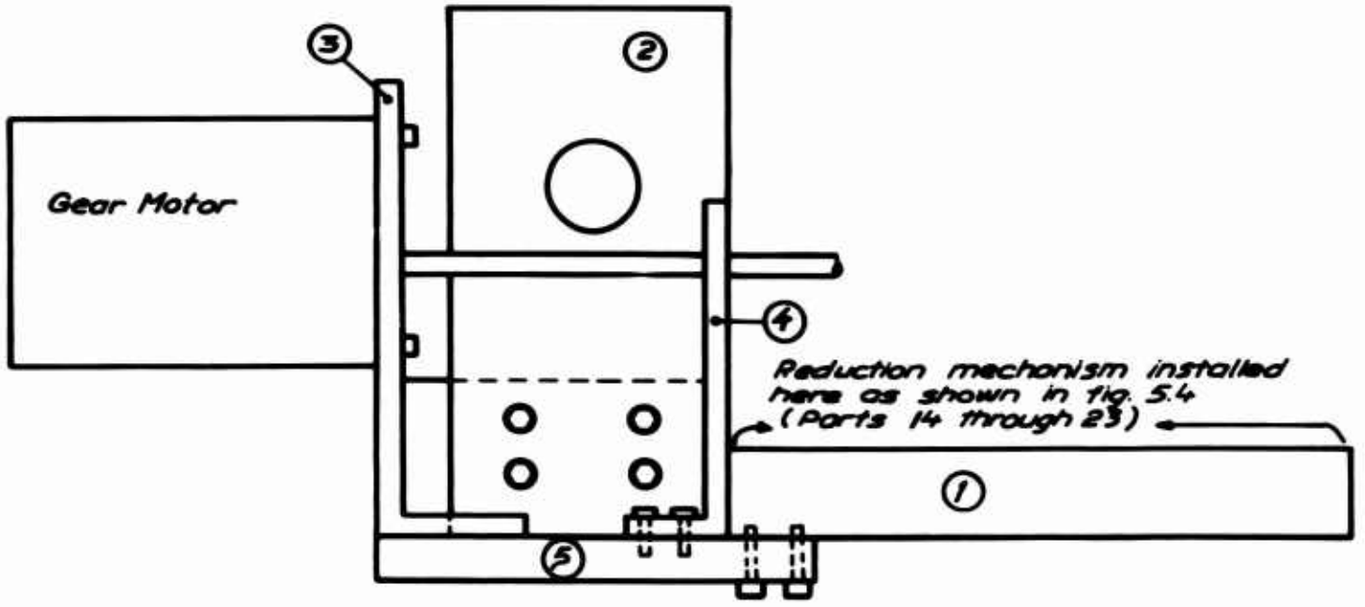

FIG. 5.5 REAR VIEW OF DRIVE MECHANISM

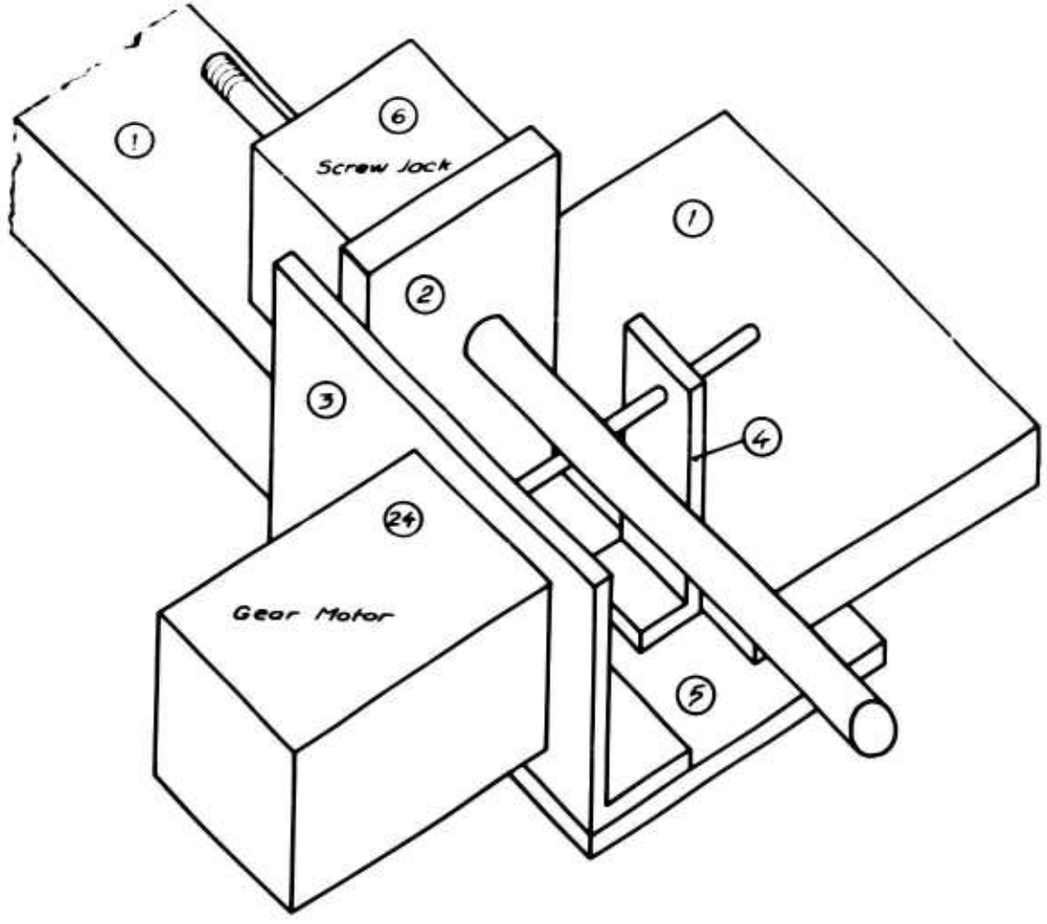

FIG. 5.6
ASSEMBLY OF PLATES AND ANGLES TO SUPPORT THE GEAR MOTOR (PART #24), THE REDUCTION SYSTEM AND THE SCREW JACK (PART #6)

Chapter 6
CONCLUSIONS AND RECOMMENDATIONS

This investigation was carried out for the purpose of developing the testing equipment and procedures necessary to evaluate the suitability of compacted stabilized soil mixes to resist surface disintegration induced by weathering forces.

It was reasoned that since disintegration of the surface in the form of loose particles of dust or scales was the result of the loss of cohesive strength, a measure of the surface tensile strength of stabilized soils would be the best criterion for evaluating their durability characteristics.

Due to a lack of precedence in performing tensile strength tests at the surface of stabilized soil samples, it was decided to design and build the simplest and most economical piece of equipment that could achieve the desired purpose.

From the experience obtained with this prototype equipment, an improved design was proposed in Chapter 5 in which corrective measures were taken to eliminate or minimize the difficulties encountered with the preliminary design. In doing so, the desire to obtain reasonably reproducible results was not the only criterion exercised. In addition, the desire for a piece of equipment that could be easily used in testing on a volume basis and testing procedures that could be easily performed by an average technician were also taken into account in the redesign.

The following conclusions and recommendations are drawn from the results of the tests performed.

1. Tests where incomplete bonding occurs between the loading caps and the specimen surface showed a significant decrease in maximum tensile strength, which in some cases was of the order of 55% lower than the average strength of the well-bonded tests. Therefore complete bonding is essential and can be achieved with the procedure given in Section 4.2.

2. Confined tests produced slightly higher maximum tensile strengths and a significant reduction in the scatter of the measured strength compared to the results of unconfined tests. The confined testing procedure is therefore recommended.

3. The tensile strength is sensitive to changes in molding density. Higher as-molded density produces samples with higher tensile strength. Further, hot curing produces samples with higher tensile strength (all samples sealed during curing) than cold curing. Both of these observations show that tensile strength measurements are a measure of the cohesive resistance of the system.

4. Eccentric application of the tensile force to the test area produces a decrease in the maximum tensile strength which results in a significant increase in the scatter of the strength measured. The revised design of the equipment and the recommended testing procedure minimize the possibility of eccentric loading.

5. While cyclic wet-dry weathering produced a 15% reduction in the tensile strength during the first two

cycles in specimen III, no further loss of strength was measured in subsequent cycles of weathering. This is believed to indicate that this soil-cement system will withstand field wetting and drying. A system that shows a progressive loss in surface tensile strength with increasing number of weathering cycles would be considered inadequate to withstand field weathering conditions.

6. The high flexibility of the system used to perform the tensile test in this investigation produced very erratic results of displacement measurements, which made it impossible to study the stress-deformation behavior of the soil-cement specimens during tensile testing. While strain measurements may not be necessary for evaluating the surface durability of stabilized soils, it would be desirable to be able to obtain such measurements. The new design proposed in Chapter 5 will make the testing apparatus sufficiently rigid to permit the recording of good displacement measurements.

7. Using an x-y plotter to record the output from the force and displacement transducers would permit faster rates of applying the tensile load without sacrificing accurracy of the measurements. This would reduce the testing time of 40-50 minutes to 5-10 minutes.

8. The preparation of the specimens by the static compacting method required great care and did not necessarily ensure uniform density. By adopting

the new design and testing procedure recommended in Chapter 5, the AASHO standard impact compaction method can be used and only the bottom surface of the test specimen needs to be used for tension tests. This should simplify sample preparation and minimize density variations at the surface subjected to tensile testing.

Further, by using AASHO compaction, the results of the tensile tests can be compared with results obtained from the ASTM Durability Test. This would permit indirect correlation of the Durability Tensile Test with field performance.

9. It is recommended to use the average of three tests to describe the tensile strength at any one level of weathering and no less than the average of two tests if one of the three tests differs from the other two by more than 20%. It is also recommended to maintain a record of diameter measurement of the specimens as well as changes in water content during cyclic weathering as shown in Table 4.4.

LIST OF REFERENCES

Clare, K. E. and Pollard, A. E., "The effect of Curing Temperature on the Compressive Strength of Soil-Cement Mixtures", Geotechnique, Vol. 4, 1954.

Lambe, T. W., (1961) "Soil Stabilization", Foundation Engineering, G. A. Leonards, Chapter 4.

Norling, L. T. (1963) "Standard Laboratory Tests for Soil-Cement Development, Purpose and History of Use", Highway Research Record, Number 36.

Sherwood, P.T. (1962) "Effect of Soil Organic Matter on the Setting of Soil-Cement Mixtures", Department of Scientific and Industrial Research, Road Research Technical Paper No. 61.

Wissa, Anwar E. Z., and Feferbaum, Z. (1969) "Influence of Molding Condition on the Effective Stress-Strength Parameters of Cement Stabilized Soil", Soil Stabilization Phase Report No. 8, Dept. of Civil Engineering, M.I.T. (under preparation).

Wissa, Anwar E. Z., and Ladd, Charles C. (1964) "Effective Stress-Strength Behavior of Compacted Stabilized Soils" Soils Publication No. 164, Department of Civil Engineering, M.I.T.

APPENDIX A

DETAIL DRAWINGS OF PARTS OF THE PROTOTYPE COMPACTION EQUIPMENT AND THE DURABILITY TENSILE TESTING APPARATUS.

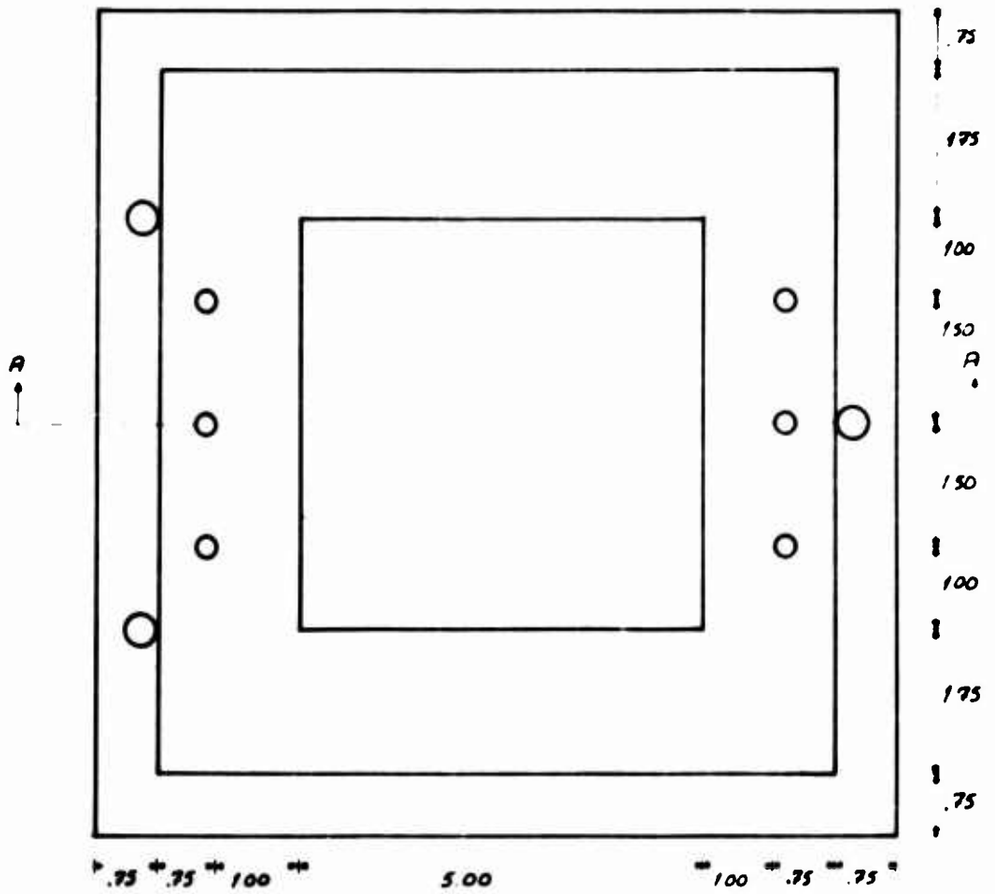

Dimensions in inches

SECTION A - A

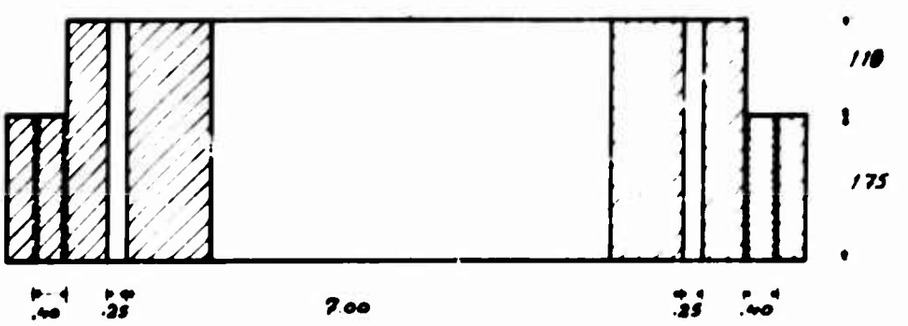

FIG. A-1 MOLD FOR COMPACTION

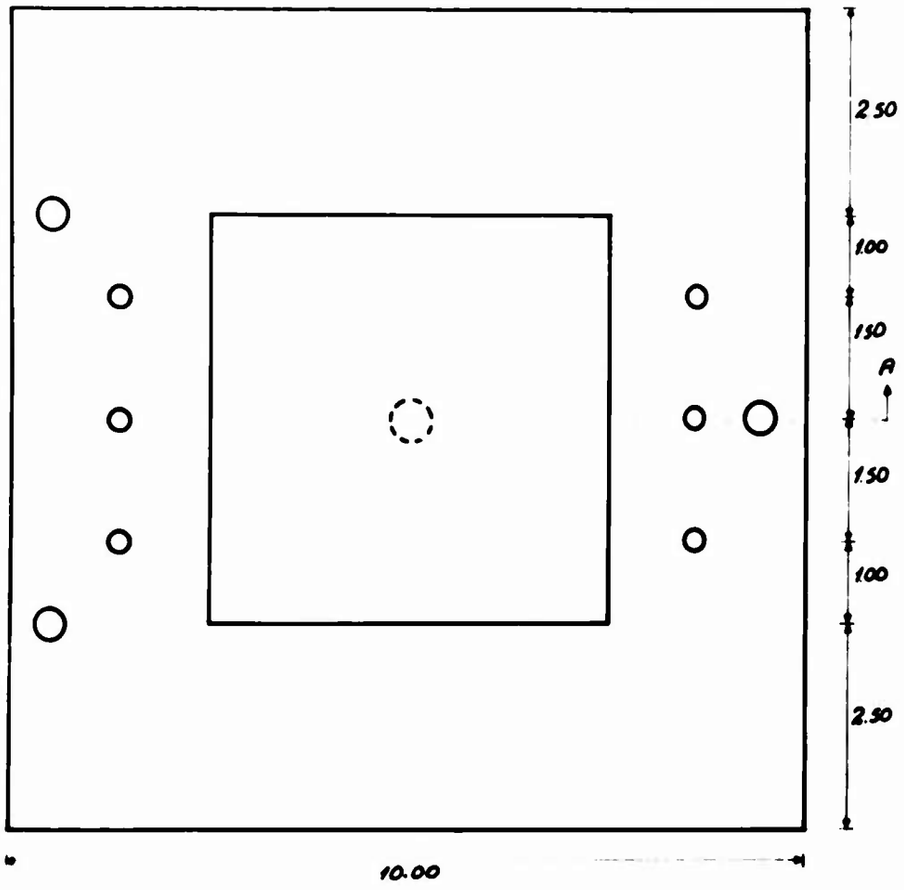

Dimensions in inches

SECTION A-A

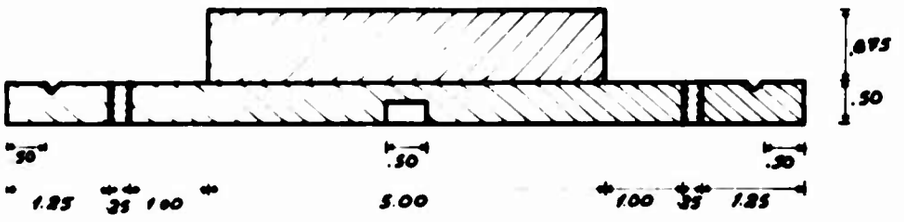

FIG. A-2 BASE

PLAN VIEW

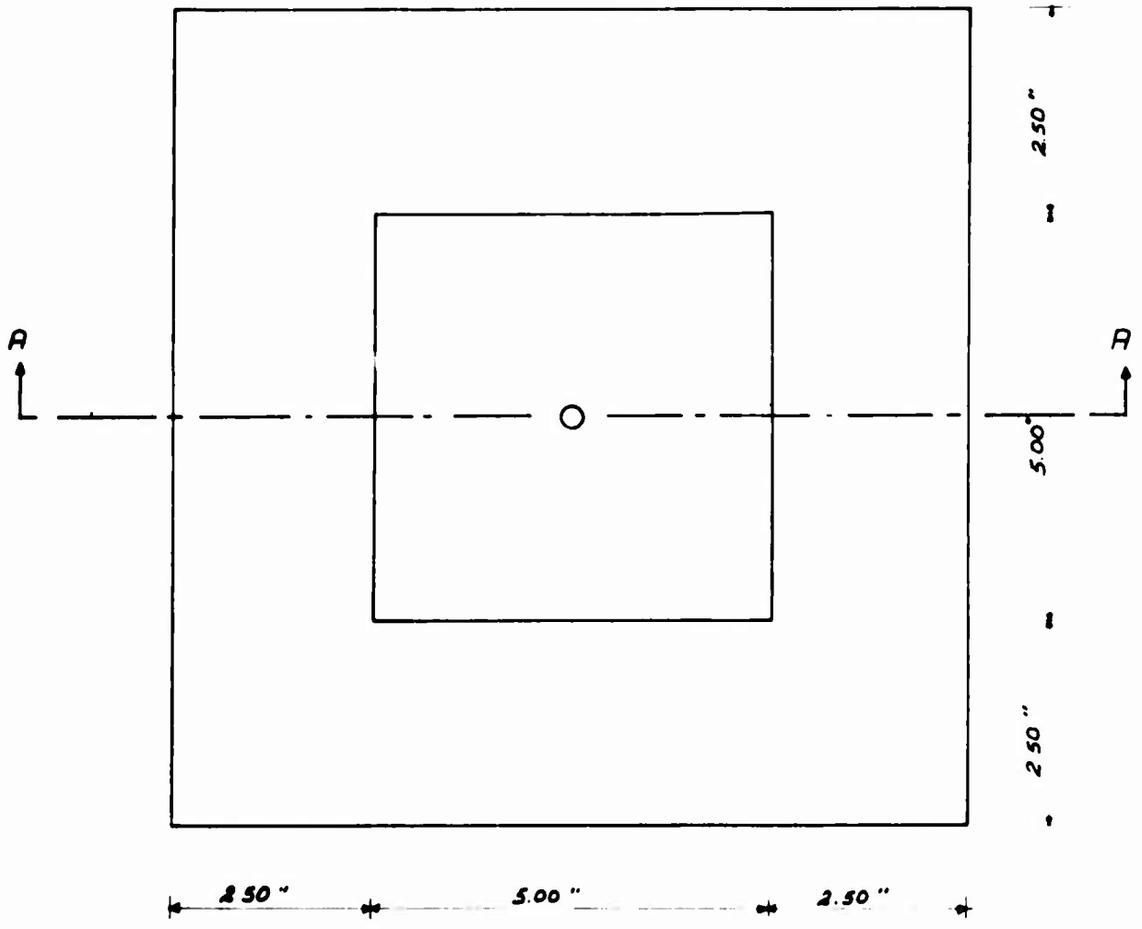

Dimensions in inches

SECTION A - A

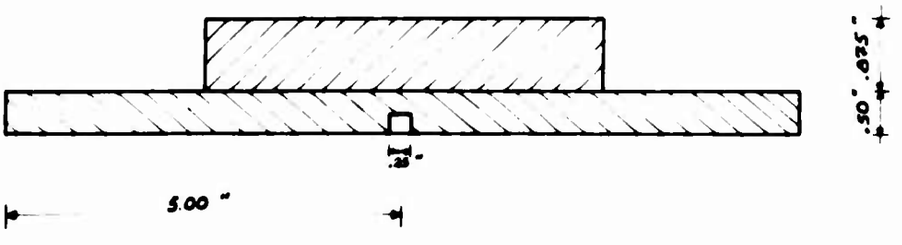

FIG. A-3 TOP PLATE FOR COMPACTION

SCREEDS

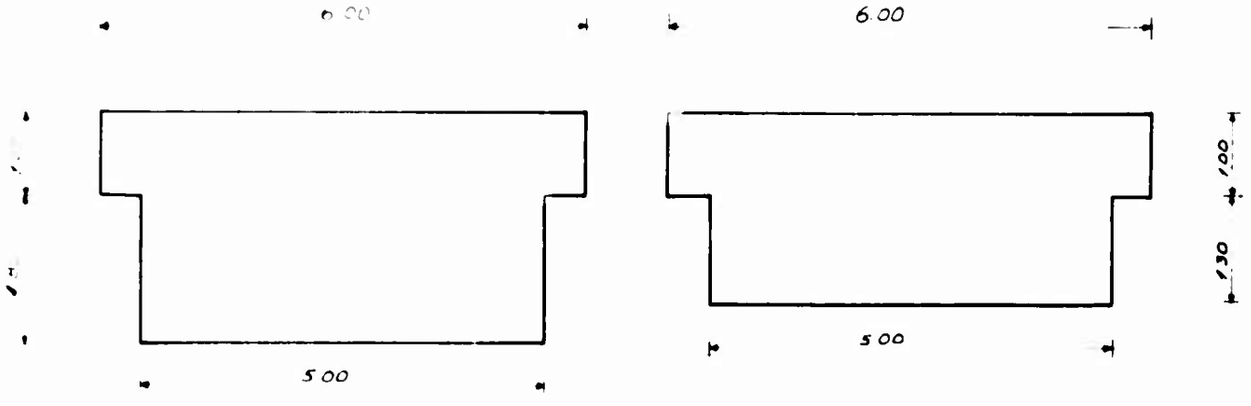

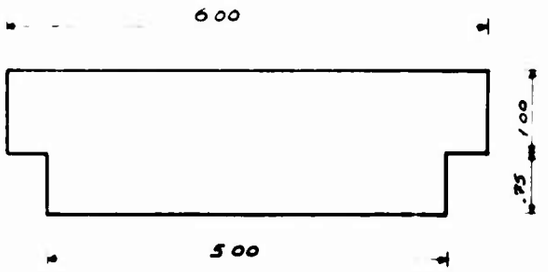

Dimensions in inches

SPACERS

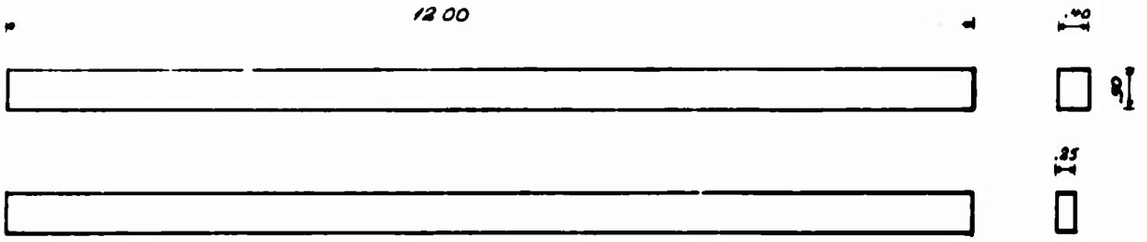

FIG. A-4 ACCESSORIES FOR COMPACTION

EXTRUDING BLOCK

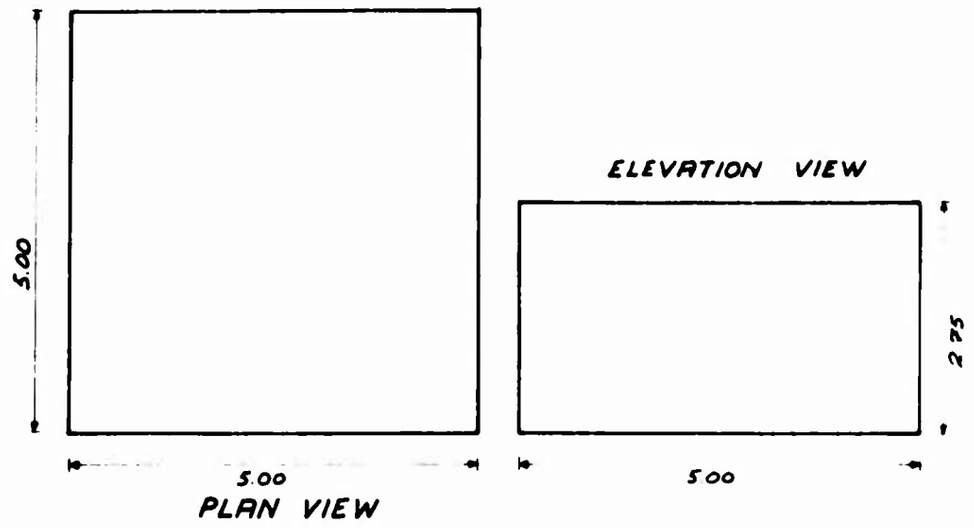

SAMPLE SUPPORT BLOCK

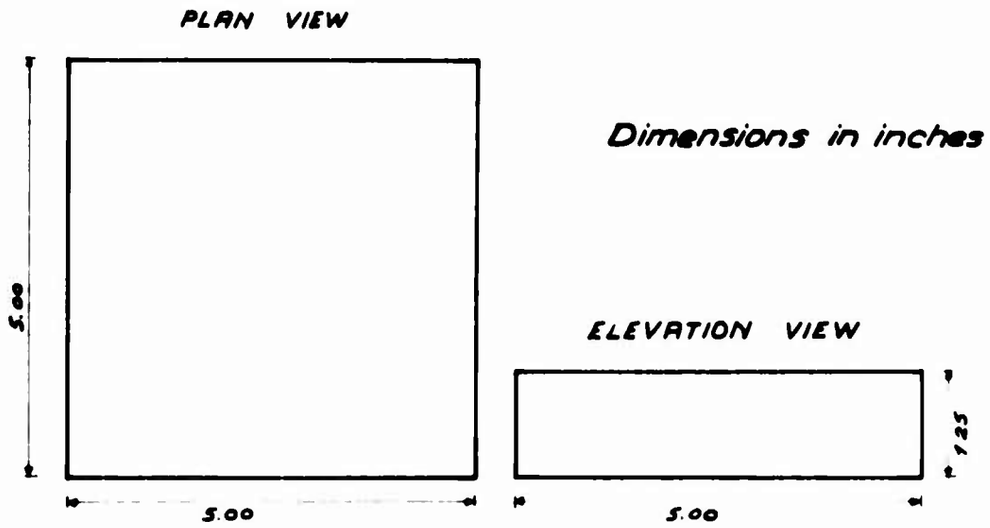

FIG. A-5 ACCESSORIES FOR COMPACTION

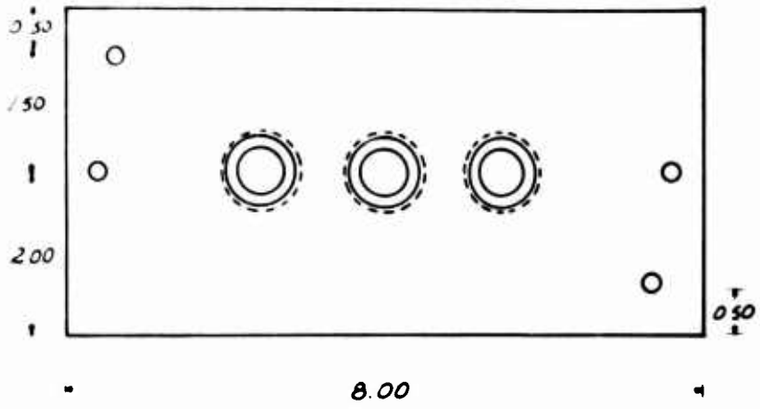

SECTION A-A

Dimensions in inches

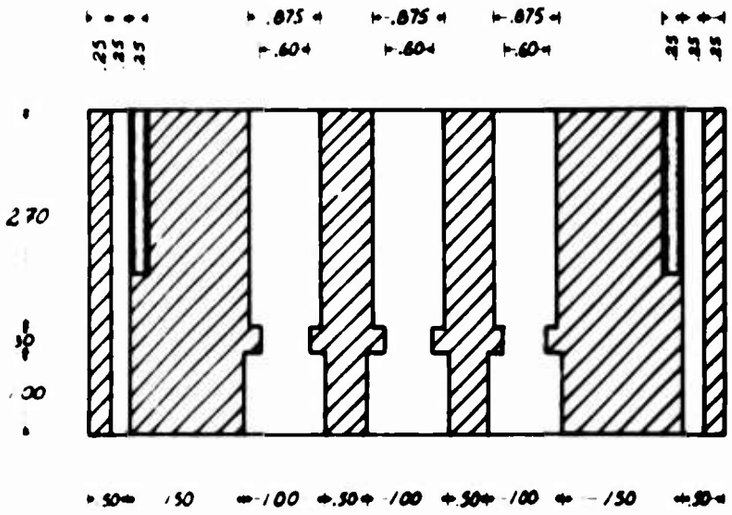

FIG. A-6 GUIDING BLOCK

TESTING CYLINDERS

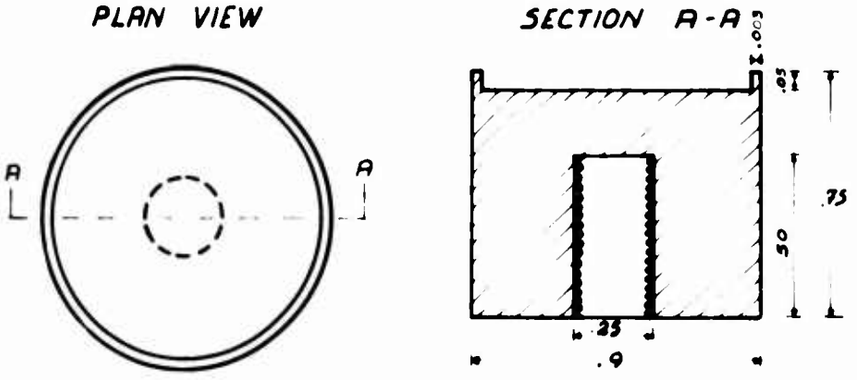

Dimensions in inches

SHAFTS

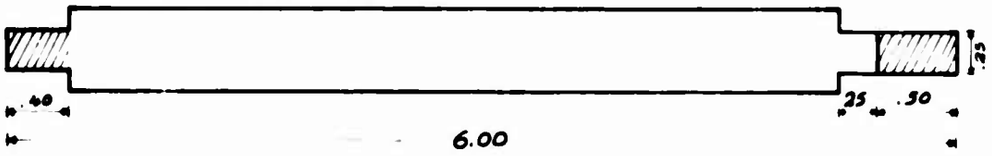

FIG. A-7 ACCESSORIES FOR TENSION TESTING

APPENDIX B

CALIBRATION DATA FOR THE MEASURING DEVICES.
WIRING SYSTEM OF THE TRANSDUCER'S OUTPUT
TERMINAL BOX.

DCDT CALIBRATION DATA

TABLE B-1

Dial Reading (in.)	Output Voltage "Vo" (mv.)	Input Voltage "Vi" (Volts)	Vo/Vi ($\frac{mv}{v.}$)
0.9500	2.3781	6.3653	0.3736
0.9000	2.0531	6.3653	0.3225
0.8500	1.7238	6.3655	0.2708
0.8000	1.3903	6.3654	0.1659
0.7500	1.0559	6.3654	0.1659
0.7000	0.7207	6.3654	0.1132
0.6500	0.3854	6.3654	0.0606
0.6000	0.0507	6.3654	0.0080
0.5500	-.2852	6.3654	-0.0448
0.5000	-.6196	6.3655	-.0973
0.4500	-.9543	6.3655	-.1499
0.4000	-1.2886	6.3655	-.2024
0.3500	-1.6224	6.3654	-.2549
0.3000	-1.9553	6.3655	-.3072
0.2500	-2.2848	6.3655	-.3589
0.2000	-2.6048	6.3655	-.4092
0.1500	-2.9092	6.3656	-.4570
0.2500*	-2.2845	6.3656	-.3589
0.3500	-1.6235	6.3655	-.2550

*Displacement reversed to re-check previous calibration points.

Table B-1 (continued)

0.4510	-.9542	6.3655	-.1499
0.5500	-.2855	6.3654	-.0449
0.6500	0.3862	6.3655	+.0607
0.7500	1.0567	6.3654	+.1660
0.8500	1.7250	6.3654	+.2710
0.9500	2.3807	6.3653	+.3740

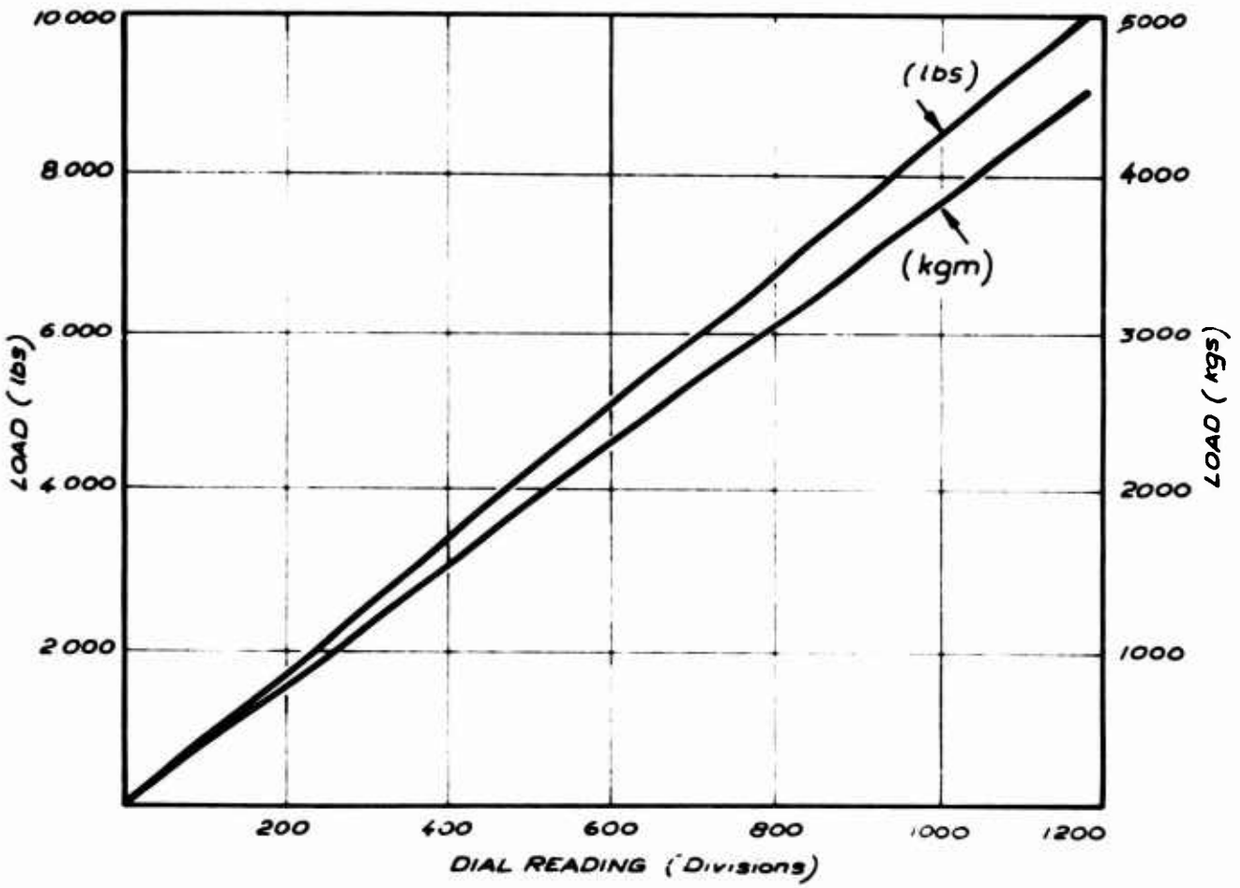

FIG. B.1 PROVING RING NO. 1320 (10.000 lbs. coposity)

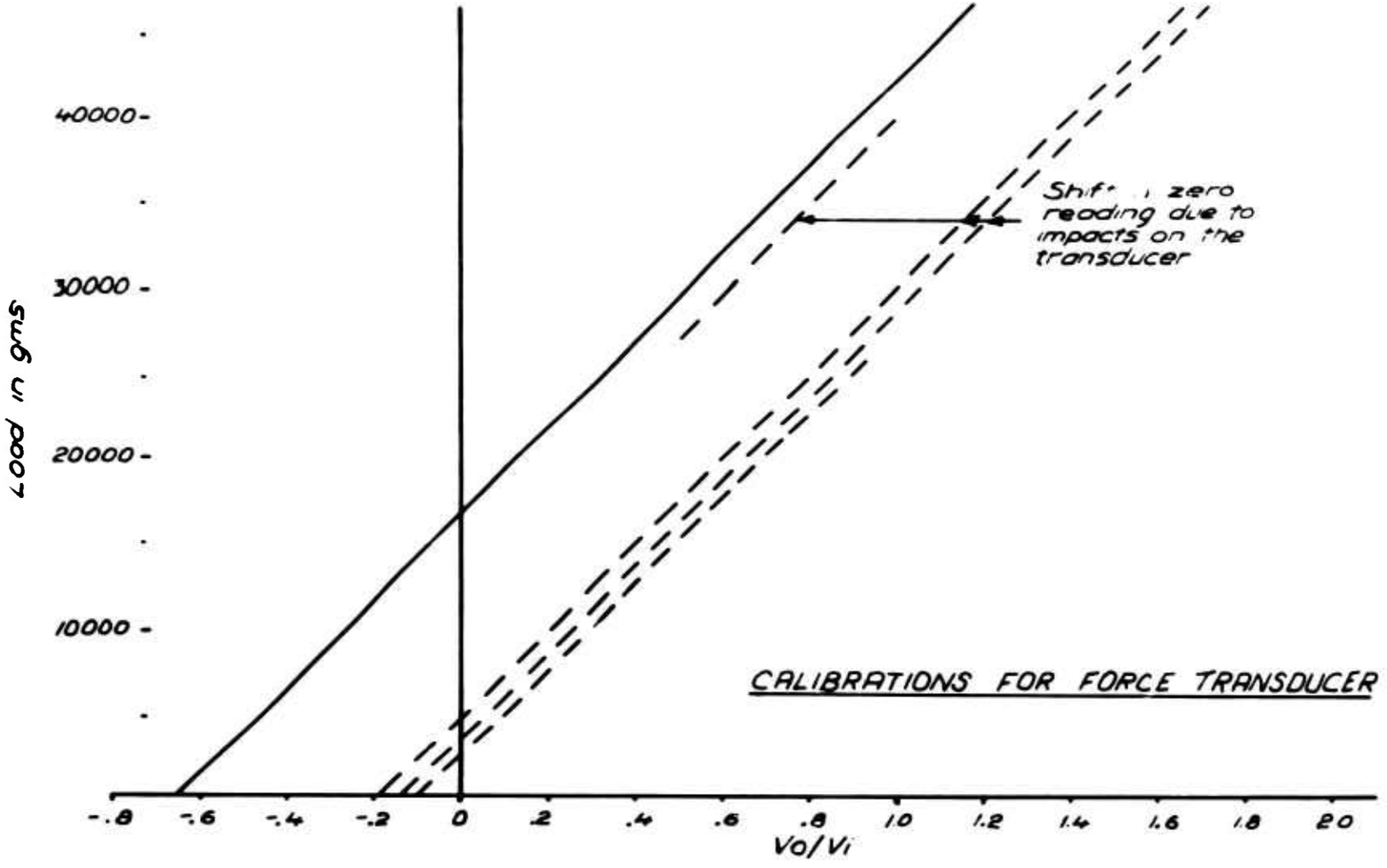

FIG. B.2 FORCE TRANSDUCER CALIBRATIONS

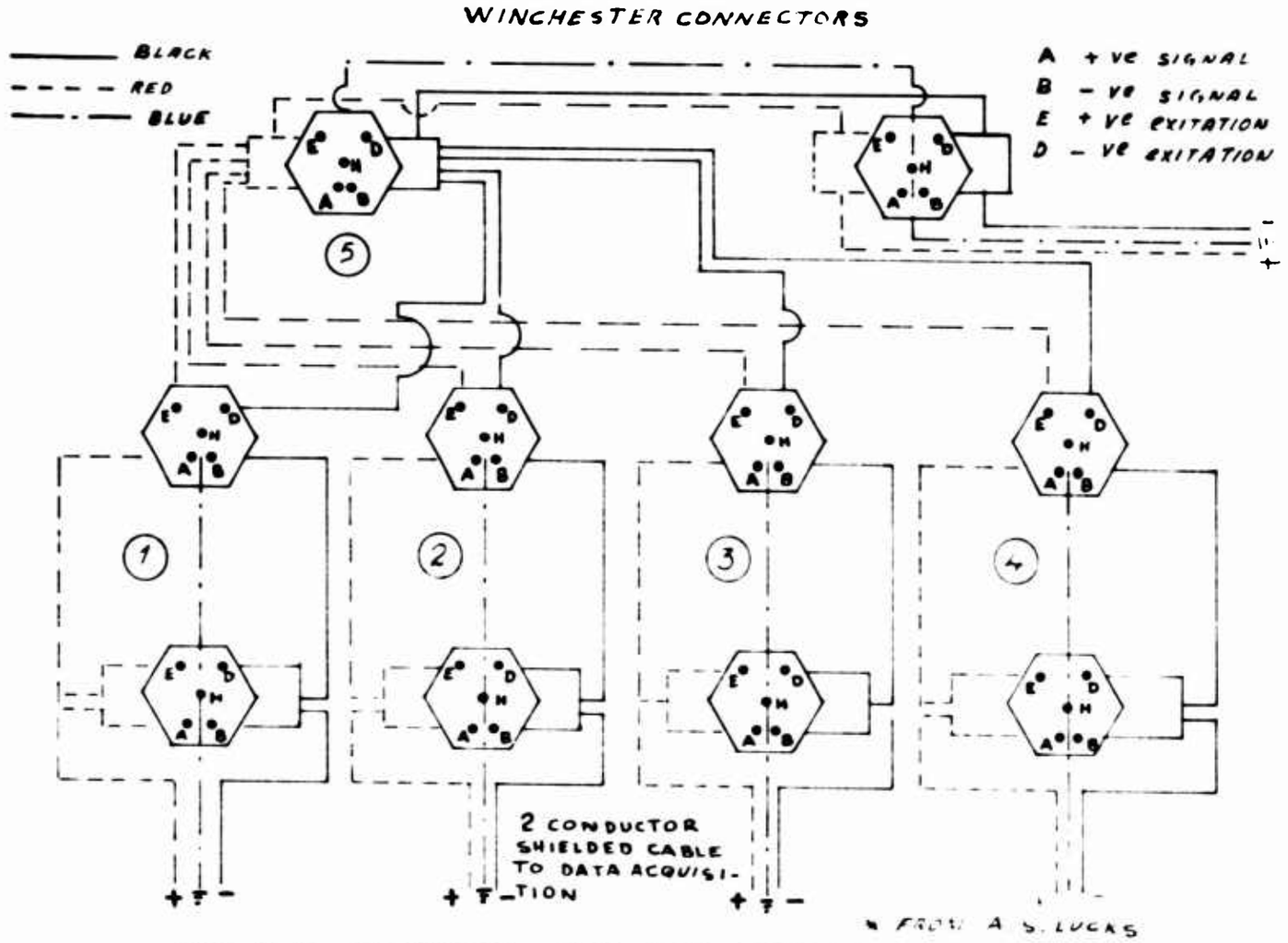

FIG B 3 TERMINAL BOX FOR TRANSDUCERS

APPENDIX C

PROPERTIES OF UNTREATED M-21 SOIL AND M-21 + 5% PORTLAND CEMENT, AND COMPACTION DATA OF SPECIMENS I, II, AND III.

Table C-1

PROPERTIES OF UNTREATED

M-21 AND M-21+5% CMEENT

		M-21	M-21+5% Cement
Textural Composition, % by wt.			
Sand	2 mm to 0.06 mm	42	
Silt	0.06 mm to 0.002 mm	43	
Clay	< 0.002 mm	15	
Physical Properties			
Liquid Limit, %		20.5	21.2
Plastic Limit, %		14.7	17.6
Plasticity Indes, %		5.8	3.6
Specific Gravity		2.75	
Max. Dry Density(1)	lb./cu.ft.	123.0	
Optimum Water Content(1), %		13.2	
Classification			
Unified		ML-CL	
AASHO		A-4(0)	
Chemical Properties (2)			
Organic Matter, % by wt.		0.2	
Cation Exchange Capacity	mg/100gm	10	
Glycol Retention	mg/gm	22	
Mineralogical Composition(2)			
Clay Composition, % by wt.		30	
Illite: Montmorillonoid(3)		1:0	
Free Iron Oxide, % Fe_2O_3		2.9	

(1) Static compaction, 400 psi effort.

(2) For minus 0.074 mm-fractions obtained from a different batch of soil.

(3) Most montmorillonoid mineral is montmorillonite.

[From Wissa and Ladd (1964) MIT Soils Publication No. 164.]

MASSACHUSETTS INSTITUTE OF TECHNOLOGY
SOIL ENGINEERING LABORATORY
DURABILITY TENSILE TEST
TABLE C-2

Soil Classification	ML - CL	Sample Name	I
Specific Gravity	2.70	Mixing Method	Standard
Stabilization Additive	Portland Cement	Weight of Additive	45 gms
Method of Compaction	Static	Curing Method	cold
Compactive Effort	400 psi	Curing Time	58 days

Water Content			Units
Container #	26	18	gms
Wt. of Container + Wet Soil	29.62	35.900	"
Wt. of Container + Dry Soil	27.31	32.866	"
Wt. of Water	2.31	3.034	"
Wt. of Container	12.29	12.10	"
Wt. of Dry Soil	15.02	20.766	"
Water Content w	15.38	14.61	%

Volume of Specimen	0.0159 ft³
Total Weight of Specimen	2.106 lbs
Wet Density	132.35 pcf
Avg Water Content	14.99 %
Avg Dry Density	115.08 pcf

MASSACHUSETTS INSTITUTE OF TECHNOLOGY
SOIL ENGINEERING LABORATORY
DURABILITY TENSILE TEST
TABLE C-3

Soil Classification	ML-CL	Sample Name	II
Specific Gravity	2.70	Mixing Method	Standard
Stabilization Additive	Portland Cement	Weight of Additive	45 gms.
Method of Compaction	Static	Curing Method	Hot
Compactive Effort	400 psi	Curing Time	60 days

Water Content			Units
Container	27	28	gms.
Wt. of container + wet soil	43.80	49.22	"
Wt. of container + dry soil	39.95	45.12	"
Wt. of water	3.85	4.10	"
Wt. of Container	12.05	12.24	"
Wt. of dry soil	27.90	32.88	"
Water Content "w"	13.80	12.47	%

Volume of Specimen	0.0159 ft³
Total weight of Specimen	2.053 lbs
Wet density	129.0 pcf
Avg. Water Content	13.13 %
Avg. Dry Density	114.03 pcf

MASSACHUSETTS INSTITUTE OF TECHNOLOGY
SOIL ENGINEERING LABORATORY
DURABILITY TENSILE TEST
TABLE C-4

Soil Classification	ML-CL	Sample Name	III
Specific Gravity	2.70	Mixing Method	Standard
Stabilization Additive	Portland Cement	Weight of Additive	45 gms.
Method of Compaction	Static	Curing Method	Hot
Compactive Effort	—	Curing Time	14 days

Water Content			Units
Container	18	36	gms.
Wt. of container+wet soil	34.393	37.448	"
Wt of container+dry soil	31.611	34.356	"
Wt of water	2.782	3092	"
Wt of Container	12.00	12.290	"
Wt of dry soil	19.511	22.066	"
Water Content "ω"	14.25	14.01	%

Volume of Specimen	0.0159 ft³
Total weight of Specimen	2.185 lbs.
Wet density	137.33 pcf
Avg. Water Content	14.13 %
Avg. Dry Density	120.33 pcf

FIG. C. 1

GRAIN SIZE DISTRIBUTION

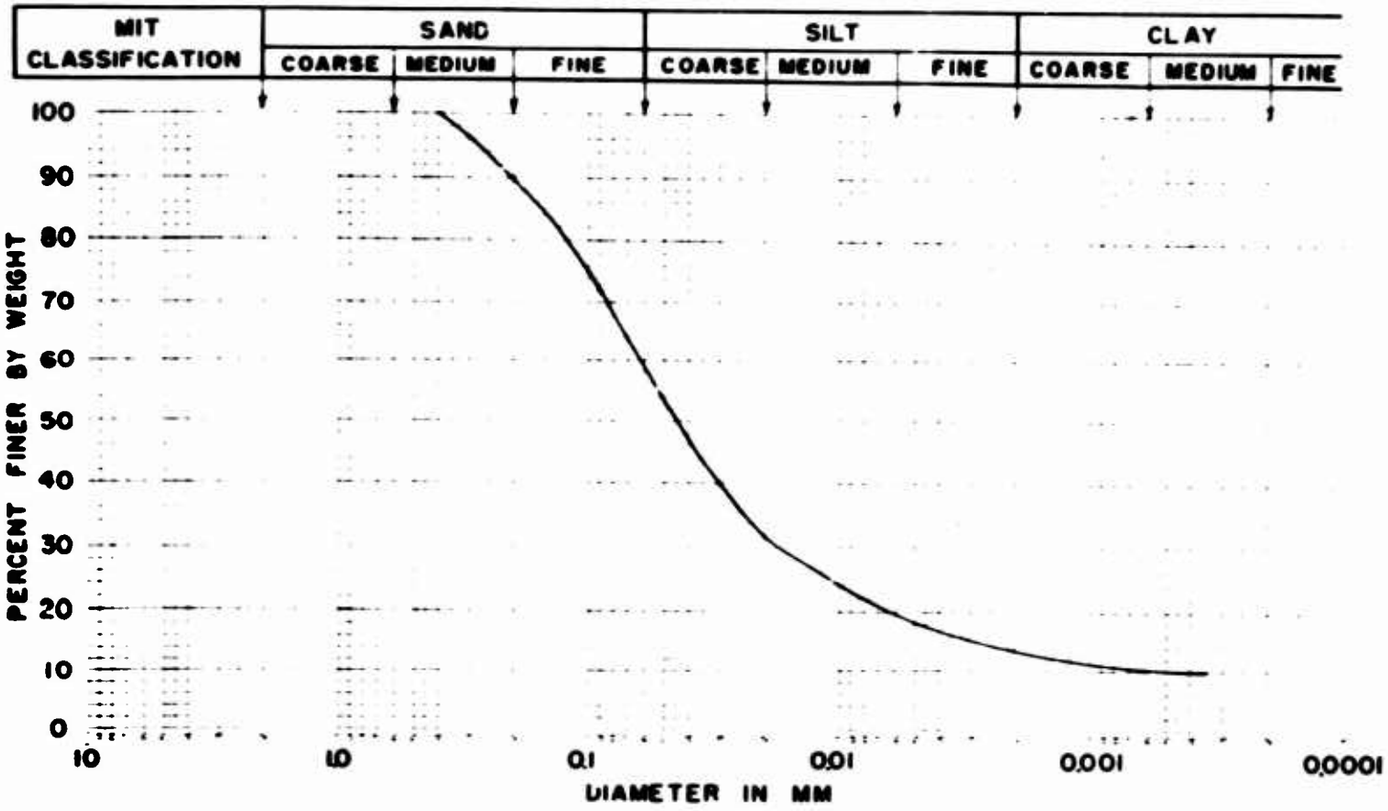

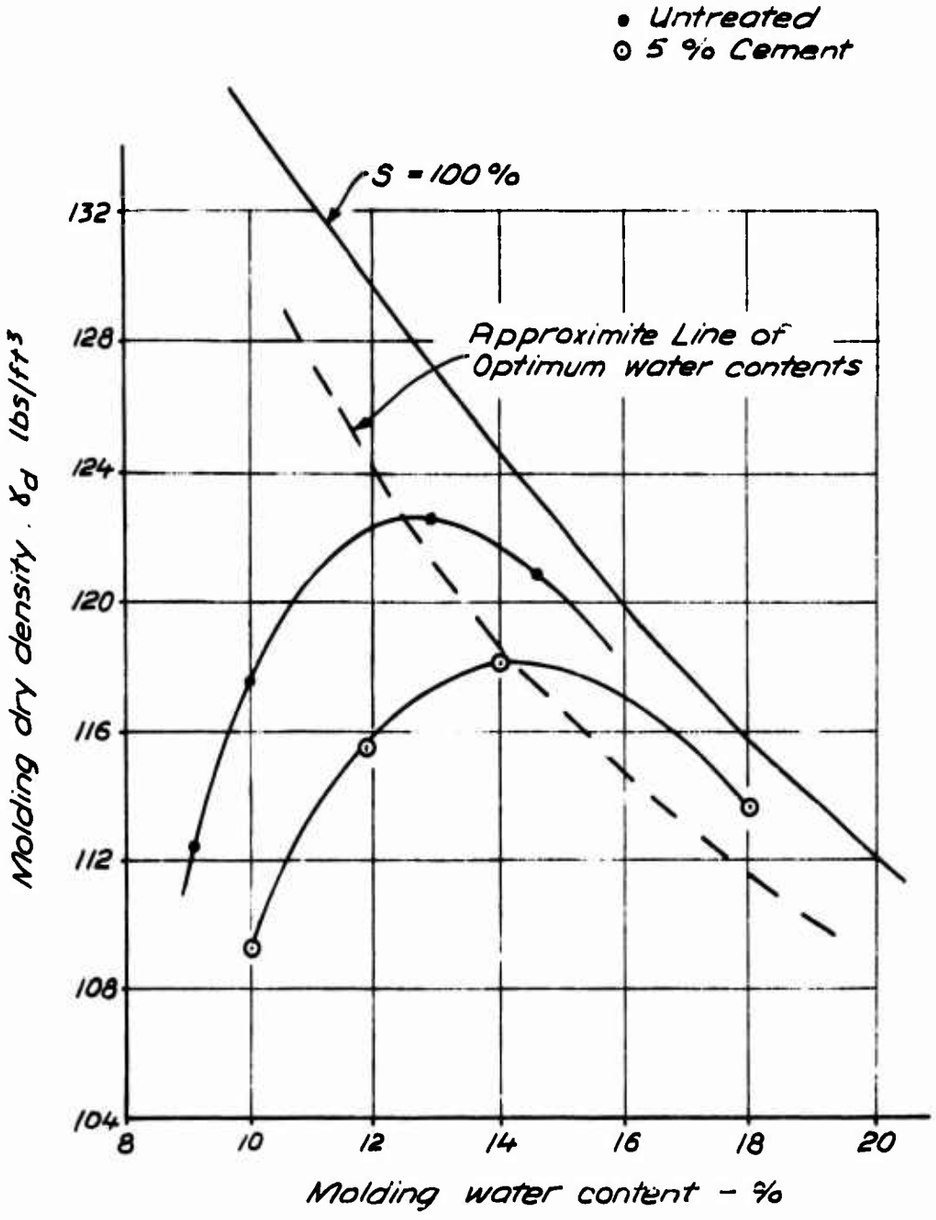

FIG. C.2
MOISTURE - DENSITY RELATIONSHIPS FOR STATIC (400 PSI) COMPACTION OF M-21 SYSTEMS

APPENDIX D

DETAIL DRAWING, ASSEMBLING INSTRUCTIONS, AND SPECIFICATIONS FOR THE REVISED DURABILITY TENSILE TESTING APPARATUS.

DI COMPACTION MOLD AND ACCESSORIES

It is recommended to make the compaction mold of stainless steel with a polished finish on the inside surface, and dimensions as shown in Fig. DI.1.

The other accessory pieces, i.e., the mold base, the top collar and the extruding piece, can be made of aluminum, having dimensions as shown in Figs. DI.2 through DI.4.

DII THE ASSEMBLY FRAME

The assembly frame is built with standard steel members with dimensions as specified in Fig. DII.1. These pieces are bolted together as shown in Fig. DII.2 through DII.4. An assembly drawing of this frame was shown in Fig. 5.1.

DIII SPECIMEN SUPPORTS, GUIDING BLOCK, AND ACCESSORIES

Part numbers refer to Figs. 5.2 and 5.3.

Part No. 1, Fig. DII.1.

This part consists of two identical standard steel channels (Fig. DII.1) to which the base plate (part No. 2) of the specimen supports assembly is bolted. The channels (base channels) are part of the assembly frame (see Fig. 5.1).

Part No. 2, Fig. DIII.1

This is a rectangular aluminum plate 1/2 in. thick, which is bolted to the base channels of the frame. On the top surface of this plate (the base plate), there are two v-shaped grooves running longitudinally (in the y-y direction of Fig. 5.3).

Part No. 3, Fig. DIII.2

This is a rectangular aluminum plate 1/2 in. thick with two longitudinal side walls. On the bottom of the plate, there are two longitudinal v-shaped steel keys which fit into the grooves cut into part no. 2. This permits sliding of part no. 3 and all the other parts attached to it longitudinally with respect to the assembly frame.

Located at the center of each of the side walls of this part is a fine-adjustment screw (screw #4 in Fig. 5.2). The function of these screws is to locate part no. 4 and all the other parts attached to it, transversely (x-x direction) with respect to part no. 2 and the assembly frame. On the top of the rectangular base plate of this part, there is a v-shaped groove, similar to that described for part no. 2, which runs transversely across the plate width (at right angles to the grooves in part no. 2).

Part No. 4, Fig. DIII.3

This is a 1-in.-thick aluminum plate with two longitudinal side walls. The bottom of the plate has two v-shaped steel keys which fit into the grooves in the top of the plate of part no. 3, permitting this part and all other parts attached to it, to slide transversely with respect to the assembly frame with the aid of the

fine-adjustment screws no. 4 previously mentioned.

In the center of each side wall of part no. 4 there is a vertical threaded hole into which bolts no. 1 screw (see Fig. 5.3).

Around the center of the plate is the lower half of a 6-in. I.D. ball race that is press-fitted into it. The dimensions of the groove to take the ball race has not yet been fixed pending details from the ball-race supplier. The depth of this groove and the corresponding groove in Part 5 will be selected to give 1/16-inch clearance between parts no. 4 and 5.

Part No. 5, Fig. DIII.4

This part is a circular plate 10-1/4 inches in diameter with a cut 6-1/8 inch in diameter and 1/2 inch deep to house a porous stone and the soil-cement specimen.

On the bottom side of the plate, the upper half of the ball race mentioned in the description of part no. 4 is press fit. In this way, part no. 5 and all the other parts attached to it can rotate around a central axis with respect to part no. 4 and all the other parts below it.

The porous stone is 6 inches in diameter and is placed on the bottom of the cut. The soil specimen is placed on the porous stone. There is 1/8-inch clearance between the diameter of the cut and the diameter of the specimen; this is necessary to introduce the soil specimen without damage.

A thin index mark, not shown in the drawings, is placed on the top side of the plate along a diameter. When the sample is placed in the cylinder, the reference

pin embedded in its side after compaction is lined up with the index mark. In this manner, after the specimen has been taken out of the testing assembly to subject it to weathering cycles, it can be relocated back into its original position before performing more tensile tests.

The selection of the testing sites is achieved by means of six pins, 2 in. long, screwed 1/2 in. in the plate part no. 5, at equal distances around the circumference (at 60°).

The guiding block, which is part no. 6, can then be located in six different circumferential positions which are determined by the six pins.

An outer O-ring groove on the top surface of the plate accommodates a Lucite ring (Fig. 5.3). The Lucite ring is bolted to the base plate. This provides a water chamber for soaking the specimens during testing.

Part No. 6, Fig. DIII.5

This part is the guiding block, which is a sector of a solid cylinder with a central angle of 140°, 3.5 in. in radius, and 4 in. high. It contains three bored holes through which the testing shafts run guided by two high-precision ball bushings for linear motion. Three one-inch-deep holes in the bottom of the block located on a radius of 3-3/8 in., one in the center radius of the sector and the other two at 60° on each side of it, match up with any three of the locating pins in part no. 5. Therefore, the guiding block can be located with respect to part no. 5, in six different circumferential positions 60° apart. If this is done, the testing shafts will mark a total of 18 different testing locations, twelve of them

on a circumference having a radius of 2-1/4 in. from the center of the specimen to the center of the shaft location, and the remaining six on a circumference of 1-1/8 in. radius. In this manner, because the loading caps are 0.9 in. in diameter, it is possible to select 18 tension test sites on one surface of a specimen that has a diameter of six inches with a minimum of 1/4-in. separation between adjacent test sites.

Part No. 7, Fig. DIII.6

This part is a Lucite ring which can be attached to part no. 5 as shown in Fig. 5.3. The function of this part is to provide a watertight reservoir around the place where the soil specimen is located. This permits running tensile tests on the soil specimen in a submerged condition.

Part No. 8, Fig. DIII.7

This part, named "clamping ring and bar", is an aluminum ring with two arms as shown in Fig. DIII.7. The function of this piece is to hold the guiding block sector fixed during testing. The procedure is to place the clamping piece over the top surface of the guiding block, passing the two bolts no. 1 (Fig. 5.3) through the holes in the extreme of the arms of the clamping piece, prior to testing.

The clamping piece is then fixed by means of the nuts no. 1, since the bolts are screwed into part no. 4 and then the clamping piece holds parts no. 4, 5, and 6 together with the soil specimen as a unit.

Part No. 9, Fig. DIII.8

This part, which has been named the "assembly-holding bar", consists of two identical rectangular steel bars, which are slotted as shown in Fig. DIII.8.

The assembly-holding bars are fastened to the base channels of the frame by bolts no. 2 in Fig. 5.2. Details of these bolts are given in Fig. DIII.9. The assembly-holding bars clamp the shoulders of part no. 4. When the nuts no. 2 are fastened, part no. 4 is fixed. In order to move the assembly longitudinally, nuts no. 2 must be loosened. This movement is needed to align the test sites at the two testing radii with the force-application system.

DIV FORCE-APPLICATION SYSTEM (DRIVE MECHANISM)

Part numbers of the drive mechanism refer to Figs. 5.4, 5.5 and 5.6. Detail drawings of the parts are given in Figs. DIV.1 through DIV.8 and specifications for commercially available pieces are given in Table DIV.1.

Parts no. 1 through 5 are pieces of aluminum plate and angles assembled as shown in Fig. 5.6. They support the gear motor, the reduction system, and the screw jack (part no. 6).

Parts no. 7, 10, and 12 are stainless steel shaft couplings (see Fig. DIV.6).

Part no. 8 is a 60 Rockwell case-hardened stainless steel shaft 10-3/4 in. long and 1/2 in. diameter threaded at both ends.

Part no. 9 is the housing for two Thomson linear bearings which guide the shaft described as part no. 8.

Part no. 11 is a 500-lb. capacity load cell for tensile force (BLH type T3P2B).

Part no. 13 is the testing shaft.

5.2.3.1 Operation

The output shaft of the gear motor rotates at a speed of 30 rpm. Part no. 18, which is an INSCO multi-speed changer (Model no. 06753), can be set at different reduction ratios between a 1:1 and 1:30; therefore, if a ratio of 1:30 is selected, for example, the rotation of the output shaft (part no. 22 would be 1 rpm. This shaft feeds Part no. 14 which is a step-function speed reducer (INSCO Model no. 00140), in which different reduction ratios between 1:1 and 1:1000 can be selected. If, for example, a ratio of 1:1000 is selected, the output shaft (part no. 23) would rotate with a speed of 1×10^{-4} rpm. This rotation is the input to the worm gear screw jack (part no. 6), which has a ratio of 5:1 (it takes 20 turns of the worm gear for 1 in. displacement of the lifting screw). Therefore the lifting screw has a minimum linear rate of displacement of 5×10^{-6} in./min.

The fastest possible rate of displacement of the lifting screw is 1.5 in./min. However, the maximum load that can be safely applied at the faster speeds is considerably less than the 450 kg. that can be applied at slower speeds due to the torque capacity of the motor and reduction gears at the fastest speed. This limitation is only of academic interest since the deformation at failure in the surface tension test is in the order of 0.001 inches and therefore fast drive speeds are undesirable.

TABLE DIV-1

SPECIFICATIONS FOR COMMERCIALLY AVAILABLE

PIECES OF EQUIPMENT

Part No. in Fig. 5.3	Quantity	Manufacturer	Description
18	1	INSCO	Multi-speed changer model No. 06753
14	1	INSCO	Step-function Speed reducer Model No. 00140
24	1	INSCO	Gear motor (Product No. 07308)
6	1	Templeton, Kenly & Co.	Simplex Uni-Lift, Model JM010, 1000-lb. capacity 5:1 Ratio
11	1	BLH	Load cell Type T3P2B
	2	Thomson	Linear bearing Series XA, No. XA-81402
	4	Sterling Instrument	3/16" bore, flanged ball bearings No. GM-2S

Part No. in Fig. 5.3	Quantity	Manufacturer	Description
17	1	Metal Bellows Corp.	ECONALIGN Flexible coupling No. W2-S45 (one end 0.187" bore, one end 0.250" bore)
15	1	Metal Bellows Corp.	ECONALIGN Flexible coupling No. W2-S5 (both ends 0.375" bore)
16	1	Sterling Instrument	Sleeve coupling No. S023-1
20	1	Sterling Instrument	Sleeve coupling, 0.375" bore both ends

PLAN VIEW

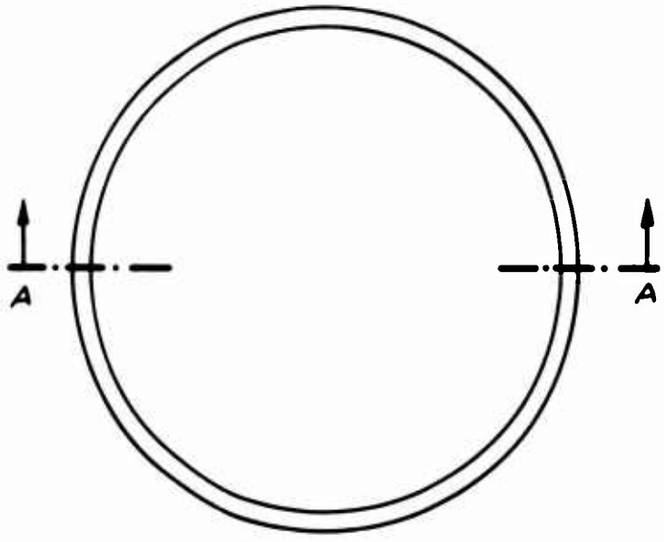

SECTION A-A

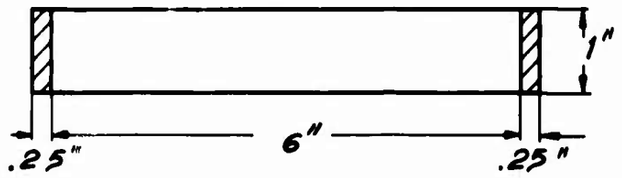

FIG. D1-1 COMPACTION MOLD

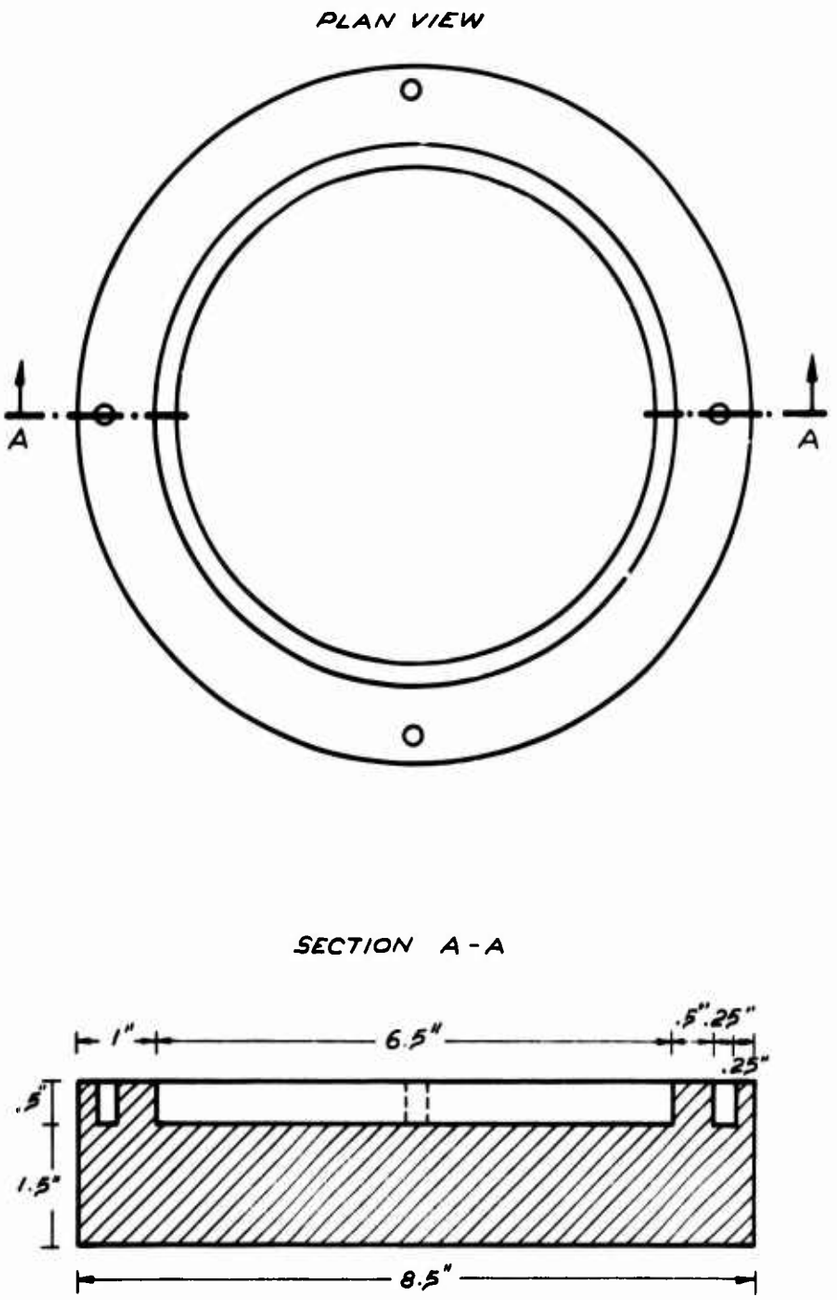

FIG. DI-2 COMPACTION MOLD BASE

PLAN VIEW

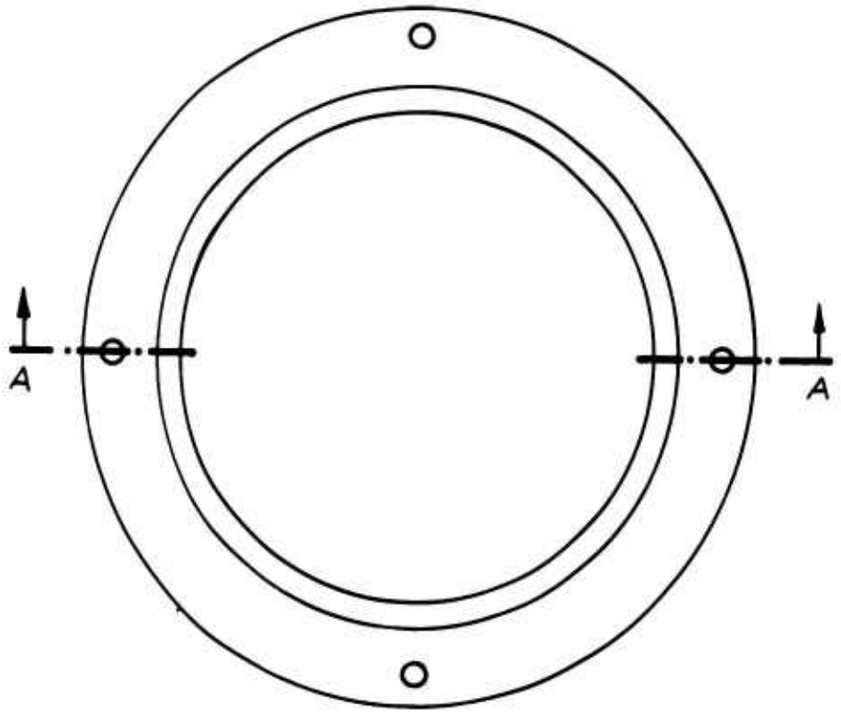

SECTION A-A

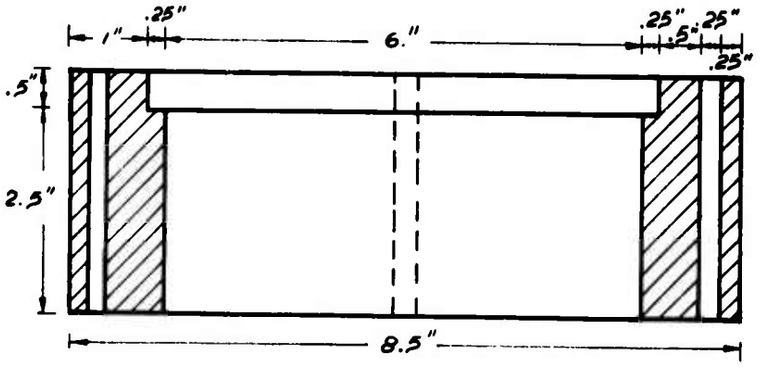

FIG. DI-3 TOP COLLAR FOR COMPACTION

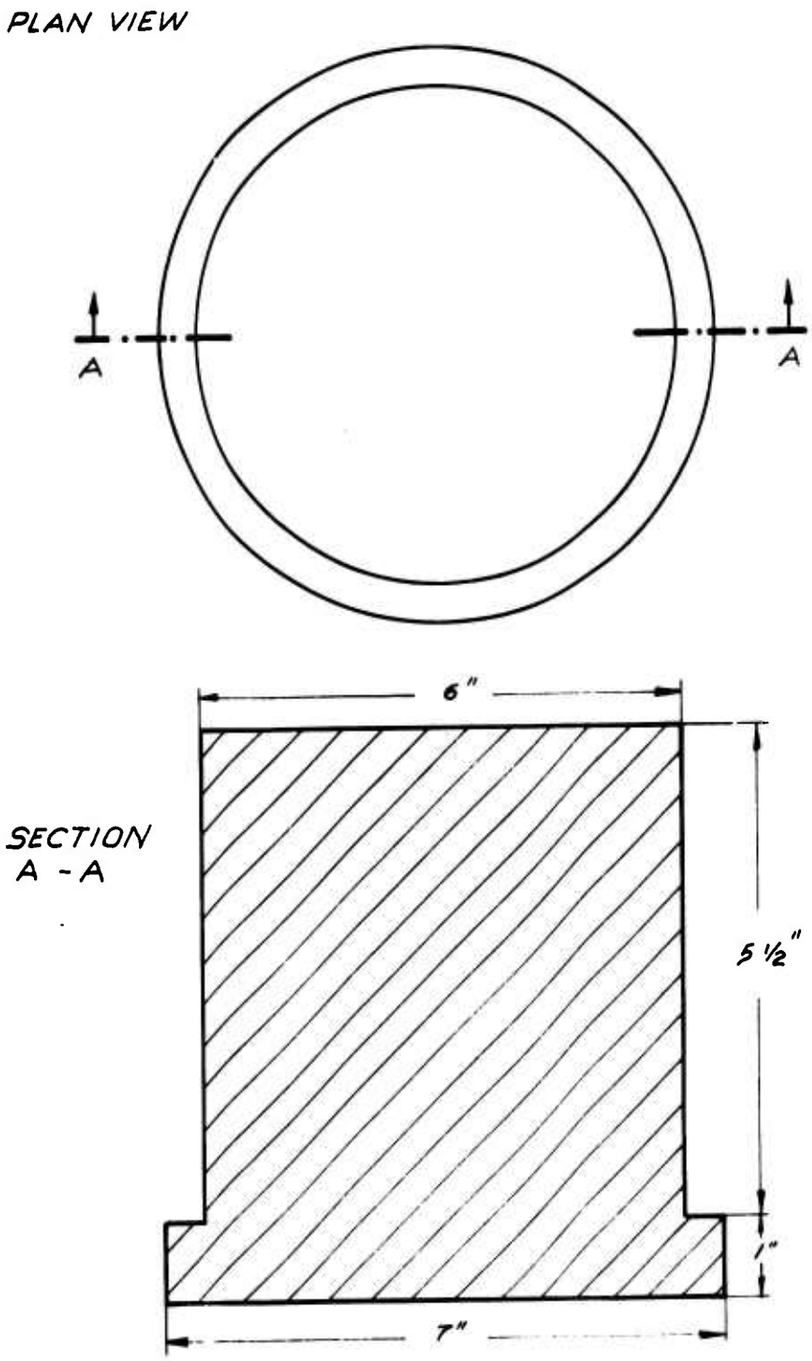

FIG. DI-4 EXTRUDING PIECE

ANGLES

2

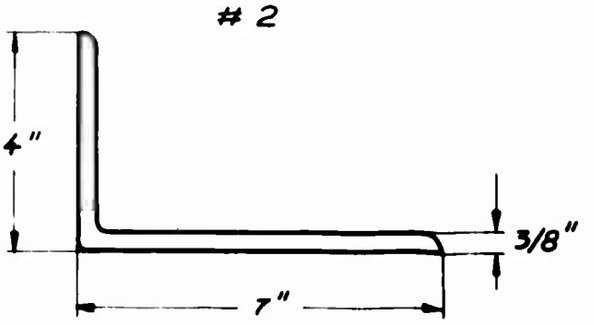

CHANNELS

1

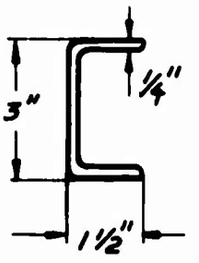

BARS # 3

AMOUNT	l (in)
2	22
2	17

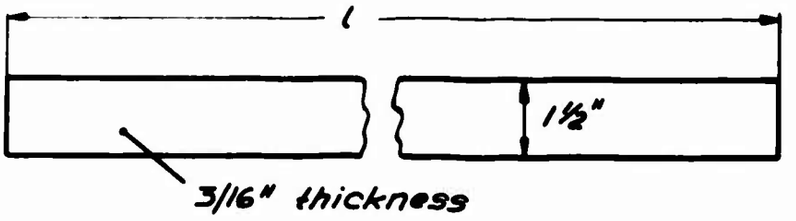

BOLTS # 4

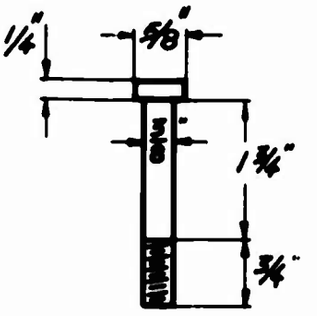

FIG. D II-1 STANDARD MEMBERS FOR ASSEMBLY FRAME

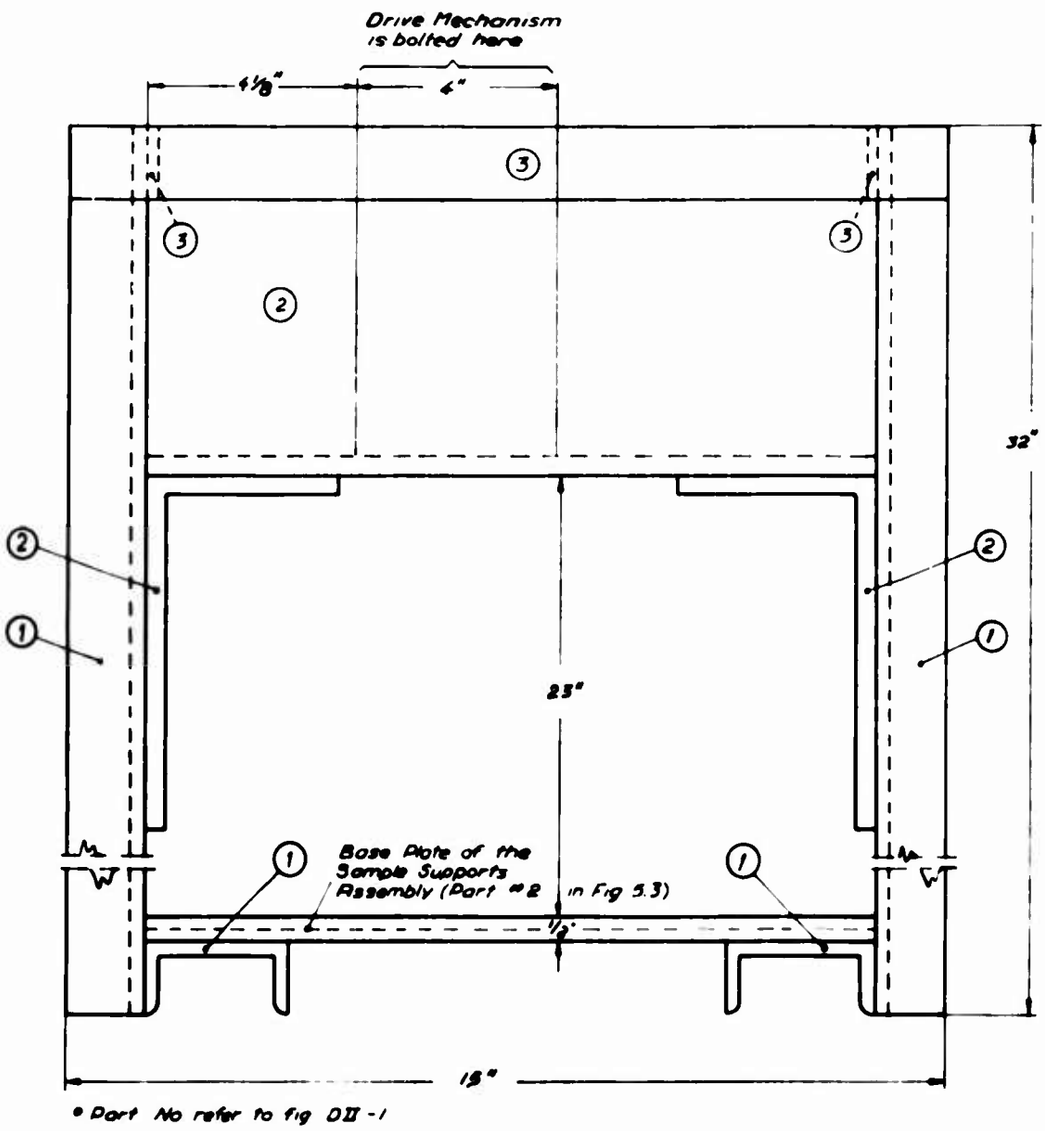

FIG DII-2 FRONT VIEW OF ASSEMBLY FRAME

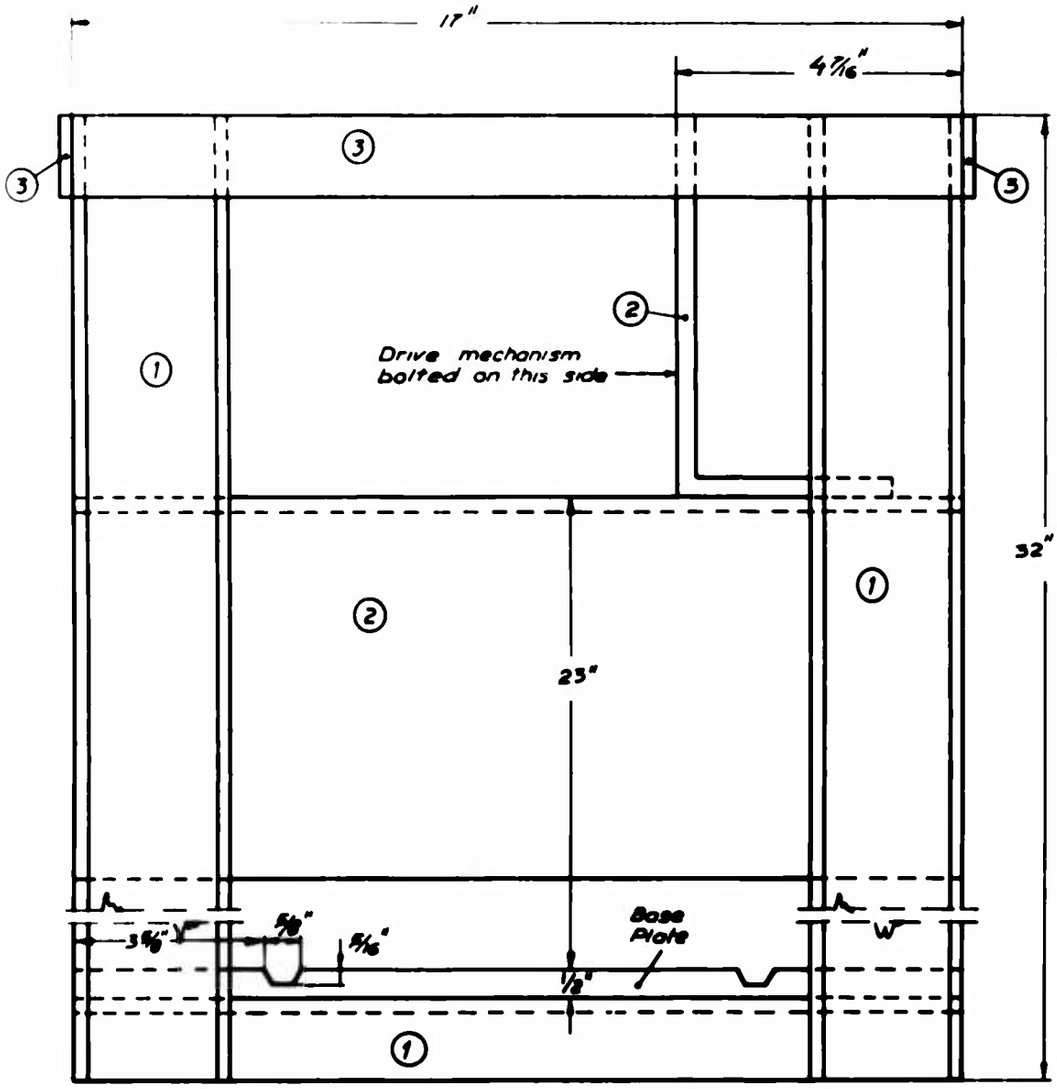

FIG. D II-3 SIDE VIEW
OF ASSEMBLY FRAME

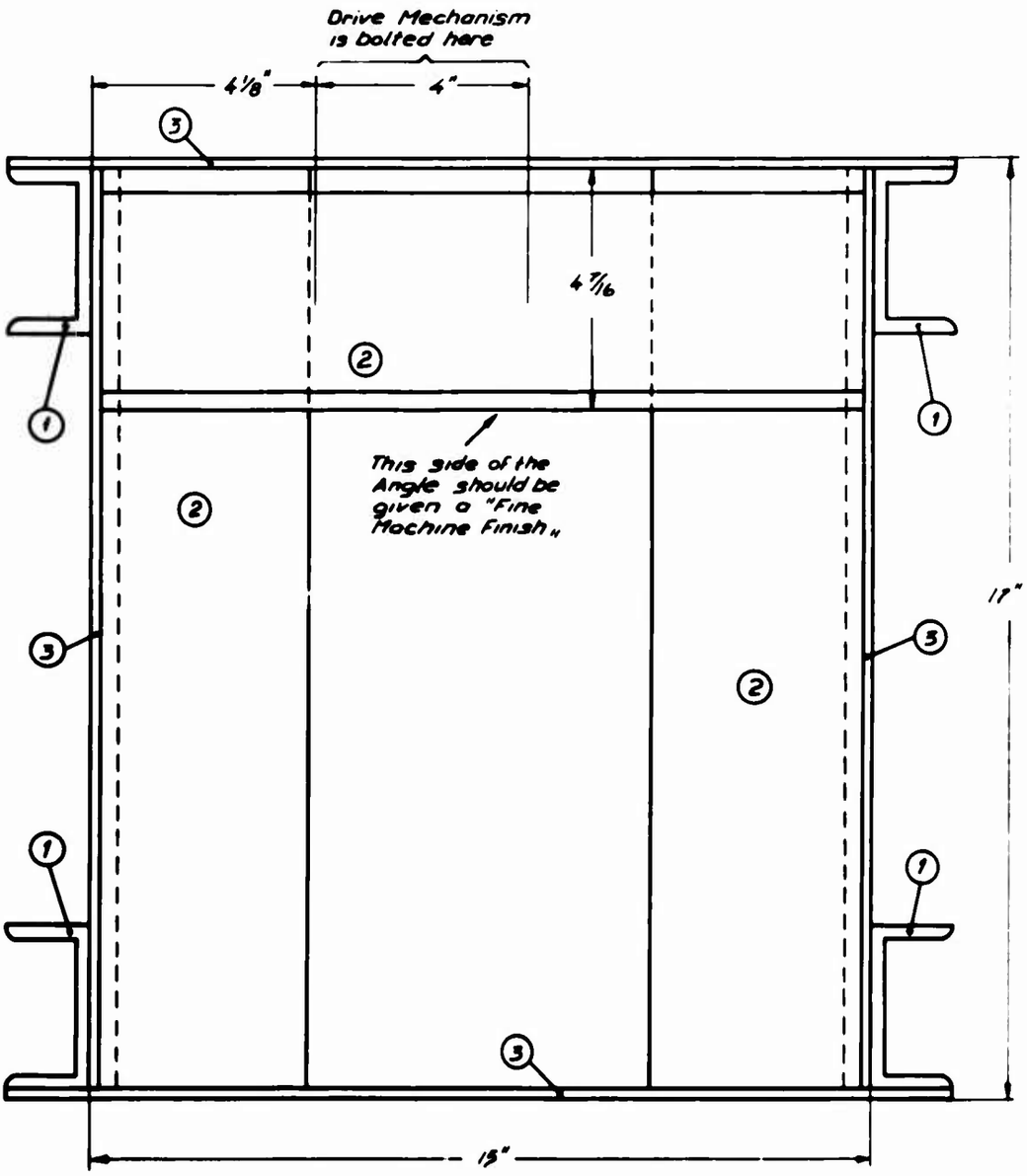

FIG. DII-4 TOP VIEW OF ASSEMBLY FRAME

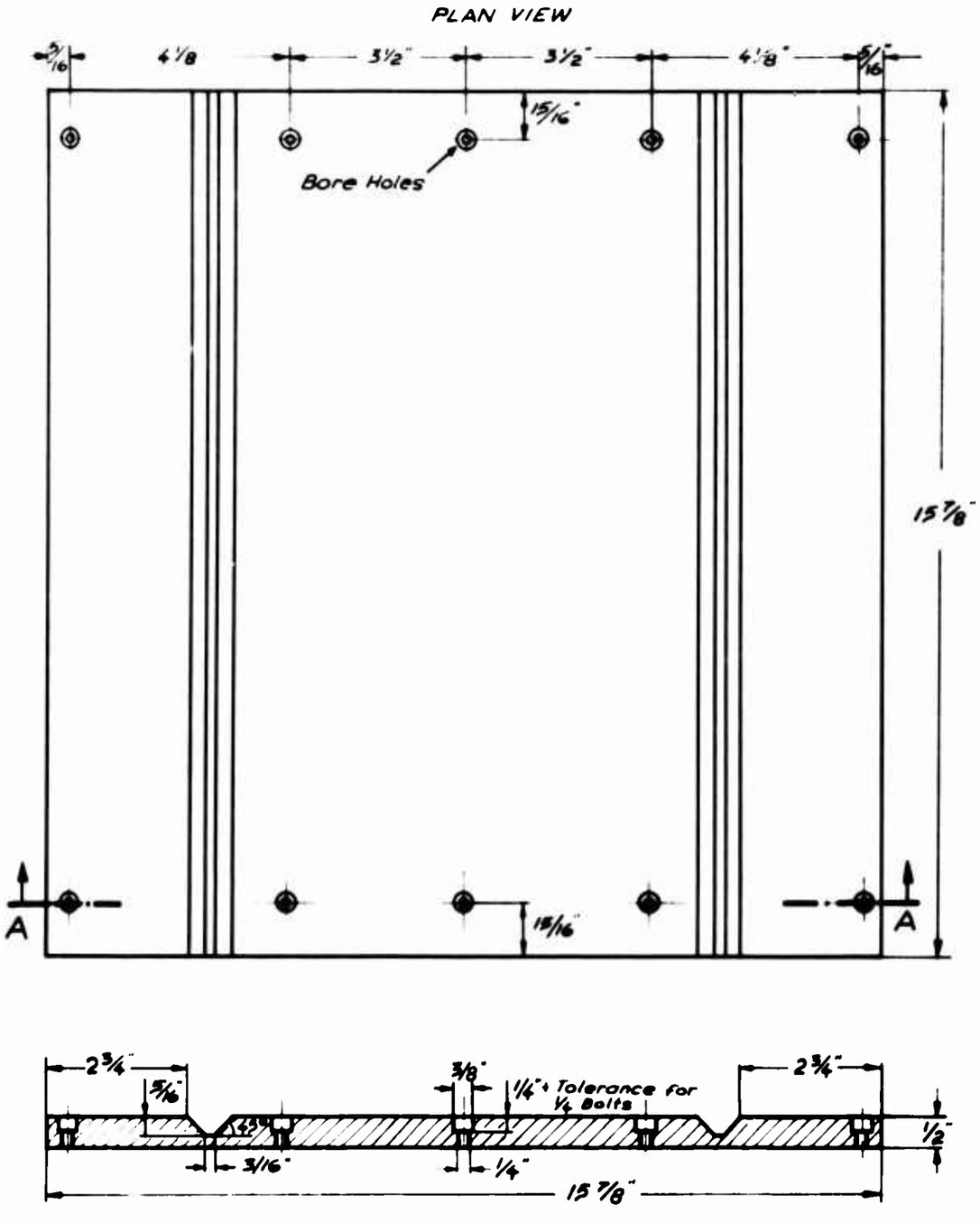

FIG. D III-1 BASE PLATE
(PART NO. 2)

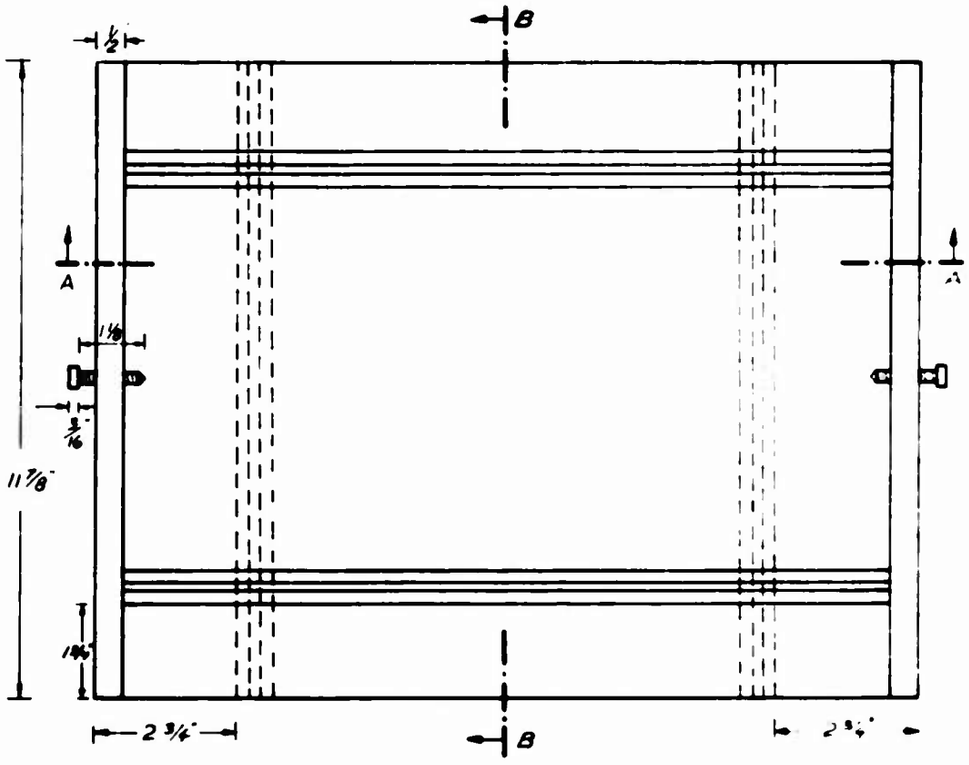

SECTION A - A

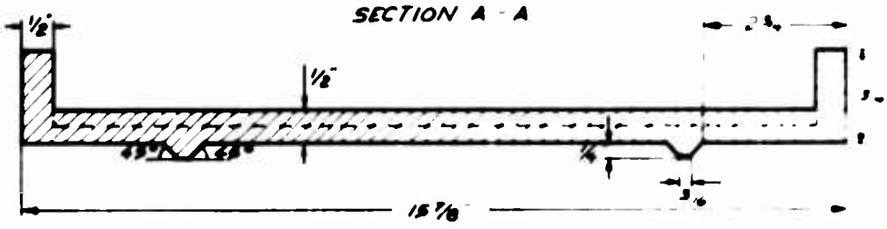

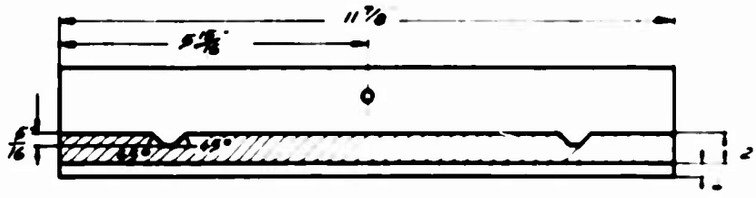

SECTION B - B

FIG. D III-2 LONGITUDINAL SLIDING BASE

(PART NO. 3)

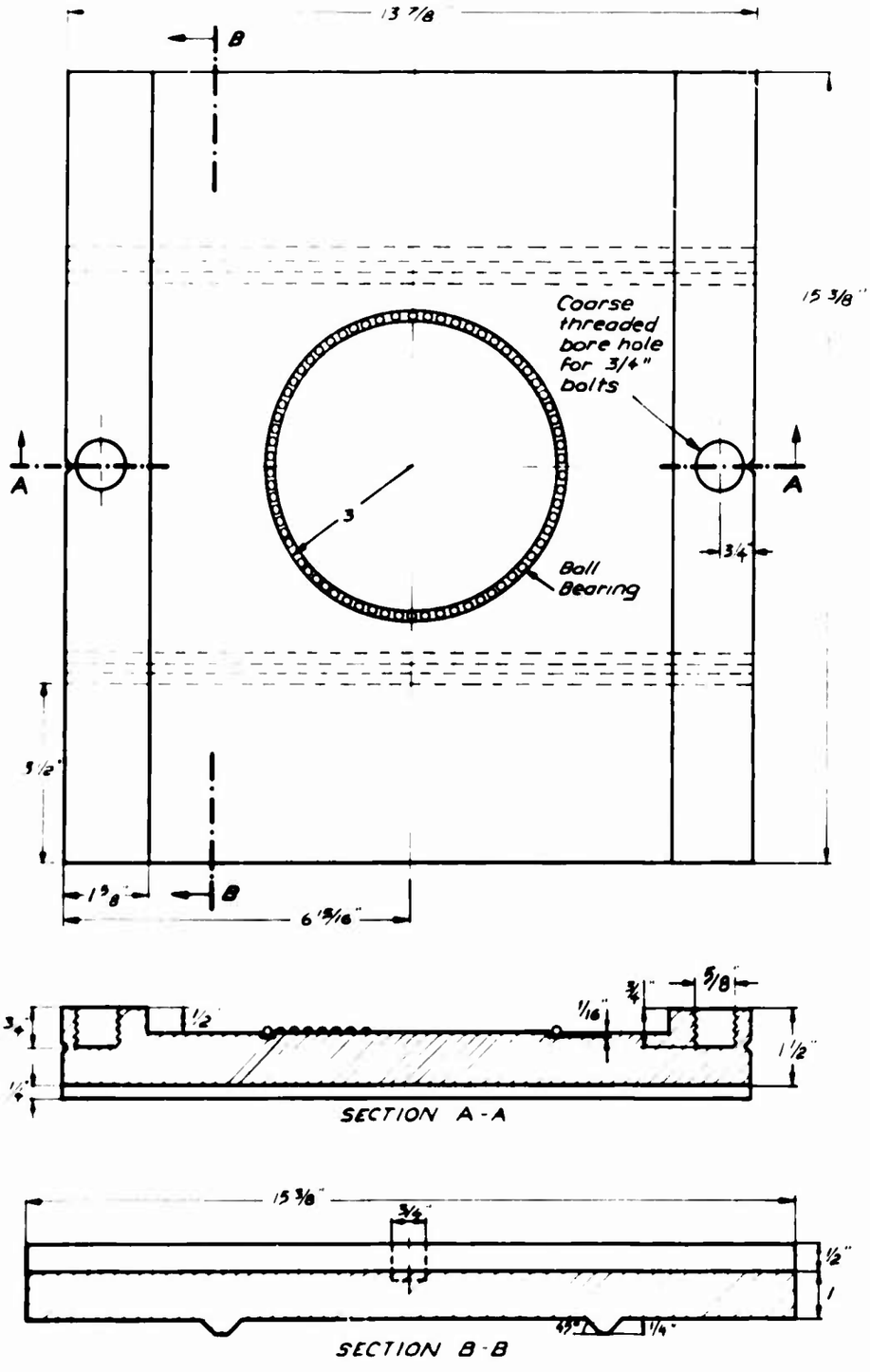

FIG. D III-3 TRANSVERSE SLIDING BASE (PART NO. 4)

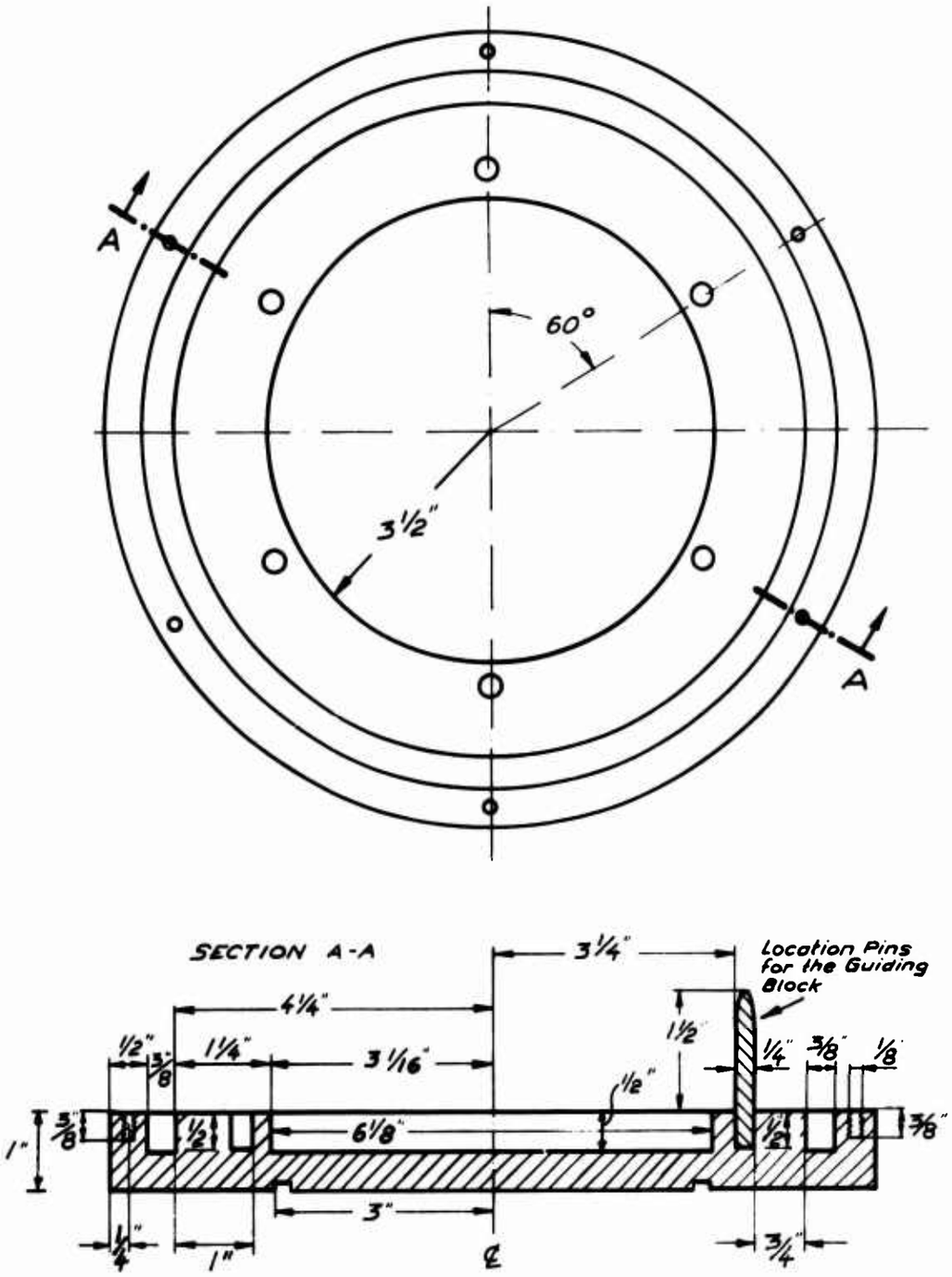

FIG. D III-4 ROTORY BASE

(PART NO. 5)

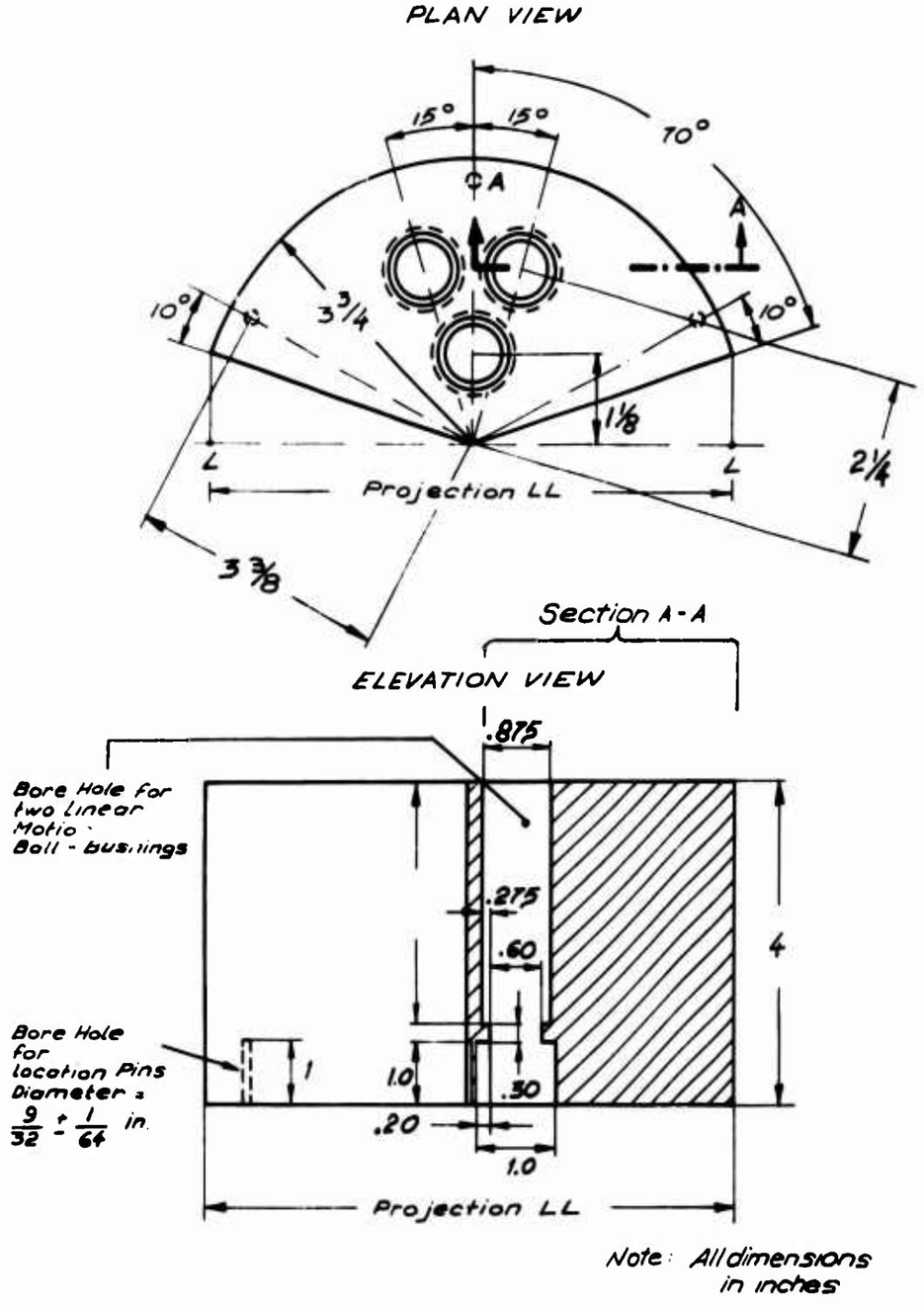

FIG. D III - 5 GUIDING BLOCK

(PART NO. 6)

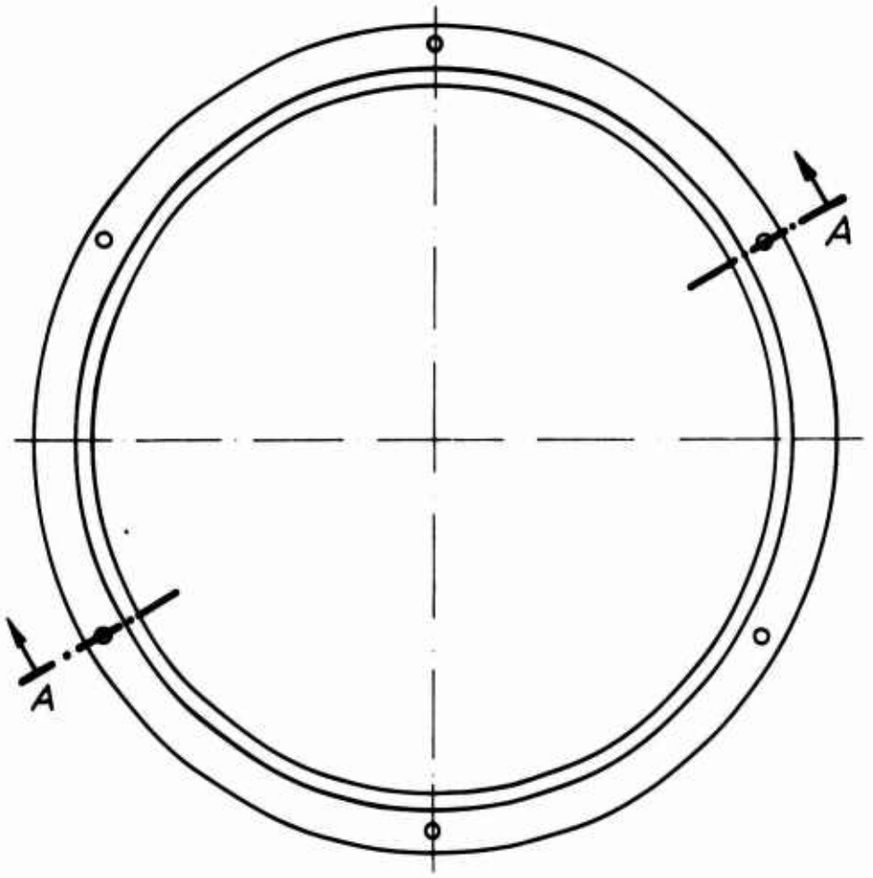

SECTION A-A

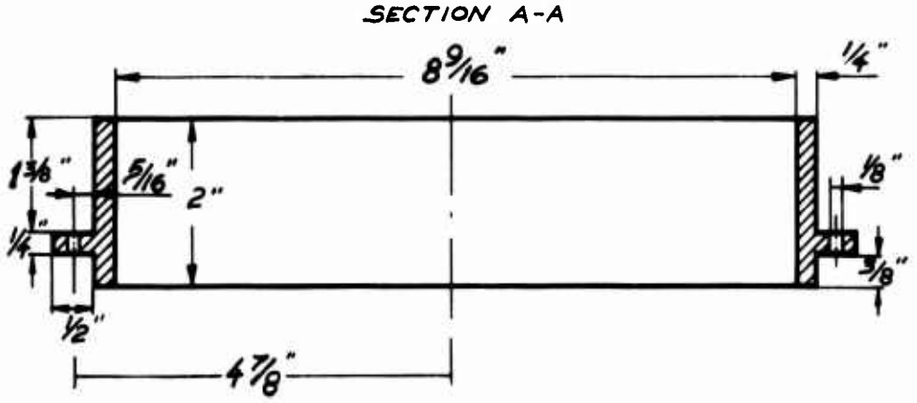

FIG. D III - 6 LUCITE CYLINDER (PART NO. 7)

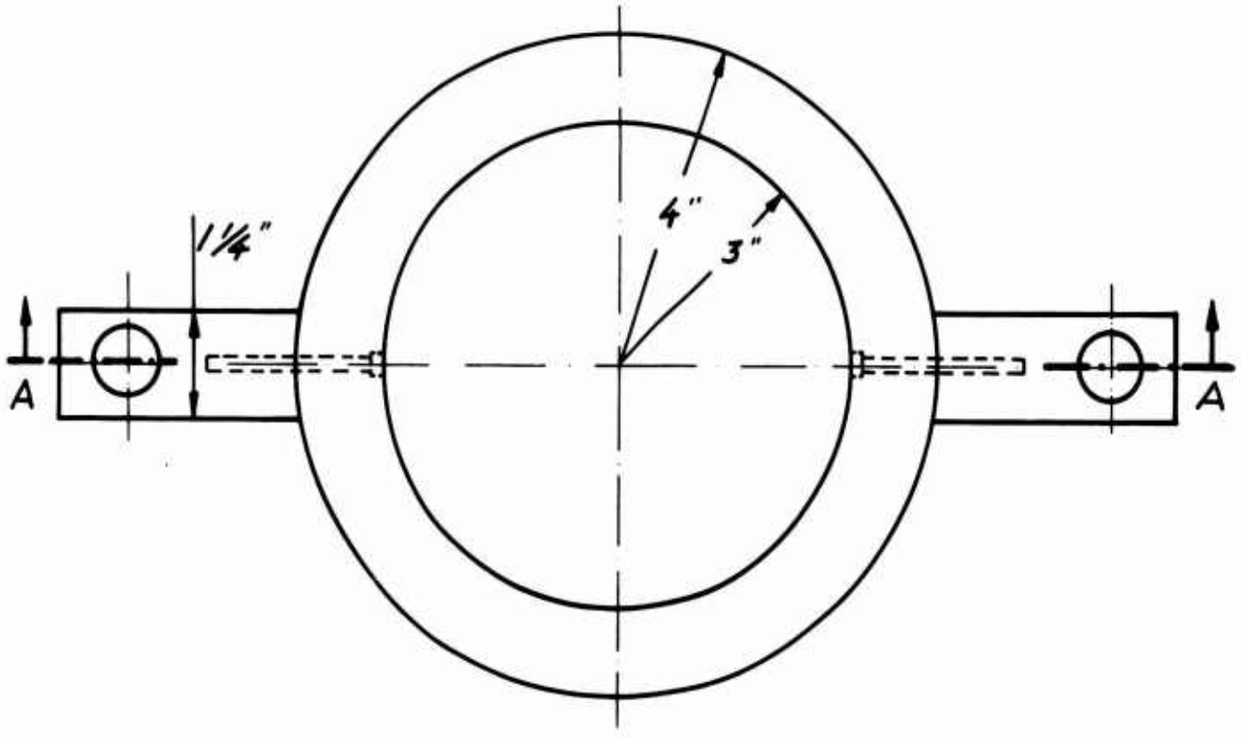

SECTION A - A

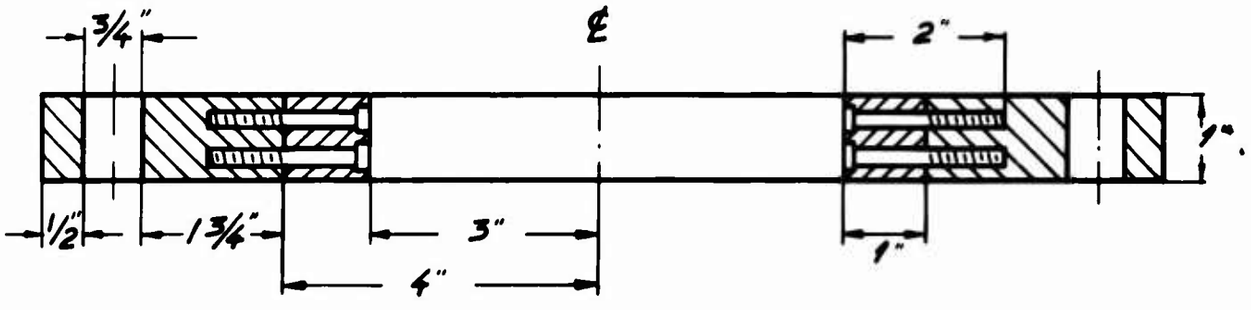

FIG. DIII-7 RING AND BAR CLAMPING PIECE (PART NO 8)

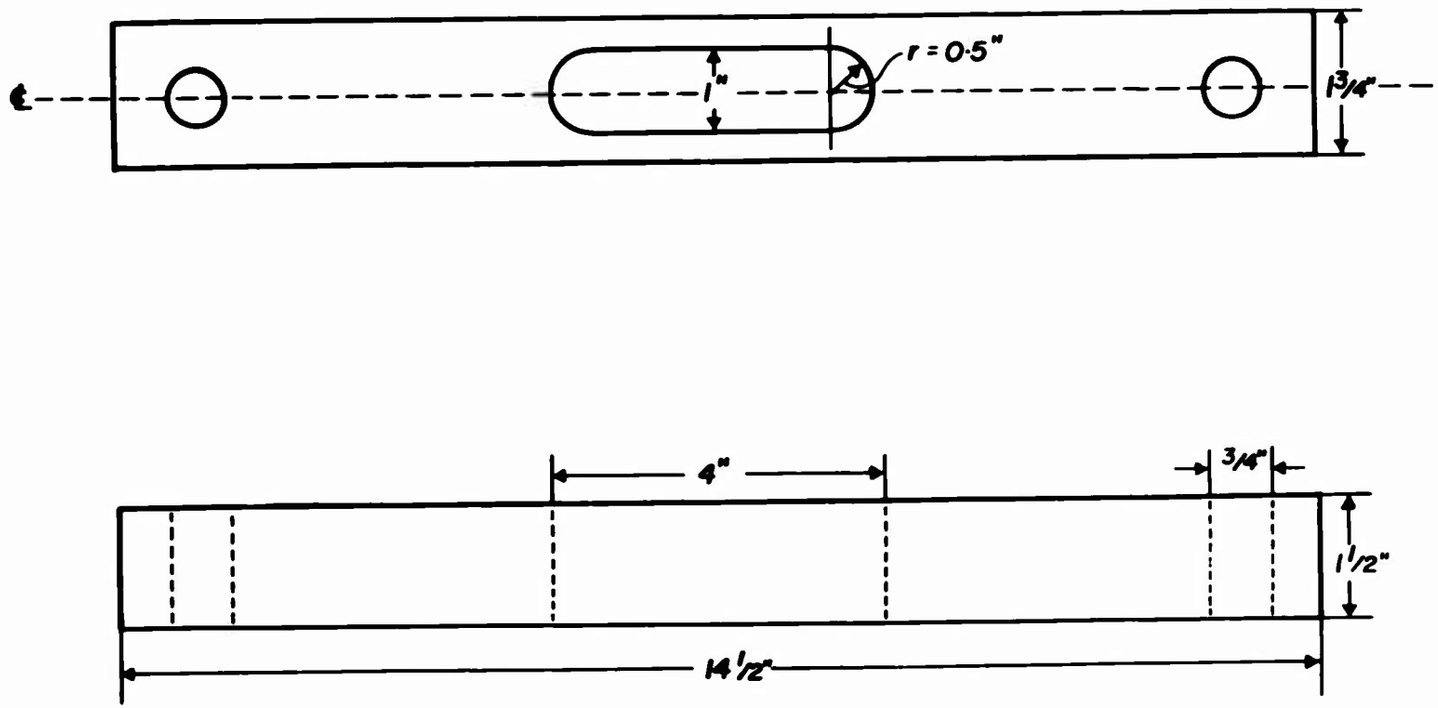

FIG. D III - 8 ASSEMBLY - HOLDING BARS

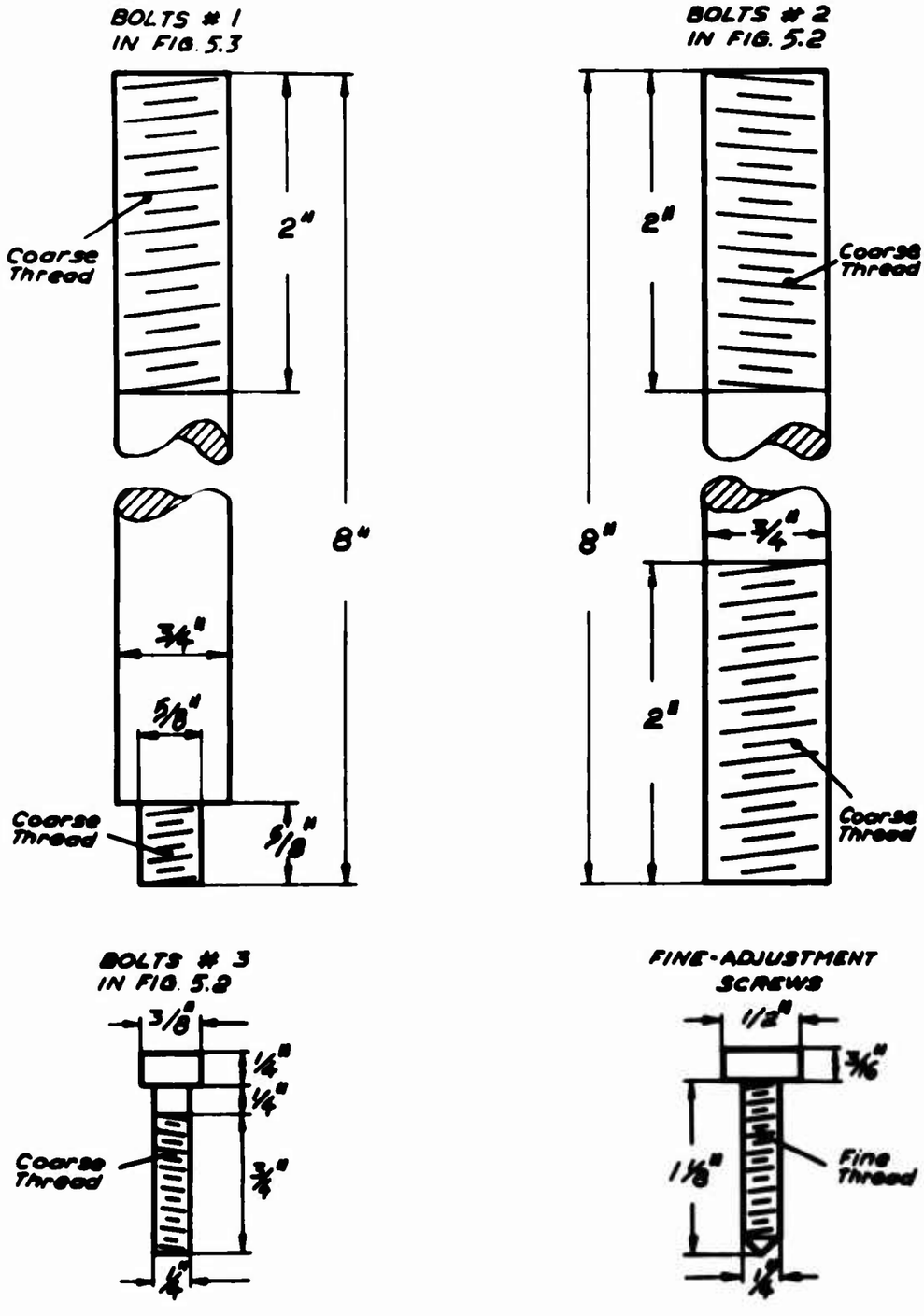

FIG. D III - 9 SPECIAL BOLTS

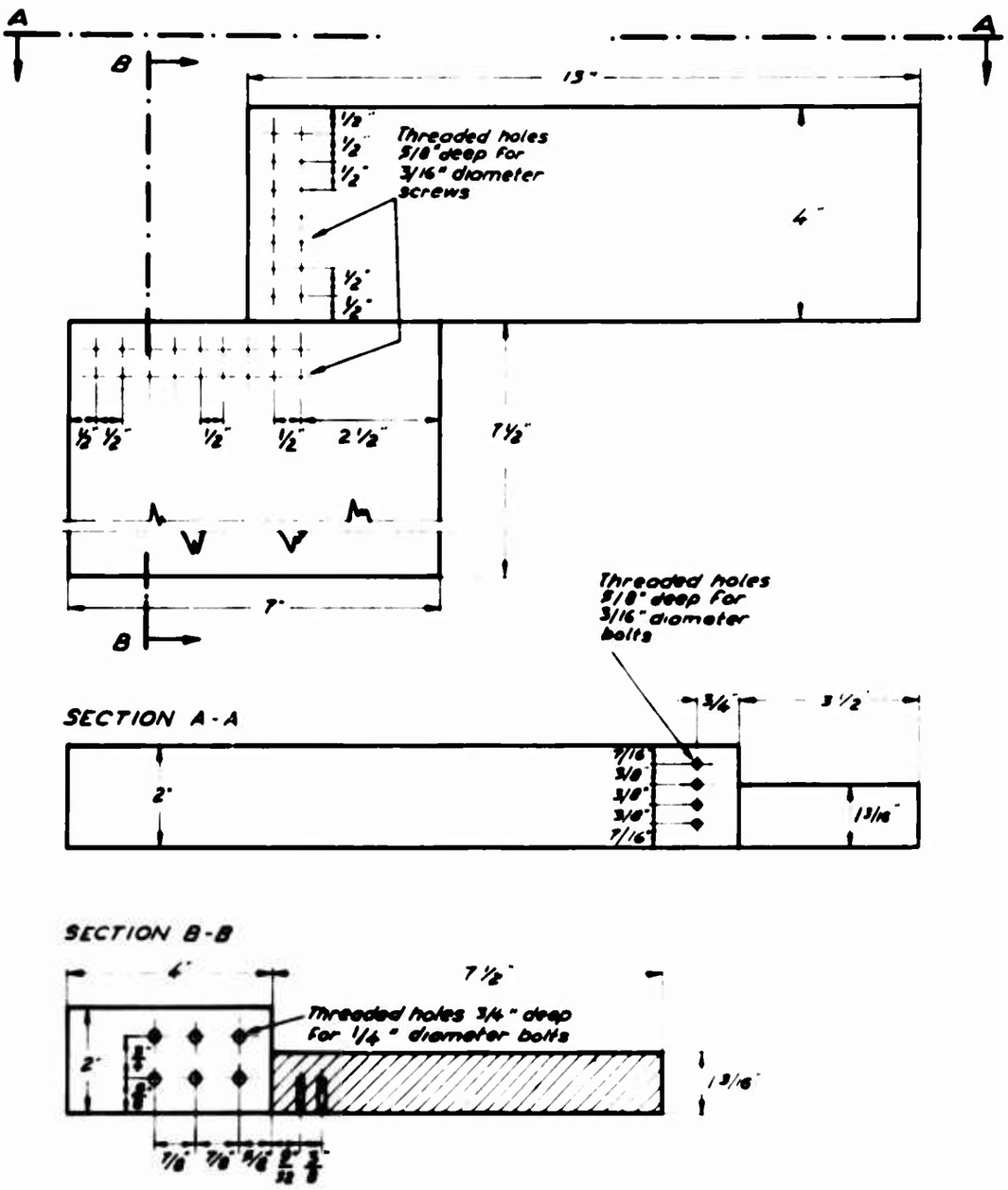

FIG D IV-1 FORCE-APPLICATION SYSTEM

PART #1

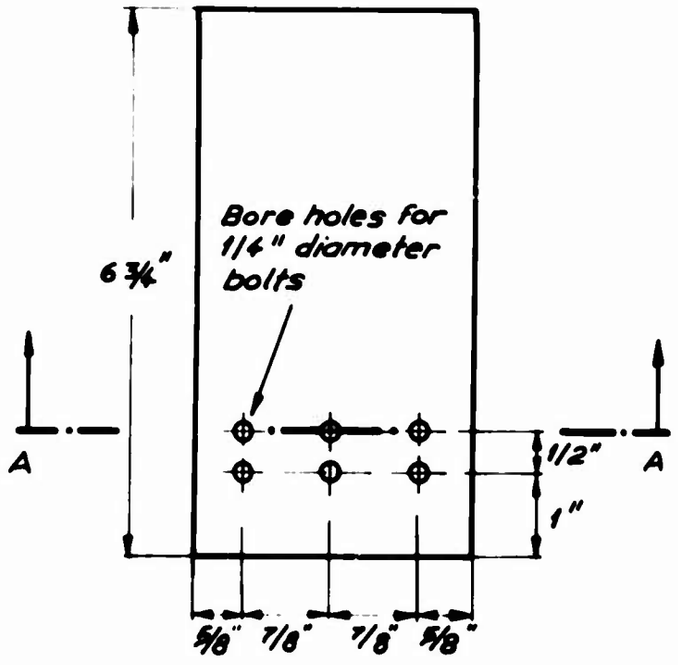

Material : Aluminum

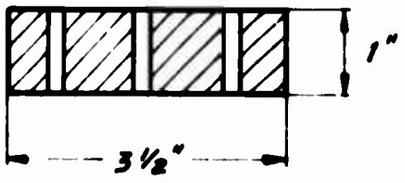

SECTION A-A

FIG. D IV-2 FORCE-APPLICATION SYSTEM
PART # 2

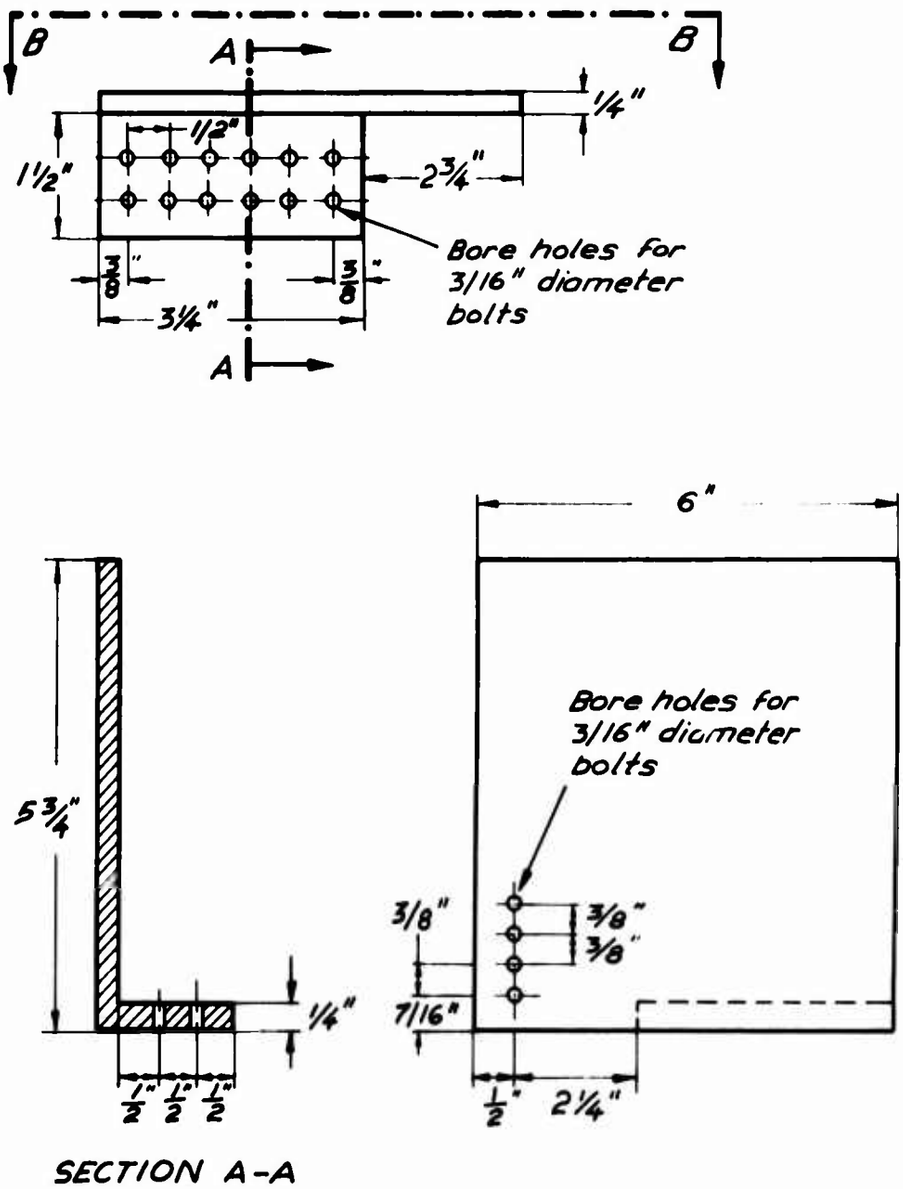

FIG. D IV-3 FORCE-APPLICATION SYSTEM
PART #3

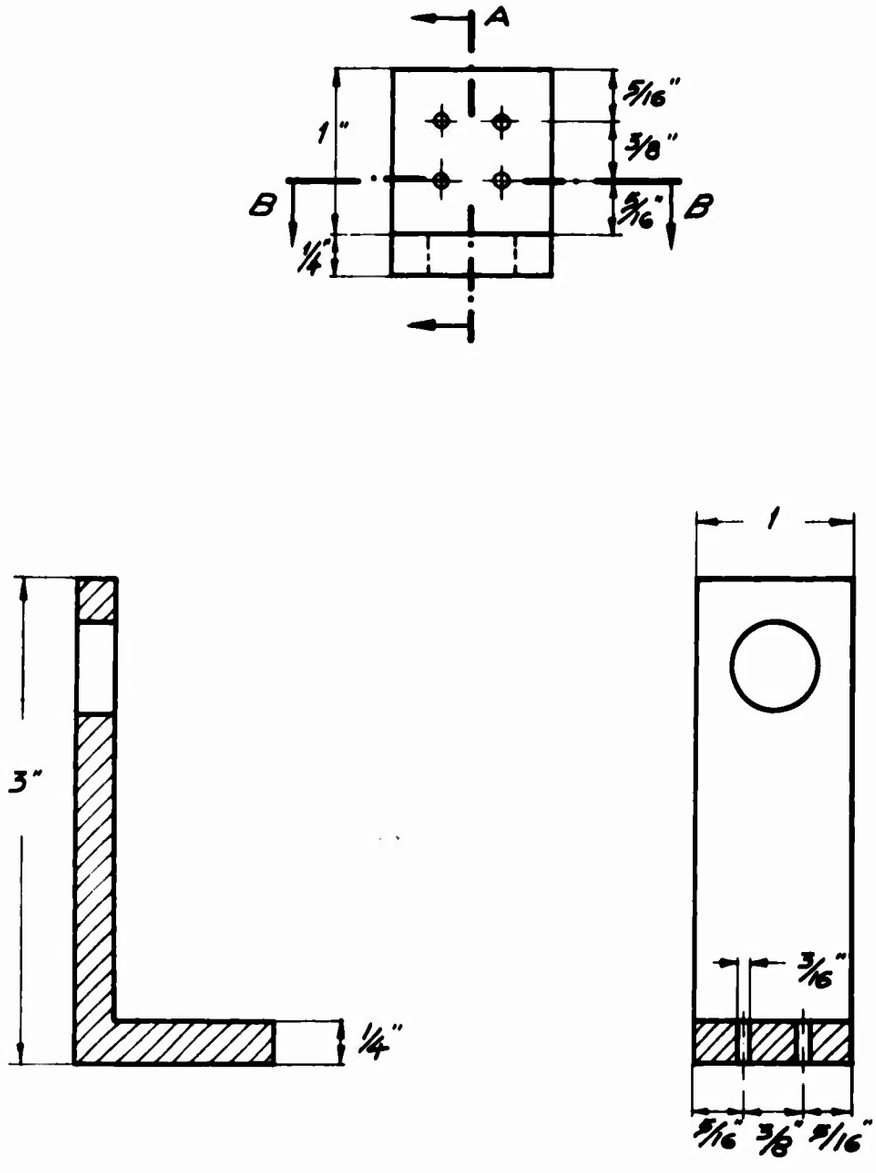

FIG. D IV - 4 FORCE - APPLICATION SYSTEM
PART # 4

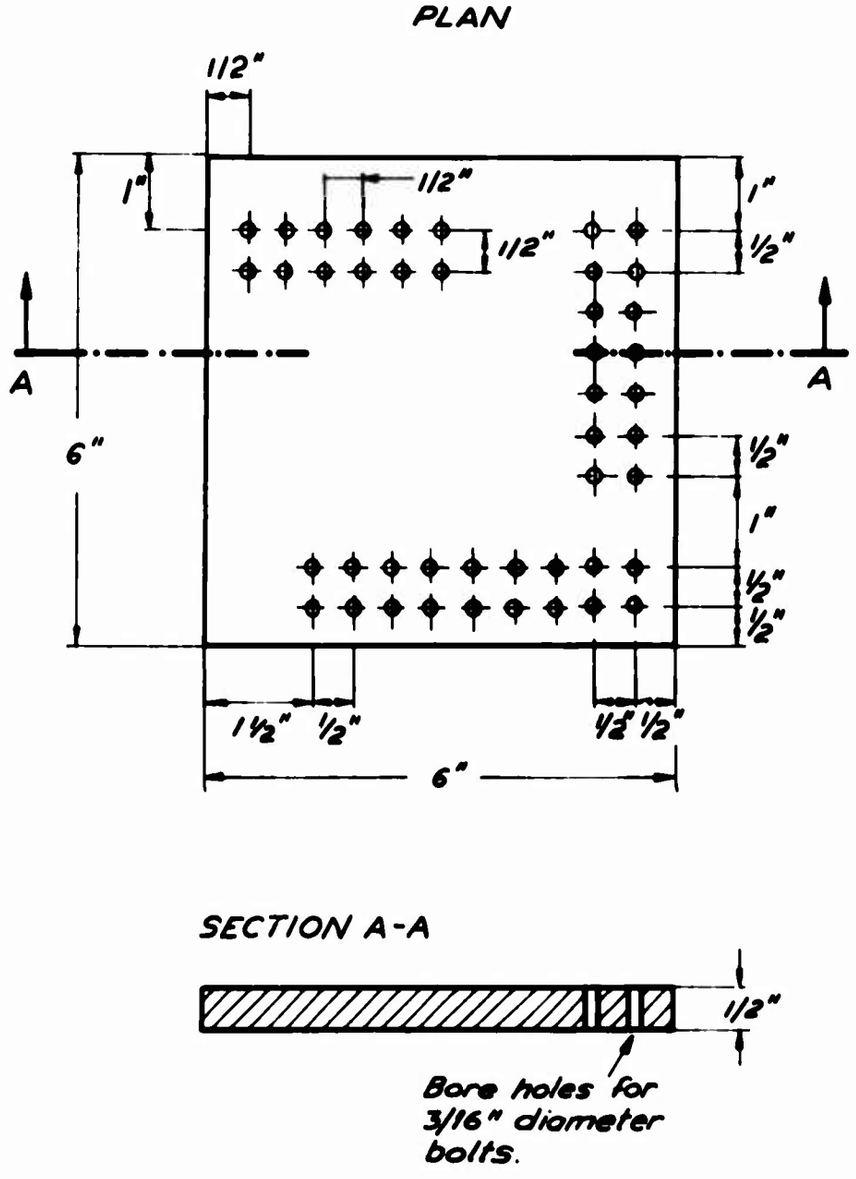

FIG. D IV - 5 FORCE - APPLICATION SYSTEM
PART # 5

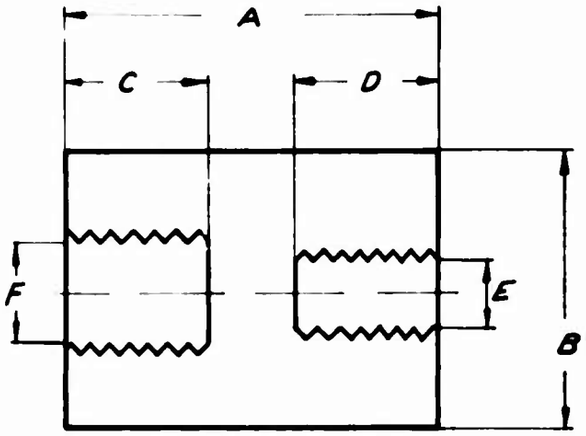

COUPLING#	A	B	C	D	E	F
1	1 1/2	1	3/4	1/2	1/4 - 20 NF	3/8 - 24 UNF - 2A
2	2	1	7/8	7/8	1/4 - 20 NF	1/4 - 20 NF
3	3	1	2 1/4	1/2	1/4 - 20 NF	1/2 - 20 NF

NOTES :

DIMENSIONS . IN INCHES
MATERIAL . 304 STAINLESS STEEL
TOLERANCES : 1/64"

FIG. D IV - 6 FORCE - APPLICATION SYSTEM COUPLINGS PARTS # 7, 10 AND 12

MOUNTING BRACKETS FOR REDUCER SHAFTS PARTS 4, 19 & 21

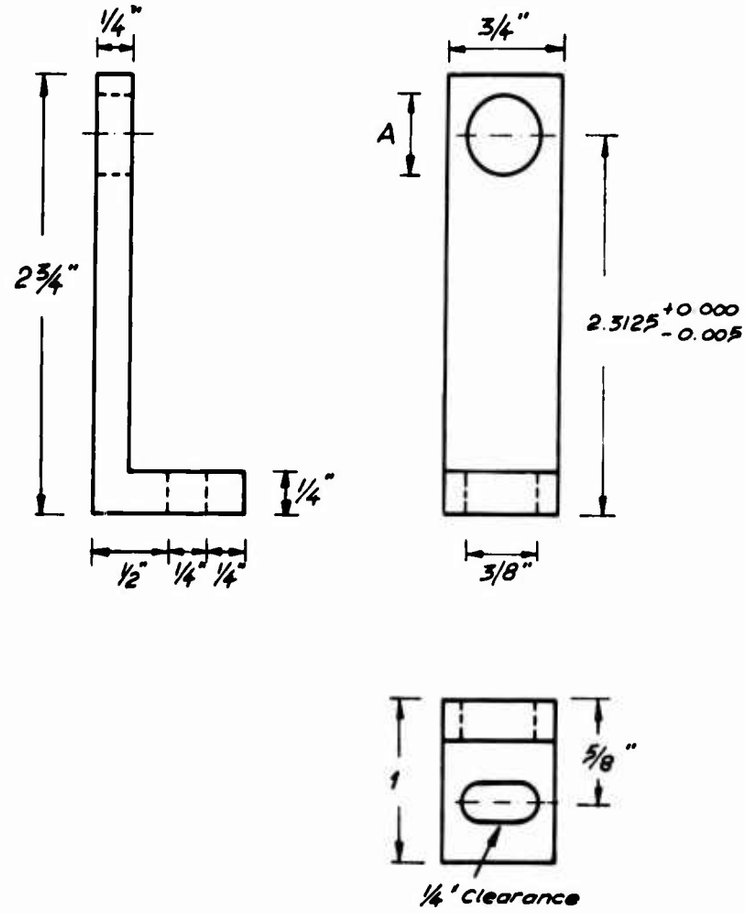

NOTES:

3 BRACKETS REQUIRED

DIMENSION "A" PUSH FIT FOR STERLING INSTRUMENT

BEARING No GM 25 O.D. = 0.5000" +.0000 -.0002

MATERIAL : 304 STAINLESS STEEL

TOLERANCES : 1/64" EXCEPT WHERE OTHERWISE SPECIFIED

FIG. D IV-7 FORCE-APPLICATION SYSTEM BRACKETS PARTS # 4, 19 AND 21

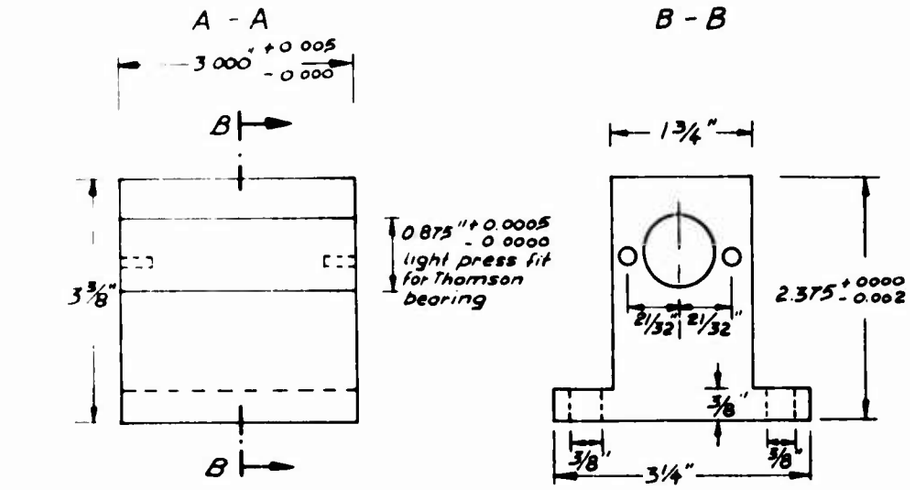

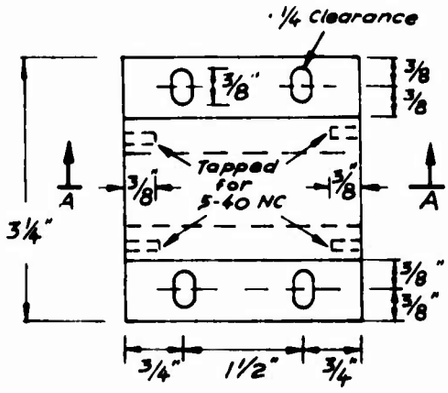

THOMSON LINEAR BEARING AB1420

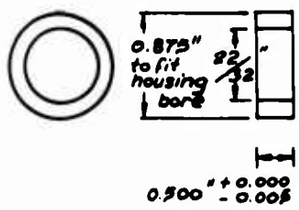

SPACER PART 34

BEARING RETAINING COVERS

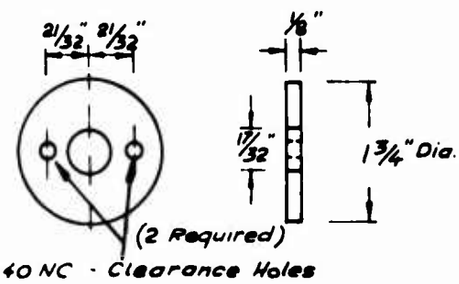

Notes:
Material: 304 Stainless Steel
Tolerances: 1/64" unless otherwise Stated

FIG. D IV-8 LINEAR BEARING HOUSING PART #9

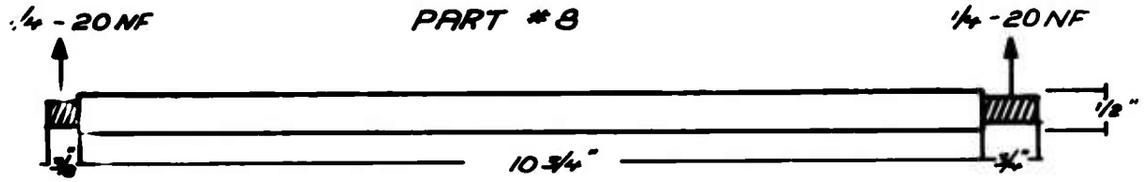

Stainless steel
60 Rockwell case hardened
Tolerance 1/64"

TESTING SHAFT (PART # 13)

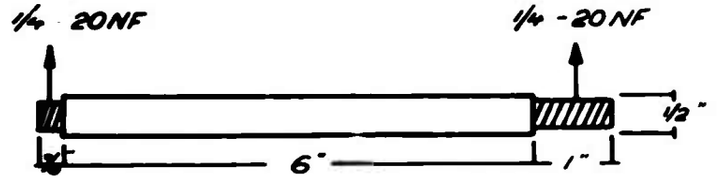

Stainless steel
60 Rockwell case hardened
Tolerance 1/64"

FIG. D IV-9 TESTING SHAFT AND PART # 8

Security Classification

DOCUMENT CONTROL DATA - R & D

(Security classification of title, body of abstract and indexing annotation must be entered when the overall report is classified)

1. ORIGINATING ACTIVITY (Corporate author)
Soil Mechanics Division, Department of Civil Engineering, Massachusetts Institute of Technology, Cambridge, Massachusetts

2a. REPORT SECURITY CLASSIFICATION
Unclassified

2b. GROUP

3. REPORT TITLE
SOIL STABILIZATION; Phase Report No. [illegible], A DURABILITY TEST FOR STABILIZED SOILS

4. DESCRIPTIVE NOTES (Type of report and inclusive dates)
Phase Report No. [illegible]

5. AUTHOR(S) (First name, middle initial, last name)
Anwar E. Z. Wissa
Jose [illegible]. [illegible]

6. REPORT DATE
June 19[illegible]

7a. TOTAL NO. OF PAGES
1[illegible]

7b. NO. OF REFS
6

8a. CONTRACT OR GRANT NO.
DA-[illegible]-eng-[illegible]

b. PROJECT NO.
DA 1T06[illegible] A-[illegible]

c.

d.

9a. ORIGINATOR'S REPORT NUMBER(S)
Soils Publication No. 239
Research Report No. R69-32

9b. OTHER REPORT NO(S) (Any other numbers that may be assigned this report)
U. S. Army Engineer Waterways Experiment Station Contract Report No. [illegible], Phase Report No. 7

10. DISTRIBUTION STATEMENT
This document has been approved for public release and sale; its distribution is unlimited.

11. SUPPLEMENTARY NOTES
Conducted for U. S. Army Engineer Waterways Experiment Station, CE, Vicksburg, Mississippi

12. SPONSORING MILITARY ACTIVITY
U. S. Army Materiel Command
Washington, D. C.

13. ABSTRACT

This report describes and evaluates a new testing procedure for determining the surface durability of stabilized soils by measuring the change in tensile strength at the surface of test specimens (slabs) subjected to laboratory cycles of weathering. This test, called the Durability Tensile Test, is shown to be potentially a more direct and reproducible method than the standard ASTM Durability Test for evaluating stabilized soils. A prototype apparatus has been constructed to measure the surface tensile strength over approximately 4.0 cm^2 circular areas of a [illegible]-inch-square slab, one inch thick. Preliminary tests on three slabs show that the measured strength is related to the effective cohesion of the soil system. For example, increases in curing or dry density which result in an increase in effective cohesion also produce an increase in measured tensile strength. Weathering cycles which have been shown elsewhere to cause a loss in effective cohesion, also result in a loss in tensile strength. Therefore the Durability Tensile Test appears to be a rational method of evaluating durability characteristics. Based on the experience obtained with the prototype apparatus, a modified version is recommended to improve reproducibility and to simplify the testing procedure.

DD FORM 1 NOV 65 1473 REPLACES DD FORM 1473, 1 JAN 64, WHICH IS OBSOLETE FOR ARMY USE.

Unclassified
Security Classification

14 KEY WORDS	LINK A		LINK B		LINK C	
	ROLE	WT	ROLE	WT	ROLE	WT
Soil stabilization						
Tensile strength						
Tensile tests						